UC Riverside
UC Riverside Electronic Theses and Dissertations

Title

Transcriptome-Wide Identification and Validation of Interactions Between the miRNA Machinery and HuR on mRNA Targets

Permalink

https://escholarship.org/uc/item/6bt9h0x5

Author

Li, Yahui

Publication Date

2018

Copyright Information

This work is made available under the terms of a Creative Commons Attribution-NonCommercial-ShareAlike License, available at https://creativecommons.org/licenses/by-nc-sa/4.0/

Peer reviewed|Thesis/dissertation

eScholarship.org Powered by the California Digital Library
University of California

UNIVERSITY OF CALIFORNIA
RIVERSIDE

Transcriptome-Wide Identification and Validation of Interactions Between the miRNA Machinery and HuR on mRNA Targets

A Dissertation submitted in partial satisfaction
of the requirements for the degree of

Doctor of Philosophy

in

Genetics, Genomics and Bioinformatics

by

Yahui Li

December 2018

Dissertation Committee:
Dr. Fedor V. Karginov, Chairperson
Dr. Xuemei Chen
Dr. Shou-wei Ding

Copyright by
Yahui Li
2018

The Dissertation of Yahui Li is approved:

Committee Chairperson

University of California, Riverside

ACKNOWLEDGEMENTS

I would like to express my sincere appreciation to everyone who helped me during my PhD studies at the University of California, Riverside (UCR). This work would not have been possible without their generous help.

First I would like to express my deep gratitude to my PhD advisor, Dr. Fedor (Ted) Karginov. He is always happy to answer my questions whenever I come to his office. During our weekly meetings, he guides me with incredible patience. Thanks to him, I get to achieve my initial graduate school goal in learning bioinformatics, as well as acquire interests in the exciting field, RNA biology. He is a role model scientist to me, and I shall always treasure the mindsets and knowledge I have learned from him during this PhD training.

I thank two graduate students in my lab, Erin Sternburg and Kris Dias, for being supportive colleagues and friends. They, with tremendous passions toward sciences and positive spirits in life, inspire me all along these years. I enjoyed their company.

I thank the members of my dissertation committee, Dr. Xuemei Chen and Dr. Shou-wei Ding, for their effort and time in keeping me on track in the past three years. I also thank the following UCR faculty for their guidance in the first two years of my PhD training: Dr. Weifeng Gu, Dr. Thomas Girke, Dr. Hailing Jin, Dr. Shizhong Xu, Dr. Michael

Adams from my qualifying exam committee, and Dr. Frances Sladek from guidance committee.

I also thank the following friends for their help in my research and dissertation writing. I thank Jason Estep for teaching me basic molecular biology methods and HITS-CLIP library preparation, Dr. Ruidong Li for bioinformatic technique supports, Dr. Hongru Wang for assistance in dissertation revision and bioinformatic analysis.

Lastly, to my dearest family, my parents Qinglong Li, Juan Wang, and my brother Dengchao Li, I thank for their unconditional love and support all these years. They are the rock of my life. Additionally, I want to give special thanks to my partner Dr. Hongru Wang, for his support and encouragement all along and especially during this dissertation work.

In accordance with department guidelines, Chapter 1, in full, is a reprint of a published paper in Journal of Molecular Biology (DOI: https://doi.org/10.1016/j.jmb.2017.12.006). I acknowledge the permission to use the item from the above publisher.

AUTHOR CONTRIBUTIONS

INTRODUCTION

Yahui Li wrote the manuscript.

CHAPTER 1

Fedor Karginov and Yahui Li wrote the manuscript. Fedor Karginov conceived the project. Jason Estep and Yahui Li performed the HITS-CLIP. Yahui Li performed the cloning and luciferase assays. Jason Estep generated CRISPR-based HuR KO cells and performed HuR KD experiments. Fedor Karginov analyzed the HITS-CLIP data.

CHAPTER 2

Yahui Li wrote the manuscript. Fedor Karginov conceived the project. Jason Estep and Yahui Li performed the HITS-CLIP. Yahui Li analyzed the data.

ABSTRACT OF THE DISSERTATION

Transcriptome-Wide Identification and Validation of Interactions
Between the miRNA Machinery and HuR on mRNA Targets

by

Yahui Li

Doctor of Philosophy, Graduate Program in Genetics, Genomics and Bioinformatics
University of California, Riverside, December 2018
Dr. Fedor V. Karginov, Chairperson

The 3' untranslated region (UTR) of mRNAs is extensively targeted by a myriad of RNA-binding proteins (RBPs) and microRNAs (miRNAs) for mRNA decay and translation control. HuR, a ubiquitously expressed RBP, shares many target mRNAs with miRNAs, and their combinatorial control of gene expression has been recently reported. However, the whole picture of this regulation paradigm across the transcriptome remains largely unclear. Here, we investigate the interactions between Ago2 (the core RBP in miRNA machinery) and HuR at the transcriptome-wide level. Using HITS-CLIP, we determined the binding locations and binding levels of HuR and Ago2 on mRNAs. To detect HuR-Ago2 interactions, we measured the CLIP signals of Ago2 while manipulating the protein level of HuR. Globally, occupancies of the most extreme changing Ago2 sites upon HuR knockdown were affected by the HuR's presence on the same 3'UTRs, suggesting that HuR exerts influence on Ago2 binding to mRNAs. In addition, HuR and Ago2 sites largely overlap on 3'UTRs. To study HuR-miRNA interactions at individual sites, thirteen overlapping CLIP sites were selected, and their

activities were tested by luciferase assays. Overall, we found three sites where HuR altered the miRNA repression effects, indicating their interaction at those sites. Additionally, we performed sequence analysis to determine the identities of three uncharacterized bands in HuR CLIP. Our results show that the composition of the sequences in these bands was different from the major band; instead, motif analysis implied that they might not be HuR bands, though higher depth sequencing data were required for confirmation. Taken together, we present an integrated approach to study the interactions between the miRNA machinery and HuR on a transcriptome-wide scale, and define the prevalence and versatility of their interactions on mRNA targets.

TABLE OF CONTENTS

INTRODUCTION

Combinatorial Control of Gene Expression by microRNAs and the RNA-binding Protein HuR

ABSTRACT 1

INTRODUCTION 2

REFERENCES 24

CHAPTER 1

Transcriptome-wide Identification and Validation of Interactions between the miRNA Machinery and HuR on mRNA Targets

ABSTRACT 32

INTRODUCTION 34

RESULTS 37

DISCUSSION 54

MATERIALS AND METHODS 59

REFERENCES 67

CHAPTER 2

Sequence Analysis of Minor Bands in HuR CLIP

ABSTRACT 74

INTRODUCTION 75

RESULTS 76

DISCUSSION 88

MATERIALS AND METHODS 92

REFERENCES 94

APPENDICES

Appendix A. Identifying the HuR Regulatory Sites for HuR-miRNA Interactions 96

Appendix B. Supplementary Figure S1.1-1.3 99

Appendix C. Supplementary File 2 102

Appendix D. Supplementary File 3 106

Appendix E. Supplementary File 1 108

LIST OF FIGURES

INTRODUCTION

Figure I.1. Diagrams of HuR-miRNA antagonistic and cooperative interactions on mRNA targets. 11

CHAPTER 1

Figure 1.1. Ago2 CLIP-Seq characteristics. 38

Figure 1.2. HuR CLIP-Seq characteristics. 39

Figure 1.3. CLIP-Seq analysis of HuR-Ago2 interactions on the same 3' UTR. 42

Figure 1.4. Number of CLIP sites on 3' UTRs that have both Ago2 and HuR sites. 43

Figure 1.5. CLIP-Seq analysis of Ago2-HuR overlapping sites. 46

Figure 1.6. Characteristics of Ago2-HuR overlapping sites. 47

Figure 1.7. Ago2 and HuR CLIP-Seq binding sites on the CDK16 mRNA 3' UTR, and corresponding reporter plasmid design. 51

Figure 1.8. Luciferase reporter assays testing candidate HuR-Ago2 interactions. 52

Figure 1.9. Specific miRNAs are responsible for repression at the identified sites of interaction. 54

CHAPTER 2

Figure 2.1. Phosphorimages of SDS-polyacrylamide gels show four radiolabeled ribonucleoprotein (RNP) bands in HuR CLIP. 78

Figure 2.2. Correlations of the barcode counts of identical reads between libraries prepared from same SDS-PAGE gels. 79

Figure 2.3. Annotation breakdown of unique locations from HuR CLIP libraries. 80

Figure 2.4. Top enriched motifs from HuR CLIP data sets and some of them matched with adapter sequences. 86

APPENDICES

Figure AA1. Luciferase assay testing of candidate HuR binding sites. 98

Figure S1.1. CLIP-Seq analysis of HuR-Ago2 interactions on the same 3' UTR without mRNA level normalization. 99

Figure S1.2. PCR design for monomer cloning and Golden Gate cloning design for luciferase reporter plasmid construction. 100
Figure S1.3. Luciferase assays of HuR-responsive positive control AU5. 101

LIST OF TABLES

INTRODUCTION

Table I.1. Studies of HuR-miRNA interactions on individual transcripts. 12

Table I.2. Examples of HuR influences miRNA expression levels and *vice versa*..... 17

CHAPTER 1

Table 1.1. Genomic locations of 13 candidate sites. 50

CHAPTER 2

Table 2.1. Read counts and barcode counts of HuR CLIP libraries..... 78

Table 2.2. Twenty-five overlapping miRNAs were enriched in all CLIP libraries. 82

Table 2.3. Comparison of motifs from major and minor band libraries and their subsampled libraries. 85

Table 2.4. Top enriched motifs and their occurrences in major and minor band data sets. 88

APPENDICES

Supplementary File 3. Expression levels of candidate miRNAs..... 106

Supplementary File 1b. Monomers coordinates..... 109

Supplementary File 1c. HuR sites coordinates..... 110

INTRODUCTION

Combinatorial Control of Gene Expression by microRNAs and the RNA-binding Protein HuR

ABSTRACT

The ubiquitous RNA-binding protein HuR and non-coding RNA microRNA (miRNA) regulate numerous mRNAs by modulating their stability and translation. Generally, HuR is a positive regulator and targets AU-rich elements (AREs) in 3' untranslated regions (UTRs) of mRNAs, while miRNAs are repressive factors which bind to complementary sequences in 3'UTRs. Interestingly, they share many target mRNAs. On some of those mRNAs, the functions of HuR and miRNA are dependent on each other, indicating their combinatorial regulation of mRNAs. Specifically, my research focus is studying the interactions between HuR and miRNA, which lead to the combinatorial effects on target mRNAs. In this chapter, I concentrate on introducing the topic of HuR-miRNA combinatorial regulation. First I describe the field of post-transcriptional regulation and the two important regulators, HuR and miRNA, respectively. Then, I review the current studies about HuR-miRNA combinatorial regulation on target mRNAs. I also show the cases where they mutually affect each other's expression which are different from their combinatorial regulation. Next, the relevant techniques utilized are described. Finally, I present the goals and experimental designs of my dissertation projects.

INTRODUCTION

1. Post-transcriptional regulation

In prokaryotes, transcription and translation are physically coupled. In eukaryotes, these two processes occur in the nucleus and cytoplasm, respectively, allowing for extensive post-transcriptional regulation (PTR) to shape intrinsic gene expression patterns. PTR includes control of splicing, RNA modification, mRNA transport, mRNA stability and translation. Among them, control of mRNA stability and translation in the cytoplasm are particularly effective in modulating gene expression under environmental perturbations. The major regulators for mRNA stability and translation are microRNAs (miRNAs) and RNA-binding proteins (RBPs), and they mainly bind to the 3' untranslated region (UTR) of mRNAs for the regulation.

Every mRNA is bound by multiple RBPs which determine every aspect of the mRNA's metabolism. The RNA binding property of RBPs is conferred by RNA-binding domains (RBDs). Some well-characterized RBDs are the following: RNA recognition motif (RRM, also known as RNA-binding domain RBD); K-homology (KH) domain (type I and II); RGG (Arg-Gly-Gly) box; Sm domain; DEAD/DEAH box; zinc figure (ZnF); double stranded RNA-binding domain (dsRBD); cold-shock domain; Pumilio/FBF (PUF or Pum-HD) domain; and the Piwi/Argonaute/Zwille (PAZ) domain (reviewed in (1)). RBPs recognize specific sequences or structures of mRNAs, e.g., HuR targets AU-rich elements (AREs) in mRNAs, and Dicer binds double-stranded RNAs with 3' overhangs.

But for some RBPs, the target recognition requires the guidance of small RNAs, e.g. Argonaute proteins are guided by miRNAs to target specific sites on mRNAs.

The binding preferences of RBPs can be determined by RNA binding assays (section 6.1). The consensus sequences derived from the identified RBP target sequences are termed 'binding motifs' for the RBP. RBP binding motifs tend to have low sequence diversity. Yet, the structure and the sequence context of the motifs also contribute to the binding specificity, suggesting more intricate mechanisms of RBP recognition (2).

Regulation of RBPs on the 3' UTR occurs in a highly dynamic manner. Many RBPs' binding sites co-localize within 3'UTRs, especially at miRNA binding sites and AU-rich elements (AREs) (3). HuR, as an ARE binding protein, is generally a stabilizer of mRNA decay, while miRNAs almost exclusively lead to gene repression. Recent studies show that they share many target mRNAs, allowing for potential interactions on the same mRNAs. In this chapter, I focus on introducing the combinatorial regulation of gene expression by HuR and miRNA.

2. Human Antigen R (HuR)

2.1 HuR protein structure and properties

Human Antigen R (HuR, also known as HuA and ELAV-like 1, ELAVL1) is a ubiquitously expressed RNA-binding protein that belongs to the Hu/ELAV mammalian

RBP family. First characterized in 1996 (4), HuR is a well-studied RBP that plays important roles in mRNA stabilization and pre-mRNA splicing.

HuR protein contains three tandem RNA recognition motifs (RRM1-3) and a HuR nuclear signal (HNS) within the hinge between RRM2 and RRM3. The two N-terminal RRM domains (RRM1 and RRM2) are highly conserved and most crucial for RNA binding, while the RRM3 contributes to stabilize the RNA-protein complex. HuR is predominantly localized in the nucleus, and the HNS in HuR is responsible for nuclear localization and nuclear export, which allows HuR to shuttle between the nucleus and cytoplasm (5,6). HuR shuttling can be induced by many stimuli, including ultraviolet radiation (UVR), lipopolysaccharide (LPS), chemical compounds, alterations in the microenvironment, cytokines, viral infection and hormone treatment (reviewed in (7)). The shuttling property allows for HuR function in a dynamic manner during various cellular processes.

2.2 HuR targets and regulation mechanism

In human cell lines, HuR targets mostly 3'UTRs and introns of mRNAs. The numbers of HuR target mRNAs range from 2128 to 7252 in various studies (8-11). HuR binds to AREs in 3'UTRs extensively. ARE is the cis-element involved in ARE-mediated decay (AMD). HuR generally acts as a stabilizer in AMD in that overexpression of HuR protects mRNAs from AMD (5,12). Mechanism-wise, HuR protects mRNAs through competing with decay factors for ARE binding, e.g., HuR and a decay factor TTP have a

competition interaction on IL-3 and GM-CSF mRNAs (13,14). When examining deadenylation and decay of c-fos ARE containing mRNA, HuR was shown to stabilize through protecting the mRNA body from degradation (12). In addition, HuR's stabilizing function is directly related with its translocation into cytoplasm under stress or during cell cycle transitions. For example, HuR stabilizes p21 mRNA under UV stress and stabilizes cyclin A and B1 cell in a cycle-dependent manner (15).

2.3 HuR and diseases

HuR regulates many important genes that are involved in cancer and inflammation. Generally, HuR enhances proliferation, represses apoptosis, increases angiogenesis, reduces immunosurveillance, and facilitates invasion and metastasis (reviewed in (16). For example, HuR positively regulates pro-angiogenic factors HIF-1α (17), VEGF (18), and COX-2 (19) by binding to their mRNAs in cultured cells or tumor samples. Given HuR's broad regulation capacity, HuR could be a potential therapeutic target for cancer and inflammation.

HuR's overall levels or cytoplasmic levels are shown to have prognosis potential in different cancer types but with varied effects. Total HuR levels predicted poor survival in colorectal adenocarcinoma (20). HuR is also shown to be a prognostic indicator in breast cancer, but is positively correlated with low reoccurrence of early stage cancer patients (21).

3. miRNAs, Argonaute and RISC complex

3.1 miRNA biogenesis and RISC complex

microRNAs (miRNAs) are a class of ~22 nucleotide (nt) small non-coding RNAs that extensively regulate gene expression at the post-transcriptional level. Generally, the miRNA gene is transcribed into primary miRNA (pri-miRNA), and then processed by the RNases III enzyme Drosha and its co-binding protein DGCR8 (collectively known as the Microprocessor) into a ~70nt hairpin-containing pre-miRNA. The pre-miRNA is exported to the cytoplasm and sliced by another RNase III enzyme Dicer into a ~22nt double-stranded miRNA duplex. One strand is the mature miRNA which is loaded into Argonaute (Ago) protein, together with other cofactors Dicer, TRBP and GW-182, to form the functional RNA-induced silencing complex (RISC).

In animals, RISC is guided by miRNAs to target the 3'UTR of mRNAs through imperfect complementarity. The seed region of miRNAs is crucial for target recognition, which is at the 5' end spanning nucleotides 2 to 7 (22). The recognition by imperfect complementarity allows miRNAs to have widespread mRNA targets. It is predicted that over 60% of human mRNAs are targeted by miRNAs (23).

There are four proteins in the Ago subfamily in human, i.e. Ago1, Ago2, Ago3 and Ago4. Ago2 is the only member that has endonuclease activity (24,25). Ago2 is the most abundant Argonaute protein in the commonly used cell lines HEK 293T and HeLa S3, occupying about 60% of the overall Argonaute protein levels (26). The four human Ago

homologs bind to similar miRNA and mRNA pools (27,28). Therefore, Ago2 is commonly used to characterize miRNA function and binding specificity.

3.2 miRNA regulation mechanism

In animals, miRNAs mediate two modes of gene silencing: mRNA decay and translational repression. On the one hand, miRNAs promote mRNA decay by recruiting deadenylases (mainly the CCR4-NOT complex) and increase the accessibility of the poly(A) tail to deadenylases. After deadenylation, target mRNAs are decapped and digested by 5'-3' exonuclease (29-33). On the other hand, miRNAs mediate translational repression by three major mechanisms, i.e. (1) poly(A)-binding protein (PABP) displacement through GW182 protein (also known as TNRC6), (2) recruiting translational repressors, and (3) facilitating eIF4A disassociation from the cap-binding complex eIF4F. These mechanisms occur concurrently or occur with different kinetics to increase the silencing effect (reviewed in (34)). Recent genome-wide studies suggest that translational repression generally precedes mRNA decay, but mRNA decay is the major outcome of miRNA mediated repression, and it has been shown that mRNA decay accounts for the most (≥84%) of reduced protein output (35).

3.3 miRNAs and medicine

miRNAs are important in both normal development, differentiation, growth control and human diseases such as cancer. miRNAs can either act as tumor suppressors or oncogenes (oncomiRs). Accordingly, miRNA therapies have been developed and several

potential drugs have already reached clinical trials including a mimic of the tumor suppressor miRNA miR-34 for treating cancer, and antagomiRs targeting miR-122 for hepatitis treatment (reviewed in (36)).

4. Combinatorial control of gene expression by the RNA-binding protein HuR and miRNAs

miRNAs and HuR target a wide range of mRNAs and they share many target mRNAs (10,37). Examples of their interactions on individual transcripts have emerged. The HuR-miRNA interactions could be either cooperative where one RBP facilitates the function of the other, or antagonistic where the RBP attenuates the function of the other. In this section, the studies of HuR-miRNA interactions are reviewed, and the evidence of their interaction at the binding level and the mechanisms of their interactions are also discussed.

4.1 Studies of HuR-miRNA interactions on individual mRNAs.

HuR-miRNA interactions have been implicated in regulating many essential genes, with well-characterized examples summarized in Table I.1. We will discuss these interactions in terms of the antagonistic and cooperative manner.

4.1.1 Antagonistic interaction

In the very first study of interplay between HuR and miRNA, Bhattacharyya and colleagues (38) reported that HuR antagonized miR-122 to de-repress cationic amino acid

transporter 1 (CAT-1) mRNA under starvation stress conditions. The expression of CAT-1 was repressed by the liver-specific miR-122 in the normal condition while de-repressed in starvation stress accompanied by CAT-1 mRNA translocation from P-bodies (PBs) to polysomes. The authors found that both the de-repression and the translocation of CAT-1 mRNA required the presence of HuR. In the meantime, upon starvation, HuR shuttled to the cytoplasm and bound an ARE region in CAT-1 mRNA. Accordingly, it was proposed that HuR antagonize the miR-122 on CAT-1 mRNA under starvation stress, and therefore relieved the miRNA-meditated repression of CAT-1 mRNA (Figure I.1A).

Similar HuR-miRNA antagonistic interactions were found to control the expression of p53, TOP2A, ERBB2 and IL-8 (Table I.1, (39-42)), where HuR antagonizes miRNA when HuR cytoplasmic level increases. Specifically, in these studies, the elevated cytoplasmic HuR levels were induced by UV stress (39), specific cell cycle phase (40) and the abnormal gene expression in cancer cells (41,42).

4.1.2 Cooperative interaction

HuR generally is a stabilizer in the AMD pathway while miRNAs largely mediate gene repression, but they have been shown to cooperatively regulate the expression of some transcripts.

Kim et al. (43) reported that HuR cooperatively interacted with let-7 to repress the expression of a proto-oncogene, c-Myc. HuR was required for let-7's binding to the c-

Myc mRNA to repress c-Myc. Conversely, let-7 was also required for HuR to repress c-Myc expression. HuR did not directly bind to the let-7 machinery, but instead bound to a site that was over 100nt away from the let-7 binding site, so it was proposed that HuR binding on mRNA perhaps changed the local RNA conformation to facilitate let-7 binding to the target site. A follow-up study showed that let-7 binding on c-Myc mRNA increased the HuR binding strength on the mRNA, supporting the cooperative interaction (44). Additionally, Thorne et al. (45) found that HuR and miR-19b interacted cooperatively to repress the expression of P-glycoprotein (ABCB1). Interestingly, HuR was shown to directly bind to miR-19b for the co-regulation. Another HuR-miRNA cooperative interaction was found to control the expression of RhoB (46). HuR and miR-19a/b bound to adjacent sites on RhoB 3'UTR in an interdependent manner to inhibit RhoB expression, and loss of this interaction under UV stress led to de-repression of RhoB mRNA (Figure I.1B).

Opposite to the resulting repression in above studies, the cooperative interaction of HuR and miR-200a up-regulates the expression of c-Jun as reported in (47). miR-200a is unconventionally shown to stabilize c-Jun mRNA, which is dependent on the presence of HuR. Additionally, overexpression of miR-200a increased HuR binding on c-Jun mRNA, supporting the cooperative interaction model. The HuR binding site is within a long ARE that covered the miR-200a site. miRNA binding was proposed to trigger a conformational change of the c-Jun 3'UTR which promoted the interaction of miR-200a.

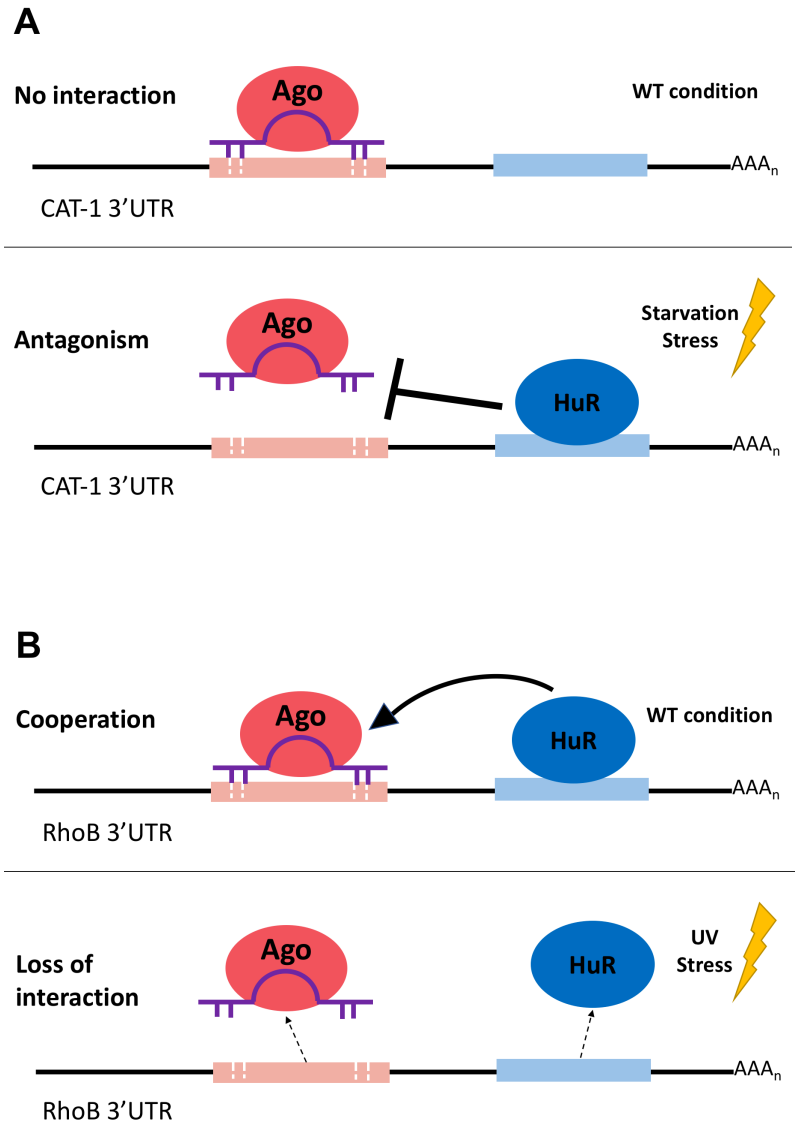

Figure I.1. Diagrams of HuR-miRNA antagonistic and cooperative interactions on mRNA targets.

A) HuR antagonizes miR-122 on CAT-1 mRNA during starvation stress condition, but no such interaction in WT condition. B). HuR cooperatively interacts with miR-19 to repress RhoB expression, while the interaction is lost during UV stress condition.

Table I.1. Studies of HuR-miRNA interactions on individual transcripts.

	mRNA	miRNA	Cells [1]	Interaction effect	Preliminary mechanism	Effect on mRNA binding levels [2]	Site distance	Ref.
Antagonism	CAT1	miR-122	Huh7	De-repression	HuR translocation	NA	>10nt	(38)
	TOP2A	miR-548c-3p	HeLa	De-repression	HuR translocation	HuR ↔ miRNA	>10nt	(40)
	Stim1	miR-195	IEC-6	De-repression	NA	HuR → miRNA	>10nt	(48)
	p53	miR-125b	MCF7	De-repression	HuR translocation	HuR → miRNA	1 nt	(39)
	ERBB2	miR-26a/b	MCF7, T47D	De-repression	Increased HuR levels	HuR ↔ miRNA	>10nt	(41)
	IL-8	miR-4312	BxPC3, SW1990	De-repression	Increased HuR levels	miRNA → HuR	>10nt	(42)
Cooperation	c-Myc	let-7	HeLa	Repression	NA	HuR → miRNA	>10nt	(43)
	RhoB	miR-19a/b	HaCaT	Repression	NA	HuR ↔ miRNA	9 nt	(46)
	c-Jun	miR-200a	HEK 293T	Stabilization	NA	miRNA → HuR	Overlapping	(47)
	ABCB1	miR-19b	MCF7	Repression	Co-binding	HuR → miRNA	Overlapping	(45)

Table I.1. Notes.

[1] Huh7: hepatocarcinoma cells; HeLa: cervical carcinoma cells; IEC-6: rat intestinal crypt cells; MCF7 and T47D: breast carcinoma cells; BxPC3 and SW1990: pancreatic ductal adenocarcinoma cells; HaCaT: keratinocyte cells; HEK 293T: embryonic kidney cells. Unless noted, the cell lines are from human origin.
[2] →: one factor affects the other factor's occupancy on mRNAs. ↔: reciprocal effect on mRNA binding levels.

4.2 Evidence of HuR-miRNA interactions at the binding level

RBPs bind to target mRNAs to regulate their metabolism, and their mRNA binding levels dictate the strength of the RBP regulation on mRNAs. The interactions between HuR and miRNA (or Ago2) largely affect each other's binding strength (occupancy) on mRNAs. To detect that, RBP occupancy is measured while the other RBP levels are manipulated, and a change in RBP occupancy upon the altered level of the other RBP indicates an interaction between the two RBPs at the binding level.

In most of the studied cases, evidence of HuR-miRNA interactions at the binding level were provided (Table I.1). In studies on TOP2A, EERB2 and RhoB mRNAs, the interactions between HuR and the miRNA (or Ago2) affect both factors' occupancy on mRNAs in a reciprocal fashion. For example, for the TOP2A 3'UTR, HuR overexpression decreased the association of TOP2A mRNA with miR-548c-3p. In turn, miR-548c-3p overexpression decreased HuR binding to TOP2A mRNA. However, in most cases, the interactions only affect one RBP's occupancy on the mRNA. In the studies on c-Myc, Stim1, p53 and ABCB1 mRNAs (39,43,45,48), HuR effect on Ago2 (or miRNA) occupancy on mRNAs was successfully detected while the Ago2 (or miRNA)

effect on HuR was not detected or not shown. While in studies on IL-8 and c-Jun mRNAs, only miRNA effect on HuR occupancy was reported.

4.3 The mechanisms of HuR-miRNA interaction

The mechanisms of the HuR-miRNA interaction remain largely unclear. HuR and miRNA binding sites on target mRNAs were rarely determined and validated, which impeded the study of mechanisms.

For the cases of HuR-miRNA antagonistic interactions on CAT-1, TOP2A, p53, ERBB2 and IL-8 mRNAs, elevated cytoplasmic HuR levels were shown to induce interaction, which suggests that localization and abundance of HuR protein are important for it to interact with miRNAs. But detailed mechanisms were not characterized. Interestingly, HuR and miRNA binding sites on mRNAs were mostly separated by long distances (Table I.1). Kundu et al. (49) showed that the long-distance antagonistic interaction of HuR and miRNAs could be mediated by HuR oligomerization along mRNA.

Studies on mechanisms of HuR-miRNA cooperative interactions are also lacking. In ABCB1, HuR was shown to directly bind to miR-19, which led to a proposal that the co-binding of HuR and miRNA facilitates miRNA association and function on mRNAs (45).

4.4 Transcriptome-wide studies of HuR-miRNA combinatorial regulation

HuR-miRNA interactions have been studied at the transcriptome-wide level in a handful of reports. Mukherjee et al. (10) showed that a close HuR binding site on transcripts affected miRNA's function in mRNA stability. Globally, miRNA sites with a close HuR binding site (distance of the two binding sites < 10nt) had less of a de-stabilization effect on mRNAs, compared to the miRNA sites with HuR binding sites that are farther, suggesting the proximal HuR binding site has an antagonistic effect on miRNA's function. Conversely, however, the close miRNA binding site did not affect HuR's function in mRNA stabilization. Interestingly, HafezQorani et al. showed that a close miRNA site has an antagonistic effect on HuR's stabilization to mRNAs (50). This inconsistency between the two studies is perhaps due to the different criteria in defining close binding sites (less than 10nt vs less than 30nt).

Although transcriptome-wide studies of HuR-miRNA interactions affecting the functions of HuR and miRNAs have been reported, transcriptome-wide evaluation of HuR-miRNA interactions affecting their mRNA binding levels have not yet been shown. Here, we detect the HuR-miRNA interactions by measuring the binding levels of one RBP across the transcriptome while manipulating the levels of the other, which is further described in section 7.

5. miRNAs expression regulation by HuR directly and *vice versa*

The previous section describes the combinatorial regulation of HuR and miRNA on shared mRNAs. However, they are the targets of each other in some cases, and therefore indirectly affect the regulated mRNAs of the other factor, i.e. HuR is the target or regulator of miRNAs, and care should be taken to differentiate those cases from their combinatorial regulation. Recent studies of their mutual effects on each other's expression levels are summarized in Table I.2.

5.1 miRNAs regulate HuR expression levels

A few miRNAs have been reported to target HuR mRNA to regulate its expression. miR-125b-5p is shown to repress HuR translation by binding to the 3'UTR region of HuR mRNA in liver cells (51). Similarly, miR-22, miR-133b, miR-133a-3p repressed HuR expression in colorectal cancer cells, prostate cancer cells and oral cancer cells, respectively (52-54). Interestingly, contrary to miRNA's common role as a repressor, miR-155-5p promotes HuR expression in a human epithelial colon adenocarcinoma cell line (55). In addition, studies of other miRNAs regulating HuR levels, including miR-519, miR-125a, miR-16 and miR-34a , are reviewed in (16).

5.2 HuR regulates miRNA expression levels

HuR also modulates the levels of certain miRNAs directly. HuR positively regulates let-7c expression possibly by binding to the ARE in the pre-let-7c sequence (56). In T helper

17 cells, HuR is shown to regulate levels of miR-466i, miR-409 and miR-335(57,58). Additionally, miR-16 and miR-7 expression is repressed by HuR as reviewed in (16).

Table I.2. Examples of HuR influences miRNA expression levels and *vice versa*

Regulator	Target	Effect	Cells/tissues*	Ref.
miR-125b-5p	HuR mRNA (3'UTR)	Repression	Huh7.5	(51)
miR-22	HuR mRNA (3'UTR)	Repression	CRC tissue and cells	(52)
miR-133b	HuR mRNA (3'UTR)	Repression	Prostate cancer cells	(53)
miR-133a-3p	HuR mRNA	Repression	UMSCC47	(54)
miR-155-5p	HuR mRNA (3'UTR)	Promotion	HT29	(55)
HuR	pre-let-7c	Promotion	HEK293T	(56)
HuR	miR-409, miR-335	Repression	Th17	(57)
HuR	miR-466i	Repression	Th17	(58)

* Huh7.5: liver carcinoma cells; CRC: colorectal cancer; UMSCC47: papillomavirus infected oral cancer cells; HT29: epithelial colon adenocarcinoma cells; Th17: T helper 17 cells. All cell lines are from human origin.

6. Methods to study RNA-protein interactions

To study combinatorial control by two RBPs on the same mRNAs, we first need to determine the individual RBP's interactions with target mRNAs. The RBP-RNA interactions can be detected by RNA binding assays including cross-linking and

immunoprecipitation followed by high-throughput sequencing (CLIP-Seq), electrophoretic mobility shift assay (EMSA), RNAcompete, RNA Bind-n-Seq. The structure of RNAs is important for understanding the RBP-RNA interactions, which can be determined by *in vivo* click selective 2'-hydroxyl acylation and profiling experiments (icSHAPE) and Psoralen Analysis of RNA Interactions and Structures (PARIS). In addition, the structure of RBP-RNA complexes can be revealed by X-ray crystallography and cryo-electron microscopy (cryo-EM).

6.1 RNA binding assays

CLIP-Seq

Cross-linking and immunoprecipitation followed by high-throughput sequencing, or CLIP-Seq, is a method to detect RNA-protein interactions in vivo at the transcriptome-wide level. In CLIP-Seq, cells are first treated with UV light to cross-link proteins and proximal RNAs together by covalent bonds. The protein of interest and its bound RNAs are then immunoprecipitated by a specific antibody. The RNA fragments from the protein-RNA complex are further isolated and sequenced. The first version of CLIP-Seq is also named HITS-CLIP (HIgh-Throughput Sequencing of RNA isolated by CrossLinking ImmunoPrecipitation) (59). Three other variations of CLIP-Seq have been developed subsequently: (1) Photoactivatable-Ribonucleoside-Enhanced Crosslinking and Immunoprecipitation, or PAR-CLIP, was introduced to improve the UV crosslinking efficiency by incorporating photoactive nucleosides such as 4' thiouridine (4SU) in cell culture before UV crosslinking. Particularly, the signature T to C conversion in cDNAs

facilitates the identification of RBP binding sites more precisely (28). (2) Individual-nucleotide resolution UV cross-linking and immunoprecipitation, or iCLIP, advanced the RBP site determination in a different methodology. Reverse transcription is likely to stall at the crosslinking site. In iCLIP, a modified RT primer was used to circularize cDNAs to preserve the stalled RT products, and thereby track down the crosslinking site (60). (3) Enhanced clip, or eCLIP, further increased the ligation efficiency of iCLIP by introducing a barcoded 3' RNA adapter and improving the efficiency of the ligation reaction (61). Among all variants of CLIP-Seq, HITS-CLIP, PAR-CLIP and iCLIP are more widely used while eCLIP was less used due to its relatively short history. In this study, we performed HITS-CLIP to identify RBP binding sites.

EMSA

Electrophoretic mobility shift assay (EMSA), or gel shift assay, is a classic in vitro method for detection of RNA-protein interactions. Protein-RNA complexes migrate more slowly than free RNA fragments when subjected to non-denaturing polyacrylamide or agarose gel electrophoresis, so that the protein-RNA complexes are resolved. The complexes are then visualized through the radioactivity of its bound RNAs in autoradiography. It is used to characterize HuR protein's binding specificity to ARE sequences and many target mRNAs including c-fos, Myc, IL3 mRNA (4,62).

RNAcompete and RNA Bind-n-Seq

Both RNAcompete and RNA Bind-n-Seq are in vitro high-throughput RNA-binding assays. In RNAcompete, the RBP of interest is mixed with a large excess of RNA which is prepared by synthesis. The RBPs with bound RNAs are then pulled down by a specific antibody. The bound RNAs are identified by a microarray (63,64). This method was used to build an RBP motif database containing motifs of 205 RBPs from 24 diverse eukaryotes. In chapter 2, I used HuR motifs of humans from this database as the HuR motifs in motif analysis. RNA Bind-n-Seq, or RBNS, is another in vitro binding assay for studying both the sequence and structural specificity of RBPs, with a distinction that the RBP binding RNAs are sequenced by RNA-Seq (65). Through analyzing the binding specificity of 78 human RBPs using RBNS, it was found that motif sequence is not the only characteristic for a RBP binding specificity, the flanking sequences and structures are also important determination factors, which suggests a more intricate rule in RNA-protein interactions (2).

6.2 Methods for determining RNA structure

An *in vivo* click selective 2'-hydroxyl acylation and profiling experiment, or icSHAPE, is a method to determine RNA secondary structure (66). It accurately identifies flexible (single-stranded) bases in RNA by using a probe that can react with the 2' hydroxyl group of free RNA bases. The modified RNAs are then added with biotin, purified and followed by sequencing. Another structure determination method, Psoralen Analysis of RNA Interactions and Structures, or PARIS, can directly identify base-paired helices. The

PARIS method uses the highly specific and reversible nucleic acid crosslinker psoralen-derivative 4'-aminomethyltrioxsalen (AMT) to fix base pairs in helix portion of RNAs, so that the helix can be kept in RNase treatment. The helix is reversed by UV and identified by sequencing (67).

6.3 Methods for modeling protein-RNA complex structure

X-ray crystallography and cryo-electron microscopy (cryo-EM) can reveal structure of protein-RNA complexes and decipher protein-RNA interactions on a structural basis. Currently, crystal structures of HuR binding with RNAs, as well as Argonaute binding with RNAs have been solved (68-70). Cryo-EM has been applied to successfully solve many important ribonucleoprotein (RNP) assemblies, including the spliceosome, ribosome, telomerase, and CRISPR complexes (71-74). Yet, cryo-EM on HuR-RNA complexes or miRISC complexes has not been solved. But those studies are anticipated to reveal mechanisms of the protein-RNA interactions.

7. Study goals and experiment designs

In this dissertation, I present two projects in the following chapter 1 and 2, respectively. In project 1, our goal is to identify interactions between the miRNA machinery and the RNA-binding protein HuR on mRNAs at the transcriptome-wide level, which is studied in two aspects. First, we examine interactions between Ago2 (a core factor in miRNA machinery) and HuR on the same 3'UTRs. HITS-CLIP is utilized to determine HuR and Ago2's occupancies on 3'UTRs. To detect HuR-Ago2 interactions, we perform Ago2

HITS-CLIP using cells in two conditions, control (WT) cells and HuR protein knockdown (KD) cells, and compare the Ago2 mRNA binding levels between the two conditions. Changing of Ago2 binding levels upon HuR KD is caused by a direct HuR effect on Ago2 binding, a secondary effect of HuR KD, or random noise. Here, we specifically examine the direct HuR effect on Ago2 binding, i.e. HuR-Ago2 interactions. Second, we investigate HuR-Ago2 interactions at their overlapping sites. Similar to the first analysis, we compare Ago2 binding levels of WT and HuR KD conditions to detect the global effects of HuR on Ago2 binding levels at the overlapping sites. Additionally, we evaluate their interactions on individual overlapping sites by experiments. We select high-fidelity HuR-Ago2 overlapping sites, and check whether HuR affects miRNA regulation on mRNA. The target sequences are cloned into a luciferase reporter and the activity of the sites are tested in the absence of HuR compared to WT condition. The change of miRNA repression in HuR KO condition is indicative of HuR's interaction with miRNAs at the sites.

In project 2, the goal is to address the identities of three uncharacterized bands (or minor bands) in HuR CLIP through sequence analysis, including annotation breakdowns of reads in HuR CLIP, and motif analysis. The known band with HuR-RNA complex, or major band, is used as a reference in comparison with the minor bands. If the read annotation compositions are similar between these two type of bands, then it suggests an overall reads similarity. Additionally, if HuR motifs are discovered in the CLIP library, it

means that the corresponding band contains abundant HuR binding sequences, and is therefore likely to be a HuR band.

REFERENCES

1. Meisner, N.C. and Filipowicz, W. (2010) Properties of the regulatory RNA-binding protein HuR and its role in controlling miRNA repression. *Adv Exp Med Biol*, **700**, 106-123.

2. Dominguez, D., Freese, P., Alexis, M.S., Su, A., Hochman, M., Palden, T., Bazile, C., Lambert, N.J., Van Nostrand, E.L., Pratt, G.A. *et al.* (2018) Sequence, Structure, and Context Preferences of Human RNA Binding Proteins. *Mol Cell*, **70**, 854-867 e859.

3. Plass, M., Rasmussen, S.H. and Krogh, A. (2017) Highly accessible AU-rich regions in 3' untranslated regions are hotspots for binding of regulatory factors. *PLoS Comput Biol*, **13**, e1005460.

4. Ma, W.J., Cheng, S., Campbell, C., Wright, A. and Furneaux, H. (1996) Cloning and characterization of HuR, a ubiquitously expressed Elav-like protein. *J Biol Chem*, **271**, 8144-8151.

5. Fan, X.C. and Steitz, J.A. (1998) Overexpression of HuR, a nuclear-cytoplasmic shuttling protein, increases the in vivo stability of ARE-containing mRNAs. *EMBO J*, **17**, 3448-3460.

6. Fan, X.C. and Steitz, J.A. (1998) HNS, a nuclear-cytoplasmic shuttling sequence in HuR. *Proc Natl Acad Sci U S A*, **95**, 15293-15298.

7. Wang, J., Guo, Y., Chu, H., Guan, Y., Bi, J. and Wang, B. (2013) Multiple functions of the RNA-binding protein HuR in cancer progression, treatment responses and prognosis. *Int J Mol Sci*, **14**, 10015-10041.

8. Li, Y., Estep, J.A. and Karginov, F.V. (2018) Transcriptome-wide Identification and Validation of Interactions between the miRNA Machinery and HuR on mRNA Targets. *J Mol Biol*, **430**, 285-296.

9. Uren, P.J., Burns, S.C., Ruan, J., Singh, K.K., Smith, A.D. and Penalva, L.O. (2011) Genomic analyses of the RNA-binding protein Hu antigen R (HuR) identify a complex network of target genes and novel characteristics of its binding sites. *J Biol Chem*, **286**, 37063-37066.

10. Mukherjee, N., Corcoran, D.L., Nusbaum, J.D., Reid, D.W., Georgiev, S., Hafner, M., Ascano, M., Jr., Tuschl, T., Ohler, U. and Keene, J.D. (2011) Integrative regulatory mapping indicates that the RNA-binding protein HuR couples pre-mRNA processing and mRNA stability. *Mol Cell*, **43**, 327-339.

11. Lebedeva, S., Jens, M., Theil, K., Schwanhausser, B., Selbach, M., Landthaler, M. and Rajewsky, N. (2011) Transcriptome-wide analysis of regulatory interactions of the RNA-binding protein HuR. *Mol Cell*, **43**, 340-352.

12. Peng, S.S., Chen, C.Y., Xu, N. and Shyu, A.B. (1998) RNA stabilization by the AU-rich element binding protein, HuR, an ELAV protein. *EMBO J*, **17**, 3461-3470.

13. Raghavan, A., Robison, R.L., McNabb, J., Miller, C.R., Williams, D.A. and Bohjanen, P.R. (2001) HuA and tristetraprolin are induced following T cell activation and display distinct but overlapping RNA binding specificities. *The Journal of biological chemistry*, **276**, 47958-47965.

14. Ming, X.F., Stoecklin, G., Lu, M., Looser, R. and Moroni, C. (2001) Parallel and independent regulation of interleukin-3 mRNA turnover by phosphatidylinositol 3-kinase and p38 mitogen-activated protein kinase. *Mol Cell Biol*, **21**, 5778-5789.

15. Wang, W., Caldwell, M.C., Lin, S., Furneaux, H. and Gorospe, M. (2000) HuR regulates cyclin A and cyclin B1 mRNA stability during cell proliferation. *Embo j*, **19**, 2340-2350.

16. Srikantan, S. and Gorospe, M. (2012) HuR function in disease. *Front Biosci (Landmark Ed)*, **17**, 189-205.

17. Galban, S., Kuwano, Y., Pullmann, R., Jr., Martindale, J.L., Kim, H.H., Lal, A., Abdelmohsen, K., Yang, X., Dang, Y., Liu, J.O. *et al.* (2008) RNA-binding proteins HuR and PTB promote the translation of hypoxia-inducible factor 1alpha. *Mol Cell Biol*, **28**, 93-107.

18. Levy, N.S., Chung, S., Furneaux, H. and Levy, A.P. (1998) Hypoxic stabilization of vascular endothelial growth factor mRNA by the RNA-binding protein HuR. *J Biol Chem*, **273**, 6417-6423.

19. Dixon, D.A., Tolley, N.D., King, P.H., Nabors, L.B., McIntyre, T.M., Zimmerman, G.A. and Prescott, S.M. (2001) Altered expression of the mRNA stability factor HuR promotes cyclooxygenase-2 expression in colon cancer cells. *J Clin Invest*, **108**, 1657-1665.

20. Yoo, P.S., Sullivan, C.A., Kiang, S., Gao, W., Uchio, E.M., Chung, G.G. and Cha, C.H. (2009) Tissue microarray analysis of 560 patients with colorectal adenocarcinoma: high expression of HuR predicts poor survival. *Ann Surg Oncol*, **16**, 200-207.

21. Ortega, A.D., Sala, S., Espinosa, E., Gonzalez-Baron, M. and Cuezva, J.M. (2008) HuR and the bioenergetic signature of breast cancer: a low tumor expression of

the RNA-binding protein predicts a higher risk of disease recurrence. *Carcinogenesis*, **29**, 2053-2061.

22. Bartel, D.P. (2009) MicroRNAs: target recognition and regulatory functions. *Cell*, **136**, 215-233.

23. Friedman, R.C., Farh, K.K., Burge, C.B. and Bartel, D.P. (2009) Most mammalian mRNAs are conserved targets of microRNAs. *Genome Res*, **19**, 92-105.

24. Liu, J., Carmell, M.A., Rivas, F.V., Marsden, C.G., Thomson, J.M., Song, J.J., Hammond, S.M., Joshua-Tor, L. and Hannon, G.J. (2004) Argonaute2 is the catalytic engine of mammalian RNAi. *Science*, **305**, 1437-1441.

25. Meister, G., Landthaler, M., Patkaniowska, A., Dorsett, Y., Teng, G. and Tuschl, T. (2004) Human Argonaute2 mediates RNA cleavage targeted by miRNAs and siRNAs. *Mol Cell*, **15**, 185-197.

26. Petri, S., Dueck, A., Lehmann, G., Putz, N., Rudel, S., Kremmer, E. and Meister, G. (2011) Increased siRNA duplex stability correlates with reduced off-target and elevated on-target effects. *RNA*, **17**, 737-749.

27. Wang, D., Zhang, Z., O'Loughlin, E., Lee, T., Houel, S., O'Carroll, D., Tarakhovsky, A., Ahn, N.G. and Yi, R. (2012) Quantitative functions of Argonaute proteins in mammalian development. *Genes Dev*, **26**, 693-704.

28. Hafner, M., Landthaler, M., Burger, L., Khorshid, M., Hausser, J., Berninger, P., Rothballer, A., Ascano, M., Jr., Jungkamp, A.C., Munschauer, M. *et al.* (2010) Transcriptome-wide identification of RNA-binding protein and microRNA target sites by PAR-CLIP. *Cell*, **141**, 129-141.

29. Behm-Ansmant, I., Rehwinkel, J., Doerks, T., Stark, A., Bork, P. and Izaurralde, E. (2006) mRNA degradation by miRNAs and GW182 requires both CCR4:NOT deadenylase and DCP1:DCP2 decapping complexes. *Genes Dev*, **20**, 1885-1898.

30. Rehwinkel, J., Behm-Ansmant, I., Gatfield, D. and Izaurralde, E. (2005) A crucial role for GW182 and the DCP1:DCP2 decapping complex in miRNA-mediated gene silencing. *RNA*, **11**, 1640-1647.

31. Eulalio, A., Rehwinkel, J., Stricker, M., Huntzinger, E., Yang, S.F., Doerks, T., Dorner, S., Bork, P., Boutros, M. and Izaurralde, E. (2007) Target-specific requirements for enhancers of decapping in miRNA-mediated gene silencing. *Genes Dev*, **21**, 2558-2570.

32. Braun, J.E., Truffault, V., Boland, A., Huntzinger, E., Chang, C.T., Haas, G., Weichenrieder, O., Coles, M. and Izaurralde, E. (2012) A direct interaction between DCP1 and XRN1 couples mRNA decapping to 5' exonucleolytic degradation. *Nat Struct Mol Biol*, **19**, 1324-1331.

33. Lim, J., Ha, M., Chang, H., Kwon, S.C., Simanshu, D.K., Patel, D.J. and Kim, V.N. (2014) Uridylation by TUT4 and TUT7 marks mRNA for degradation. *Cell*, **159**, 1365-1376.

34. Iwakawa, H.O. and Tomari, Y. (2015) The Functions of MicroRNAs: mRNA Decay and Translational Repression. *Trends Cell Biol*, **25**, 651-665.

35. Guo, H., Ingolia, N.T., Weissman, J.S. and Bartel, D.P. (2010) Mammalian microRNAs predominantly act to decrease target mRNA levels. *Nature*, **466**, 835-840.

36. Rupaimoole, R. and Slack, F.J. (2017) MicroRNA therapeutics: towards a new era for the management of cancer and other diseases. *Nat Rev Drug Discov*, **16**, 203-222.

37. Mukherjee, N., Lager, P.J., Friedersdorf, M.B., Thompson, M.A. and Keene, J.D. (2009) Coordinated posttranscriptional mRNA population dynamics during T-cell activation. *Mol Syst Biol*, **5**, 288.

38. Bhattacharyya, S.N., Habermacher, R., Martine, U., Closs, E.I. and Filipowicz, W. (2006) Relief of microRNA-mediated translational repression in human cells subjected to stress. *Cell*, **125**, 1111-1124.

39. Ahuja, D., Goyal, A. and Ray, P.S. (2016) Interplay between RNA-binding protein HuR and microRNA-125b regulates p53 mRNA translation in response to genotoxic stress. *RNA Biol*, **13**, 1152-1165.

40. Srikantan, S., Abdelmohsen, K., Lee, E.K., Tominaga, K., Subaran, S.S., Kuwano, Y., Kulshrestha, R., Panchakshari, R., Kim, H.H., Yang, X. *et al.* (2011) Translational control of TOP2A influences doxorubicin efficacy. *Mol Cell Biol*, **31**, 3790-3801.

41. Tan, S., Ding, K., Chong, Q.Y., Zhao, J., Liu, Y., Shao, Y., Zhang, Y., Yu, Q., Xiong, Z., Zhang, W. *et al.* (2017) Post-transcriptional regulation of ERBB2 by miR26a/b and HuR confers resistance to tamoxifen in estrogen receptor-positive breast cancer cells. *The Journal of biological chemistry*, **292**, 13551-13564.

42. Li, C., Jiang, J.Y., Wang, J.M., Sun, J., An, M.X., Li, S., Yan, J. and Wang, H.Q. (2018) BAG3 regulates stability of IL-8 mRNA via interplay between HuR and miR-4312 in PDACs. *Cell death & disease*, **9**, 863.

43. Kim, H.H., Kuwano, Y., Srikantan, S., Lee, E.K., Martindale, J.L. and Gorospe, M. (2009) HuR recruits let-7/RISC to repress c-Myc expression. *Genes Dev*, **23**, 1743-1748.

44. Gunzburg, M.J., Sivakumaran, A., Pendini, N.R., Yoon, J.H., Gorospe, M., Wilce, M.C. and Wilce, J.A. (2015) Cooperative interplay of let-7 mimic and HuR with MYC RNA. *Cell Cycle*, **14**, 2729-2733.

45. Thorne, J.L., Battaglia, S., Baxter, D.E., Hayes, J.L., Hutchinson, S.A., Jana, S., Millican-Slater, R.A., Smith, L., Teske, M.C., Wastall, L.M. *et al.* (2018) MiR-19b non-canonical binding is directed by HuR and confers chemosensitivity through regulation of P-glycoprotein in breast cancer. *Biochimica et biophysica acta. Gene regulatory mechanisms*, **1861**, 996-1006.

46. Glorian, V., Maillot, G., Poles, S., Iacovoni, J.S., Favre, G. and Vagner, S. (2011) HuR-dependent loading of miRNA RISC to the mRNA encoding the Ras-related small GTPase RhoB controls its translation during UV-induced apoptosis. *Cell Death Differ*, **18**, 1692-1701.

47. Del Vecchio, G., De Vito, F., Saunders, S.J., Risi, A., Mannironi, C., Bozzoni, I. and Presutti, C. (2016) RNA-binding protein HuR and the members of the miR-200 family play an unconventional role in the regulation of c-Jun mRNA. *Rna*, **22**, 1510-1521.

48. Zhuang, R., Rao, J.N., Zou, T., Liu, L., Xiao, L., Cao, S., Hansraj, N.Z., Gorospe, M. and Wang, J.Y. (2013) miR-195 competes with HuR to modulate stim1 mRNA stability and regulate cell migration. *Nucleic Acids Res*, **41**, 7905-7919.

49. Kundu, P., Fabian, M.R., Sonenberg, N., Bhattacharyya, S.N. and Filipowicz, W. (2012) HuR protein attenuates miRNA-mediated repression by promoting miRISC dissociation from the target RNA. *Nucleic Acids Res*, **40**, 5088-5100.

50. HafezQorani, S., Lafzi, A., de Bruin, R.G., van Zonneveld, A.J., van der Veer, E.P., Son, Y.A. and Kazan, H. (2016) Modeling the combined effect of RNA-binding proteins and microRNAs in post-transcriptional regulation. *Nucleic Acids Res*, **44**, e83.

51. Shwetha, S., Sharma, G., Raheja, H., Goel, A., Aggarwal, R. and Das, S. (2018) Interaction of miR-125b-5p with Human antigen R mRNA: Mechanism of controlling HCV replication. *Virus Res*, **258**, 1-8.

52. Liu, Y., Chen, X., Cheng, R., Yang, F., Yu, M., Wang, C., Cui, S., Hong, Y., Liang, H., Liu, M. *et al.* (2018) The Jun/miR-22/HuR regulatory axis contributes to tumourigenesis in colorectal cancer. *Molecular cancer*, **17**, 11.

53. Liu, H., Song, X., Hou, J., Zhao, Z. and Chang, J. (2018) Posttranscriptional Regulation of Human Antigen R by miR-133b Enhances Docetaxel Cytotoxicity Through the Inhibition of ATP-Binding Cassette Subfamily G Member 2 in Prostate Cancer Cells. *DNA and cell biology*, **37**, 210-219.

54. House, R., Majumder, M., Janakiraman, H., Ogretmen, B., Kato, M., Erkul, E., Hill, E., Atkinson, C., Barth, J., Day, T.A. *et al.* (2018) Smoking-induced control of miR-133a-3p alters the expression of EGFR and HuR in HPV-infected oropharyngeal cancer. *PLoS One*, **13**, e0205077.

55. Al-Haidari, A., Algaber, A., Madhi, R., Syk, I. and Thorlacius, H. (2018) MiR-155-5p controls colon cancer cell migration via post-transcriptional regulation of Human Antigen R (HuR). *Cancer letters*, **421**, 145-151.

56. Song, Y., Feng, W., Shi, G.M., Chen, C. and Zhang, Y.Y. (2018) RNA-binding protein HuR regulates hsa-let-7c expression by its RNA recognition motif. *Sheng Li Xue Bao*, **70**, 1-8.

57. Chen, J., Martindale, J.L., Cramer, C., Gorospe, M., Atasoy, U., Drew, P.D. and Yu, S. (2017) The RNA-binding protein HuR contributes to neuroinflammation by promoting C-C chemokine receptor 6 (CCR6) expression on Th17 cells. *The Journal of biological chemistry*, **292**, 14532-14543.

58. Chen, J., Adamiak, W., Huang, G., Atasoy, U., Rostami, A. and Yu, S. (2017) Interaction of RNA-binding protein HuR and miR-466i regulates GM-CSF expression. *Scientific reports*, **7**, 17233.

59. Licatalosi, D.D., Mele, A., Fak, J.J., Ule, J., Kayikci, M., Chi, S.W., Clark, T.A., Schweitzer, A.C., Blume, J.E., Wang, X. *et al.* (2008) HITS-CLIP yields genome-wide insights into brain alternative RNA processing. *Nature*, **456**, 464-469.

60. Konig, J., Zarnack, K., Rot, G., Curk, T., Kayikci, M., Zupan, B., Turner, D.J., Luscombe, N.M. and Ule, J. (2010) iCLIP reveals the function of hnRNP particles in splicing at individual nucleotide resolution. *Nat Struct Mol Biol*, **17**, 909-915.

61. Van Nostrand, E.L., Pratt, G.A., Shishkin, A.A., Gelboin-Burkhart, C., Fang, M.Y., Sundararaman, B., Blue, S.M., Nguyen, T.B., Surka, C., Elkins, K. *et al.* (2016) Robust transcriptome-wide discovery of RNA-binding protein binding sites with enhanced CLIP (eCLIP). *Nat Methods*, **13**, 508-514.

62. Myer, V.E., Fan, X.C. and Steitz, J.A. (1997) Identification of HuR as a protein implicated in AUUUA-mediated mRNA decay. *EMBO J*, **16**, 2130-2139.

63. Ray, D., Kazan, H., Chan, E.T., Pena Castillo, L., Chaudhry, S., Talukder, S., Blencowe, B.J., Morris, Q. and Hughes, T.R. (2009) Rapid and systematic

analysis of the RNA recognition specificities of RNA-binding proteins. *Nat Biotechnol*, **27**, 667-670.

64. Ray, D., Kazan, H., Cook, K.B., Weirauch, M.T., Najafabadi, H.S., Li, X., Gueroussov, S., Albu, M., Zheng, H., Yang, A. *et al.* (2013) A compendium of RNA-binding motifs for decoding gene regulation. *Nature*, **499**, 172-177.

65. Lambert, N., Robertson, A., Jangi, M., McGeary, S., Sharp, P.A. and Burge, C.B. (2014) RNA Bind-n-Seq: quantitative assessment of the sequence and structural binding specificity of RNA binding proteins. *Mol Cell*, **54**, 887-900.

66. Spitale, R.C., Flynn, R.A., Zhang, Q.C., Crisalli, P., Lee, B., Jung, J.W., Kuchelmeister, H.Y., Batista, P.J., Torre, E.A., Kool, E.T. *et al.* (2015) Structural imprints in vivo decode RNA regulatory mechanisms. *Nature*, **519**, 486-490.

67. Lu, Z., Zhang, Q.C., Lee, B., Flynn, R.A., Smith, M.A., Robinson, J.T., Davidovich, C., Gooding, A.R., Goodrich, K.J., Mattick, J.S. *et al.* (2016) RNA Duplex Map in Living Cells Reveals Higher-Order Transcriptome Structure. *Cell*, **165**, 1267-1279.

68. Wang, H., Zeng, F., Liu, Q., Liu, H., Liu, Z., Niu, L., Teng, M. and Li, X. (2013) The structure of the ARE-binding domains of Hu antigen R (HuR) undergoes conformational changes during RNA binding. *Acta Crystallogr D Biol Crystallogr*, **69**, 373-380.

69. Wang, Y., Juranek, S., Li, H., Sheng, G., Tuschl, T. and Patel, D.J. (2008) Structure of an argonaute silencing complex with a seed-containing guide DNA and target RNA duplex. *Nature*, **456**, 921-926.

70. Chi, S.W., Zang, J.B., Mele, A. and Darnell, R.B. (2009) Argonaute HITS-CLIP decodes microRNA-mRNA interaction maps. *Nature*, **460**, 479-486.

71. Fica, S.M. and Nagai, K. (2017) Cryo-electron microscopy snapshots of the spliceosome: structural insights into a dynamic ribonucleoprotein machine. *Nat Struct Mol Biol*, **24**, 791-799.

72. Feigon, J., Chan, H. and Jiang, J. (2016) Integrative structural biology of Tetrahymena telomerase - insights into catalytic mechanism and interaction at telomeres. *FEBS J*, **283**, 2044-2050.

73. Jiang, F. and Doudna, J.A. (2015) The structural biology of CRISPR-Cas systems. *Curr Opin Struct Biol*, **30**, 100-111.

74. von Loeffelholz, O., Natchiar, S.K., Djabeur, N., Myasnikov, A.G., Kratzat, H., Menetret, J.F., Hazemann, I. and Klaholz, B.P. (2017) Focused classification and

refinement in high-resolution cryo-EM structural analysis of ribosome complexes. *Curr Opin Struct Biol*, **46**, 140-148.

CHAPTER 1

Transcriptome-wide Identification and Validation of Interactions between the miRNA Machinery and HuR on mRNA Targets

ABSTRACT

The 3′ UTR of mRNAs is the primary regulatory region that mediates post-transcriptional control by microRNAs and RNA-binding proteins (RBPs) in the cytoplasm. Aside from individual sequence-specific binding and regulation, examples of interaction between these factors at particular 3′ UTR sites have emerged. However, the whole picture of such higher-order regulatory modules across the transcriptome is lacking. Here, we investigate the interactions between HuR, a ubiquitous RBP, and Ago2, a core effector of the miRNA pathway, at the transcriptome-wide level. Using HITS-CLIP, we map HuR and miRNA binding sites on human 3′ UTRs and assess their co-occurrence. Additionally, we demonstrate global effects of HuR knockdown on Ago2 occupancy, suggesting a co-regulatory relationship. Focusing on sites of Ago2-HuR overlap, 13 candidates were screened in luciferase reporter assays. Eleven sites showed miRNA-dependent repression, as confirmed in Dicer-null cells. To test for HuR's role in co-regulation, we measured the reporters in HuR KO cells. Three of the miRNA sites demonstrated altered activities, indicating that HuR has an effect on miRNA repression at those sites. Our study presents an efficient search and validation system for studying miRNA-HuR interactions, which

expands our understanding of the combinatorial post-transcriptional control of gene expression at the 3′ UTR.

INTRODUCTION

The cellular regulatory networks that establish protein levels employ post-transcriptional control to a great extent and in various contexts (1,2). Since joint transcriptome and proteome measurements detect poor mRNA-protein level correlations at steady state (3,4), a significant, albeit variably estimated, effect is attributed to post-transcriptional regulation (5,6). Even more important in cells that are undergoing a transition, translational control contributes strongly to changes in protein levels upon differentiation (7), in development (8), throughout the cell and circadian cycles (9,10), and during ER stress (11). Studies of differential expression across individuals in a population, integrated with genomics, indicate that quantitative trait loci associated with protein abundance variability are largely distinct from those that explain mRNA differences, again suggesting additional layers of control (3,4,12,13). Furthermore, inter-species comparisons show that the levels of orthologous mRNAs vary more than their ribosomal occupancies or corresponding protein abundances, indicating that processes acting at the mRNA level buffer their variability (14-18). Thus, post-transcriptional control acts at steady cellular states as well as rapid and/or reversible cellular transitions, and may allow for evolutionary flexibility in transcriptional circuits.

Comparable in complexity to transcriptional regulation, mRNA control in mammalian cells is mediated by approximately 1500 RNA-binding proteins (RBPs) (19) and several hundred microRNAs (miRNAs) (20,21), and is primarily thought to involve sequence- or

structure-specific RBP binding at defined sites on the mRNA, often the 3′ UTR. miRNAs are a class of ~22 nt regulatory noncoding RNAs that associate with and guide Argonaute (Ago) proteins to repress target mRNAs through imperfect complementarity. The four human Ago homologs, Ago1-Ago4, bind to similar miRNA and mRNA pools, with Ago2 being the most studied (22-25). Among the RBPs, HuR/ELAVL1 is a ubiquitously expressed protein that binds to AU-rich element (ARE)-containing transcripts, mainly with a stabilizing role (reviewed in 26). HuR is involved in many cellular processes including cell proliferation, apoptosis, angiogenesis, and immunity (27,28).

As in transcription (29), combinatorial control by interactions between bound RBPs has emerged as a flexible and powerful model, which enables more precise targeting specificity and spatiotemporal resolution. However, less is known about the specifics and principles of such RBP interactions. Several individually characterized cases, often involving RBPs and miRNAs, (reviewed in 30,31,32), demonstrate or postulate a number of cooperative and antagonistic interaction modes, including direct steric hindrance or long-distance interactions, as well as RNA structure-mediated effects on each other's binding and activity. For example, HuR antagonizes miR-122-mediated repression of the CAT-1 mRNA in human hepatocarcinoma cells under stress (33,34). In a cooperative interaction, Pum1 binding on the 3′ UTR of p27 mRNA elevates miR221/222 accessibility, causing more Ago/miRNA-mediated repression (35).

In addition to individual cases, analysis of transcriptome-wide datasets provides evidence for RBP-miRNA interactions (36,37). Studies show an enrichment of specific AU-rich motifs in miRNA-targeted 3′ UTRs, suggesting co-regulation by additional RBPs (38,39). Conversely, predicted miRNA sites are enriched in 3′ UTRs targeted by the Pum RBPs (40) and near Pum and UAUUUAU motifs, where they impact mRNA stability (41). With the more precise identification of RBP binding site locations by CLIP-seq, proximity of HuR/ELAVL1 sites to predicted miRNA seeds (42), as well as overlap with Ago binding sites and its antagonistic effects on mRNA target levels, has been observed (43). However, transcriptome-wide effects of an RBP directly on the binding of another have not been demonstrated.

In the current study, we investigate the types and the extent of interactions between HuR and Ago2 (representing miRNA regulation) at the binding level, assessing their effect on each other's occupancy, and identify antagonistic as well as cooperative interaction signals. Furthermore, we carry out a panel of validation assays for overlapping interactions and demonstrate the occurrence of both interaction modes at specific mRNA sites.

RESULTS

Interactions between Ago2 and HuR sites on the same 3′ UTR

To globally and quantitatively assess the potential interactions between Ago2 and HuR on target mRNAs, we set out to determine their binding site locations by HITS-CLIP and to examine the cross-dependence of their occupancies. Reasoning that manipulation of HuR levels would affect Ago2 binding at interacting sites, we performed Ago2 CLIP in T-REx-293 cells under conditions of HuR depletion with two distinct siRNAs, compared to control knockdowns. HuR levels were reduced to an average of 14% and 15% among the five replicates for the two siRNAs, respectively (Figure 1.1A). Sequenced reads mapping to mRNA 3′ UTRs were collapsed into discrete, contiguous clusters (peaks), quantified by the count of uniquely barcoded 5′ ligation events in the CLIP procedure, and filtered for abundance and lack of siRNA complementarity, yielding 5045 sites, 4699 of which occurred on mRNAs with previously available abundance data (44), with a median length of 44nt (Figure 1.1C). The identified Ago2 binding sites showed enrichment for abundant miRNA seed complements (Figure 1.1B), confirming the specificity of the procedure. Changes in CLIP signal upon HuR KD for each peak were determined by DESeq2 (45).

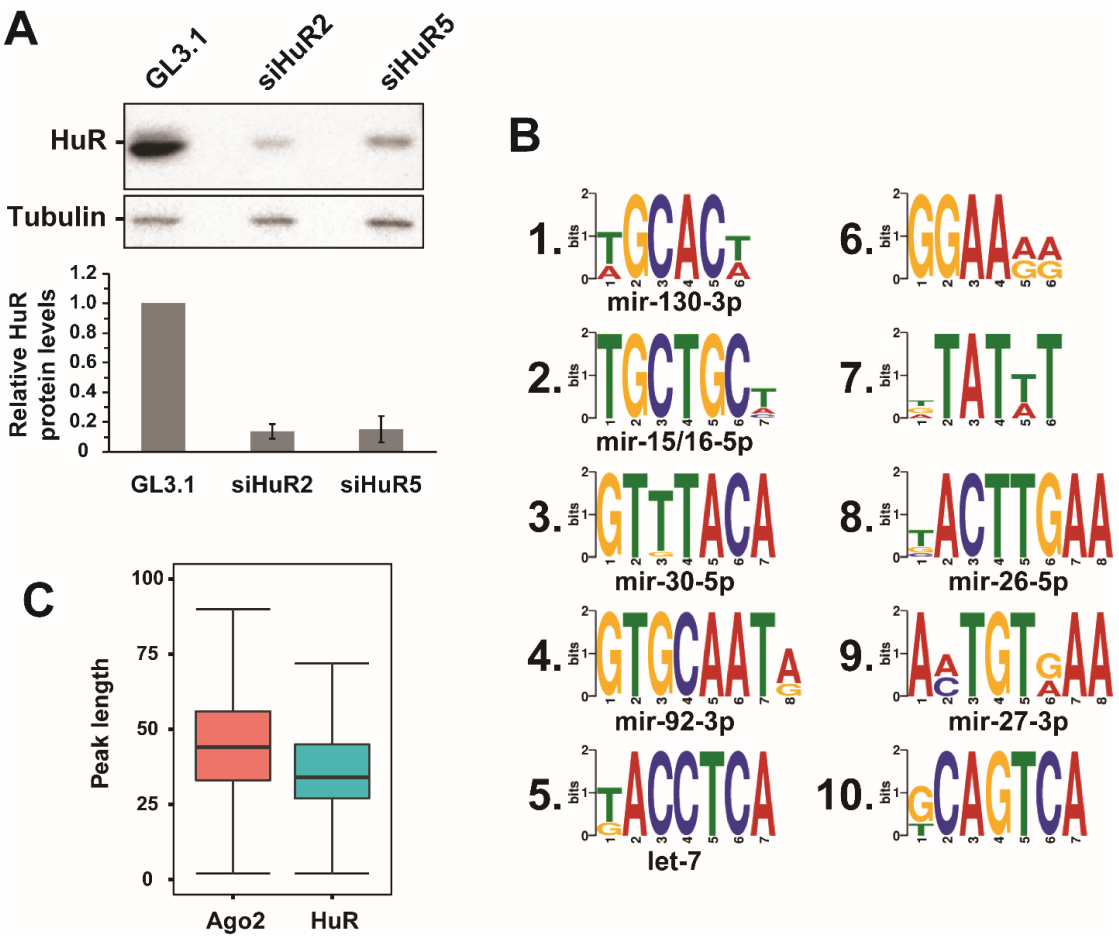

Figure 1.1. Ago2 CLIP-Seq characteristics.

A) Successful knockdown of HuR assayed by Western blot. HuR protein was knocked down by transfection of two HuR siRNAs, siHuR2 and siHuR5, in parallel. GL3.1 is a negative control siRNA targeting the firefly luciferase gene. (Bottom) Quantification of HuR protein levels from 5 replicates, normalized to tubulin and HuR levels in the GL3.1 control transfection. B) Top 10 sequence motifs enriched in Ago2 CLIP sites, determined by DREME with a minimal 6-mer motif, contain seed site complements to many abundant miRNA families. C) Boxplot of Ago2 and HuR peak length distributions.

Reciprocally, HuR CLIP was performed in triplicate under conditions where miRNA-dependent Ago binding to mRNAs was eliminated, along with WT controls. To this end, and to overcome the redundancy of the 4 mammalian Ago paralogs, we took advantage

of two 293T-derived Dicer-deficient cell lines generated by the Cullen lab (46). A robust population of HuR-bound RNA fragments was identified and excised (Figure 1.2A). Filtering for abundance, 3′ UTR mapping and intersection with RNA-seq data resulted in 2810 HuR sites, with a median length of 34 nt (Figure 1.1C). To verify the specificity of the CLIP, we computed the enrichment of all possible 6-mers in the site sequences relative to randomly sampled peaks of the same length from the same UTRs. The top 6-mers contained U-rich sequences (Figure 1.2B), consistent with previous studies (42,47-49).

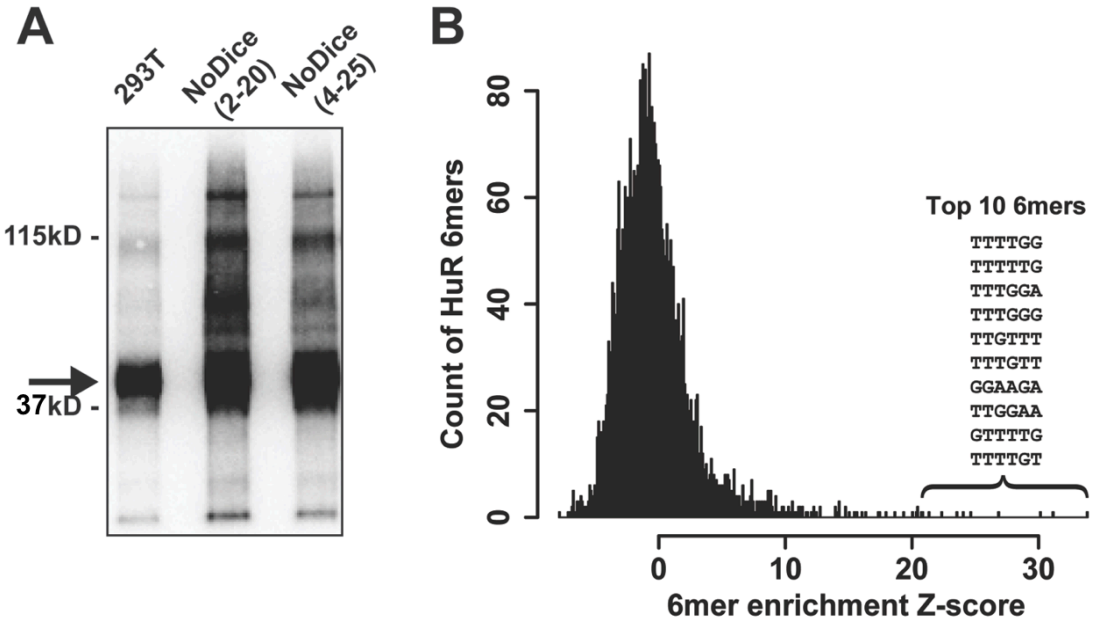

Figure 1.2. HuR CLIP-Seq characteristics.

A) HuR-RNA crosslinked complex (after labeled 3′ linker ligation), resolved on an SDS NuPAGE gel and transferred to nitrocellulose during the CLIP procedure. Dicer KO, miRNA-deficient NoDice 2-20 and 4-25 cell lines and 293T control cells were used. B) A histogram of enrichment z-scores for all possible 6mers in HuR CLIP sites. Sequences of the top 10 6mers are shown.

Ago2 and HuR were found to bind large groups of mRNAs and to co-occupy 3′ UTRs often, consistent with previous observations (43). Initially, we aimed to identify any signatures of interactions between the two RBPs on the same transcript. Considering only the longest 3′ UTR of each gene, 2653 transcripts contained Ago2 CLIP sites, and 1366 transcripts harbored HuR CLIP sites at the applied abundance cutoffs. Among them, 788 transcripts contained both Ago2 and HuR sites (Figure 1.3A). Furthermore, 56% of the 788 3′ UTRs had more than one Ago2 site, and 45% had multiple HuR sites, allowing for several combinations of interactions (Figure 1.4). To limit these combinations, we hypothesized that when multiple sites occur on the same UTR, the Ago2 peaks that show the largest shifts in occupancy (minimal and maximal log fold change, LFC) in response to HuR KD are the most likely candidates for interaction with HuR, and these sites were selected for analysis. In this model, Ago2 sites that weaken upon HuK KD represent potential cooperative interactions, and sites that strengthen suggest an antagonistic relationship (Figure 1.3B). To isolate the direct effects of HuR on such Ago2 sites, all Ago2-bound transcripts were divided into two groups: those that have HuR sites (and could potentially interact), and those that do not have HuR sites and therefore serve as non-interacting, background controls. Since changes in mRNA levels upon HuR KD can themselves contribute to the observed Ago2 CLIP signal LFC, the LFC values were normalized to the mRNA changes derived from (43).

Selecting the Ago2 site with the minimal LFC in occupancy upon HuR KD for each 3′ UTR, we examined their cumulative distributions in the two groups (Figure 1.3C). The Ago2 sites from HuR-bound transcripts showed significantly lower LFCs than the control non-interacting group (p-value=1.77×10^{-8}, Kolmogorov-Smirnov (KS) test). Thus, the presence of HuR on a 3′ UTR corresponds with more dissociation of Ago2 upon HuR KD (compared to Ago2 site behavior on HuR-free UTRs), consistent with a direct HuR-Ago2 interaction. For this class of sites, the loss of Ago2 binding upon HuR KD implies an enrichment of cooperative HuR-Ago2 interactions. Conversely, when examining the Ago2 sites with the maximal LFC from each UTR, HuR-bound transcripts exhibited significantly higher LFCs than unbound transcripts (Figure 1.3D, p-value=1.64×10^{-3}, KS test). In other words, presence of HuR on the UTR corresponds with increased Ago2 binding upon HuR KD (compared to Ago2 site behavior on HuR-free UTRs), suggesting that antagonistic interactions are enriched in this group of Ago2 sites.

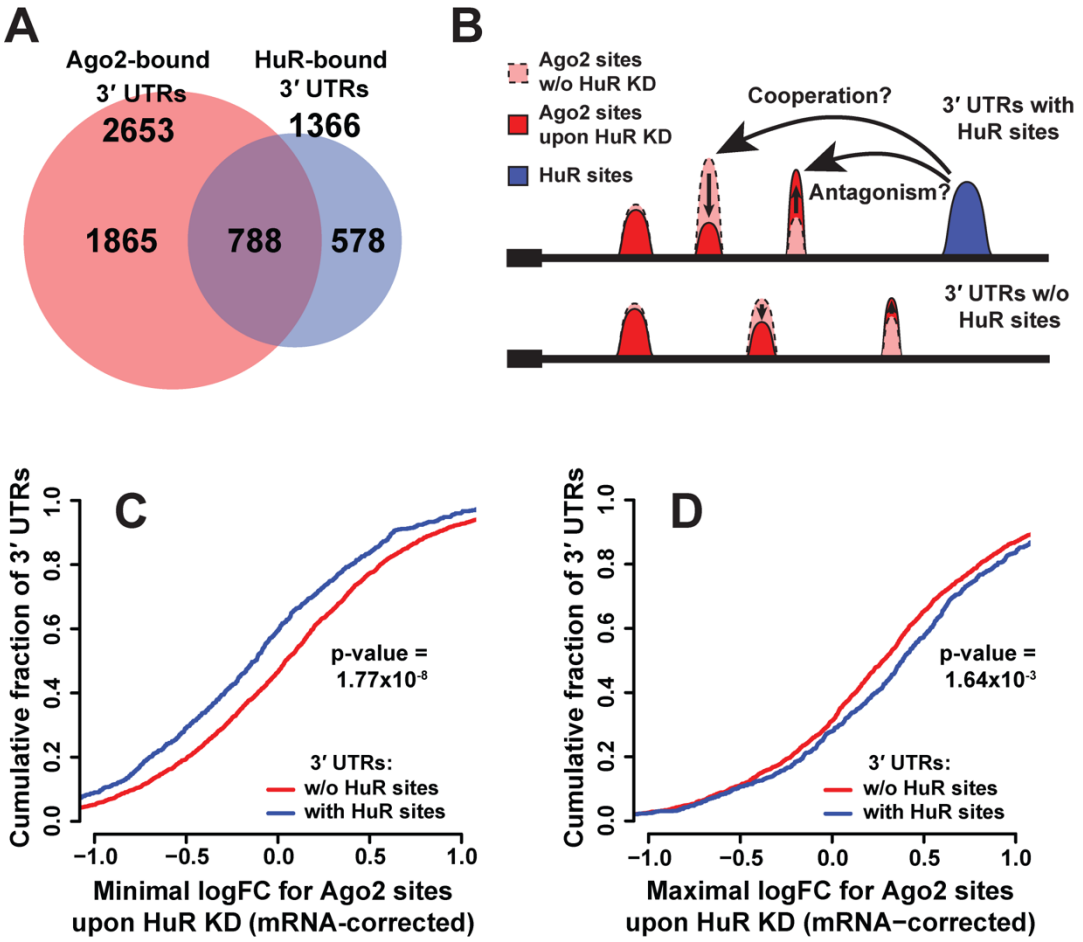

Figure 1.3. CLIP-Seq analysis of HuR-Ago2 interactions on the same 3′ UTR.

A) Number of transcript 3′ UTRs that are bound by Ago2, HuR, or both. B) A schematic of the potential cooperative and antagonistic effects of HuR presence on Ago2 site occupancy on the same 3′ UTR. Ago2 sites with minimal and maximal log fold change (logFC) upon HuR KD on each 3′ UTR are examined for HuR-Ago2 interactions. C, D) Cumulative fraction plots of the minimal (C) and maximal (D) logFC of Ago2 sites upon HuR KD on 3′ UTRs with and without HuR sites. Ago2 site CLIP signal was normalized to changes in mRNA levels upon HuR KD.

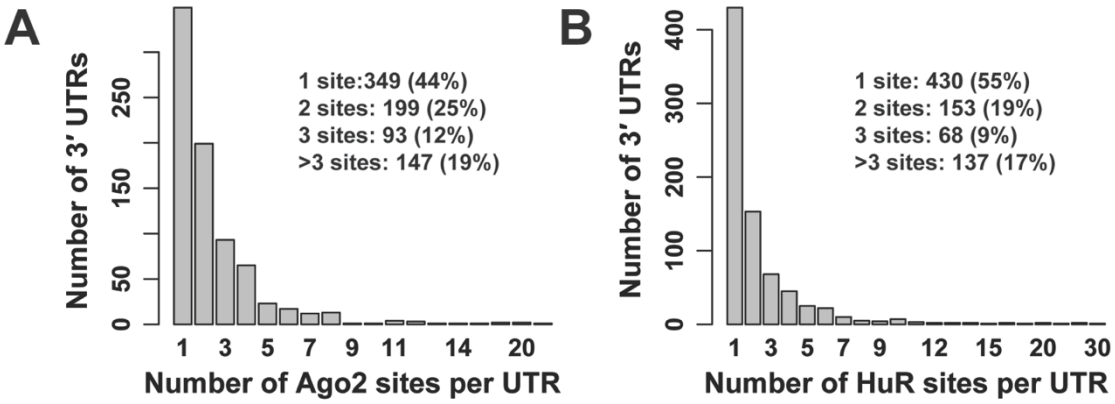

Figure 1.4. Number of CLIP sites on 3′ UTRs that have both Ago2 and HuR sites. A) Histogram of the number of Ago2 sites. B) Histogram of the number of HuR sites.

As an alternative to mRNA LFC normalization, we assayed whether the observed effects may be attributed to mRNA level changes by comparing the sum (as opposed to min or max) of LFCs for all Ago2 sites on a 3′ UTR between HuR-bound and unbound transcripts. Here, individual interactions between Ago2 and HuR would be expected to contribute less, and the mRNA level effects of HuR KD would be reflected in the sum of LFC. No statistically significant difference between the cumulative distributions was observed (p-value=0.1089, Appendix B-Supplementary Figure S1.1C). In comparison, the Ago2 minimal and maximal LFC without mRNA LFC normalization still showed differences between HuR-bound and unbound groups (p-values<0.05, Appendix B-Supplementary Figure S1.1A, B). In summary, the available CLIP data indicates that HuR cooperates and antagonizes Ago2 sites on the same transcript by affecting Ago2 binding.

To see whether Ago2 sites reciprocally impact HuR binding on the same 3′ UTR, we examined if there is a relationship between changes in Ago2 peak occupancy upon HuR KD and corresponding changes for HuR peaks upon Dicer loss. Again, the most responsive sites were hypothesized to be more likely to interact. A positive correlation between the maximal LFCs for Ago2 and HuR sites on the same 3′ UTR (correlation coefficient=0.0923, p-value=0.00954) was observed, suggesting an interaction in the binding behavior at these sites. A z-score of 2.54 based on correlations of permuted Ago2-HuR LFC pairs was calculated. Furthermore, no correlation between the sums of LFCs was observed (correlation coefficient=-0.00463, p-value=0.897), indicating that mRNA level effects are unlikely to strongly contribute to the effect. While a positive correlation in this analysis is consistent with both cooperative and antagonistic interactions, the selection of maximal (mostly positive) LFCs proposes predominantly the latter.

Interactions between Ago2 and HuR peaks on Ago2-HuR overlapping sites

In addition to analysis of interactions between Ago2 and HuR anywhere on the 3′ UTR, we examined the co-localization of their binding sites and potential interactions at such loci. Among the 4699 Ago2 peaks identified by CLIP, 482 sites overlapped with HuR sites (Figure 1.5A). Similarly, 502 of 2810 HuR peaks co-localized with Ago2 peaks (in a few cases, a single Ago2 site overlapped two HuR sites, and vice versa). From the aggregate frequency of HuR sites as a function of distance from Ago2 sites (Figure 1.5D), it is evident that such co-localized, joint binding of Ago2 and HuR occurs preferentially,

significantly more so than in controls where HuR positions were randomized on the 3′ UTR. To determine whether the overlapping peaks were genuine binding sites or resulted from cross-linking hotspots or experimental artefacts, we compared motif enrichment and signal strength properties between overlapping and non-overlapping sites. The density of TargetScan7-predicted miRNA sites (an independent measure of Ago2 CLIP validity) (50) in the vicinity of HuR-overlapping and -nonoverlapping Ago2 sites was nearly identical (Figure 1.5B), with 46% vs 45% of Ago2 sites containing seed predictions in the two categories (Figure 1.6B). Similarly, the identified top 10 HuR 6-mers were positionally enriched at both Ago2-overlapping and non-overlapping peaks (Figure 1.5C). Furthermore, the strength of CLIP signal, normalized to mRNA abundance, was very similar between the two groups, both for Ago2 and HuR sites (Figure 1.6A). Thus, Ago2 and HuR sites evolved to co-occur at specific positions with the characteristics of bona fide binding events, suggesting an interaction between the two factors at these locations. To assess the extent of interaction at overlapping sites, we compared the changes in occupancy upon HuR KD for HuR-overlapping vs. non-overlapping Ago2 sites. While the raw LFCs showed a statistically significant difference (Figure 1.6C, $p=0.0148$, KS test), normalization to changes in mRNA levels reduced the effect below significance (Figure 1.6D, $p=0.0811$). Thus, Ago2 occupancy at overlapping sites observed by CLIP may be affected by HuR levels, but at least part of the effect is explained by changes in mRNA levels. Additionally, interactions may be more difficult to detect in this analysis, as cooperative and antagonistic contributions at individual sites would cancel out.

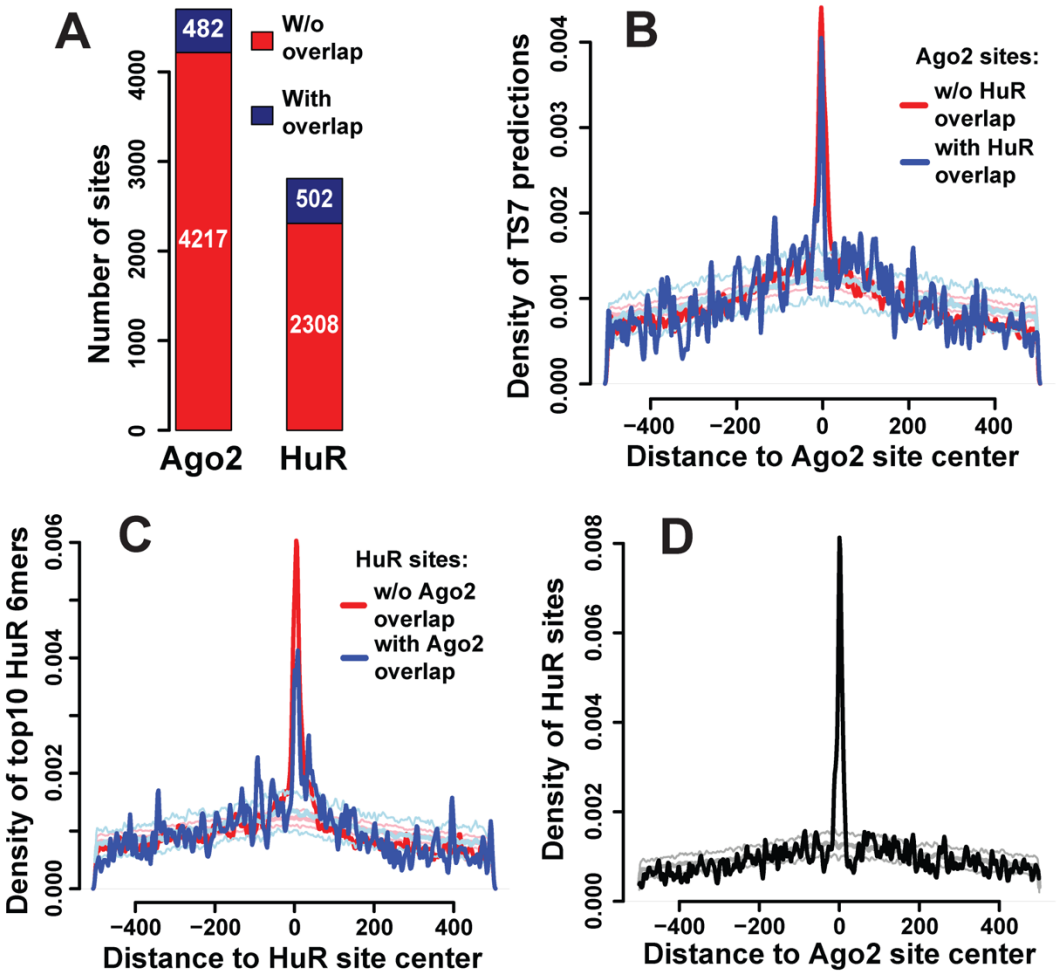

Figure 1.5. CLIP-Seq analysis of Ago2-HuR overlapping sites.

A) Number of Ago2 and HuR sites identified by CLIP-Seq, including sites of overlap. B) Comparison of TargetScan7 miRNA seed prediction density near Ago2 sites that do not (red) or do (blue) overlap with HuR sites. Light red and blue curves denote the mean (thicker line) and standard deviation (thinner line) of corresponding site position-randomized controls on the same 3′ UTR. C) Comparison of top 10 HuR site-associated 6mer density near HuR sites that do not (red) or do (blue) overlap with Ago2 sites. Light red and blue curves denote the mean (thicker line) and standard deviation (thinner line) of corresponding site position-randomized controls on the same 3′ UTR. D) Spatial distribution of HuR sites near Ago2 sites in 3′ UTR coordinates. Grey curves denote the mean (thicker line) and standard deviation (thinner line) of a HuR position-randomized control on the same 3′ UTR.

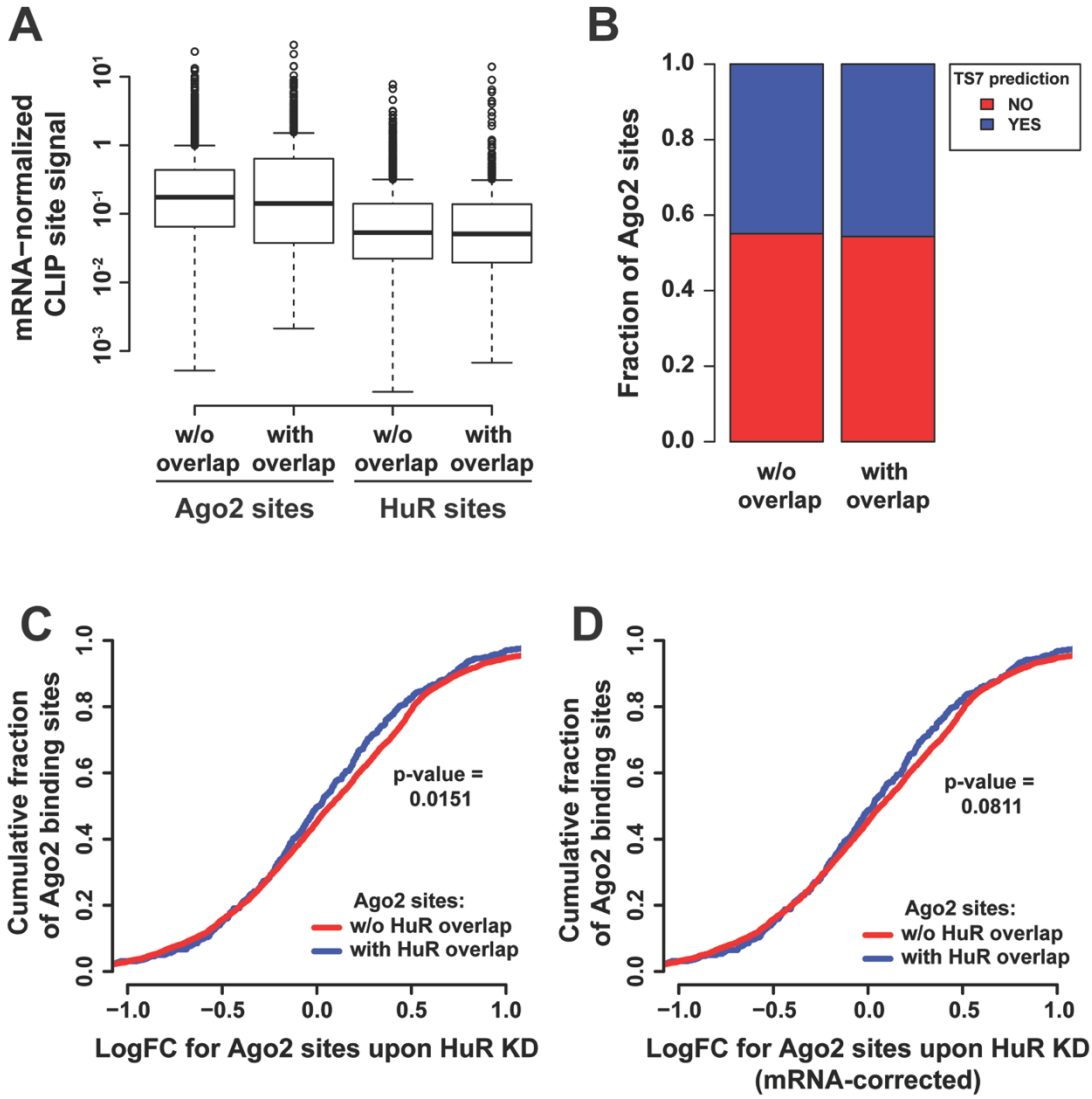

Figure 1.6. Characteristics of Ago2-HuR overlapping sites.

A) Boxplot of CLIP site signal for Ago2 and HuR sites with and without overlap. The CLIP site signal was normalized to mRNA levels from 293S cells. B) TargetScan7 miRNA seed prediction enrichment at overlapping and non-overlapping Ago2 sites. C) Cumulative fraction plot of log fold change (logFC) of Ago2 sites upon HuR KD on Ago2-HuR overlapping and non-overlapping sites. D) As in C), with CLIP site signal normalized to mRNA level changes upon HuR KD.

Evaluation of Ago2-HuR interaction on individual sites by luciferase reporter assays

To rigorously examine the occurrence of interactions at an individual level, we assayed a cohort of candidates from Ago2-HuR overlapping sites using luciferase reporters. To identify loci that are likely to represent true binding events and thus harbor potential interactions, we selected Ago2 CLIP sites based on HuR site overlap, Ago2 CLIP sites strength, presence of TargetScan miRNA seed predictions, and manual inspection (described in Materials and Methods), yielding 13 candidates for testing, listed in Table 1.1. An example locus on the CDK16 3′ UTR is shown in Figure 1.7. Ago2 sites, including 24-32 nt flanking sequences, were 4x concatenated to generate the WT reporters. In addition, mutant constructs were created by shuffling predicted miRNA seed matches to the most abundant miRNAs in the Ago2 CLIP sites, and the ratio of WT to mutant reporter expression was used to assess the regulatory activity of Argonaute at each interrogated site under several conditions. First, the constructs were measured in the T-REx-293 cell line to verify the activity of the mutated site. Twelve of the 13 candidate sites displayed WT/mut ratios that were significantly less than 1 (Figure 1.8A), indicating a repressive function for the sites. To further validate that the repression was a result of miRNA activity, we tested the constructs in NoDice 4-25 cells (46), which are deficient for miRNAs. Eleven of the 13 candidate sites demonstrated statistically significant derepression, showing their miRNA dependence (Figure 1.8A). For the majority of sites, ablation of miRNAs rendered the mutated site completely inactive (the WT/mut ratio returned to near 1). Cases where the ratio went significantly above 1 (ex., the BTG2 3′ UTR) convey that the site becomes protective rather than repressive in the absence of

miRNAs, suggesting the involvement of an additional factor, whose binding is dependent on the site. Overall, these experiments demonstrate that the vast majority of the tested candidate sites possess miRNA repressive ability.

Lastly, to examine whether HuR interacts with the miRNA machinery and affects miRNA repression, we used T-REx-293 derived HuR KO cells, HuRKO 3-D8, generated by the CRISPR-Cas9 system (51) after the Ago2 CLIP HuR KD experiments. A control construct bearing a known HuR motif (a synthetic repetitive AUUUA-containing sequence) (52) demonstrated repressive activity in T-REx-293 cells relative to the mutant reporter, indicating regulation by other ARE-binding factors. Furthermore, additional repression of the reporter was observed in the HuR KO cells, demonstrating HuR's protective activity at this site and the suitability of the cell line to detect HuR-dependent effects (Appendix B-Supplementary Figure S1.3). When the Ago2-HuR interaction candidates were tested in the HuR KO cells, significantly different extents of regulation were identified for three candidates (Figure 1.8B). The miRNA-guided repression at BTG2 and CDK16 sites was enhanced in the absence of HuR, indicating an antagonistic interaction with the miRNA machinery at these loci. In contrast, the WT/mut ratio for the MSMO1 3′ UTR site increased in HuR KO cells, signifying that HuR can also cooperatively interact with miRNAs at overlapping sites (Figure 1.8B).

Table 1.1. Genomic locations of 13 candidate sites.

The mutated miRNA seed matches in mutant constructs were indicated.

NO.	Gene	Strand	Ago2 site coordinates (in BED format)			Length/nt	Mutate miRNA seed targeting sequences in mutant constructs
			Chromosome	Start	End		
1	MYC	+	chr8	128753288	128753356	68	let-7-5p
2	BTG2	+	chr1	203277617	203277669	52	miR-25-3p, 128-3p
3	SNX17	+	chr2	27599814	27599857	43	miR-19-3p
4	NEFL	-	chr8	24809912	24809944	32	miR-25-3p, 137
5	TIMM17B	-	chrX	48750932	48750980	48	let-7-5p
6	MSMO1	+	chr4	166264168	166264205	37	miR-130-3p, 19-3p, 17-5p
7	FAM98A	-	chr2	33808881	33808936	55	miR-103-3p, 544
8	JOSD1	-	chr22	39081664	39081702	38	miR-30-5p, 495-3p
9	PNRC1	+	chr6	89794228	89794259	31	miR-19-3p
10	HOXA10	-	chr7	27210259	27210297	38	miR-15-5p
11	RNF167	+	chr17	4848326	4848356	30	miR-370-5p, 19-3p
12	CDK16	+	chrX	47088767	47088796	29	miR-25-3p
13	WEE1	+	chr11	9610599	9610645	46	miR-300, 17-5p, 302-3p

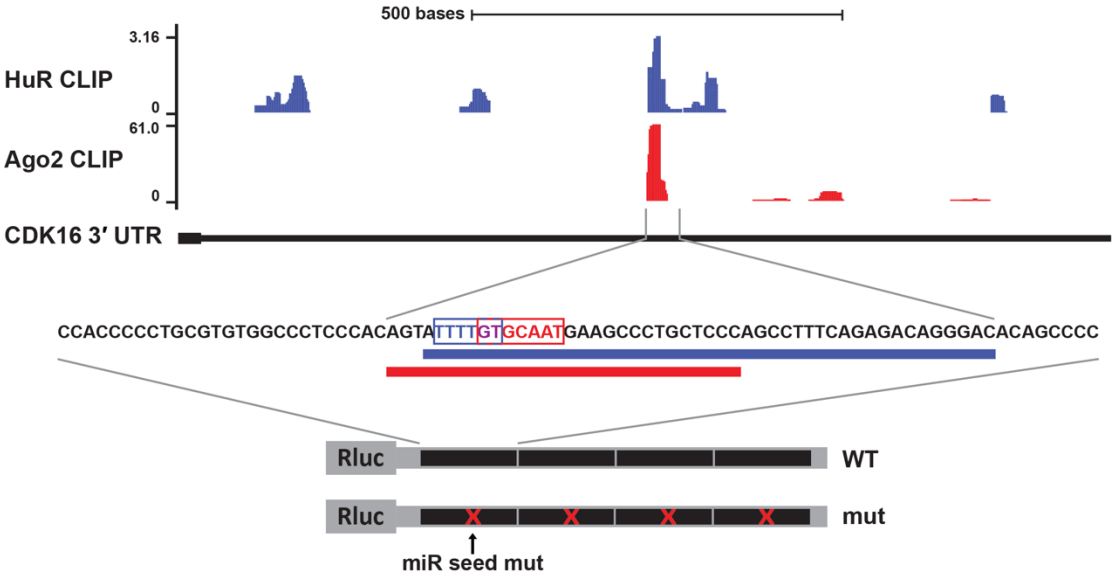

Figure 1.7. Ago2 and HuR CLIP-Seq binding sites on the CDK16 mRNA 3′ UTR, and corresponding reporter plasmid design.

UCSC genome browser-generated tracks of Ago2 and HuR CLIP sites are shown, and the region of overlap is detailed. The miR-25/92 family seed site is boxed in red, and an overlapping potential HuR motif is boxed in blue. The HuR-Ago2 overlapping site, including flanking sequences, was 4x concatenated into the 3′ UTR of the psiCHECK-2 luciferase reporter plasmid.

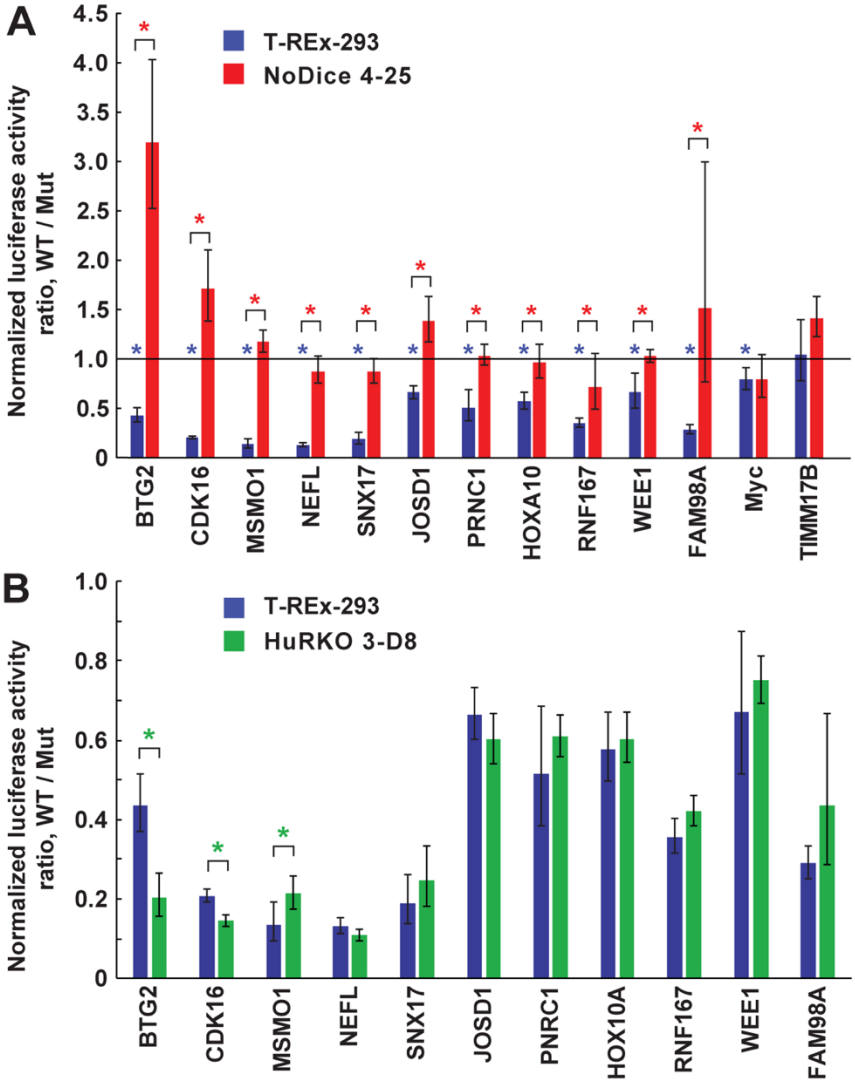

Figure 1.8. Luciferase reporter assays testing candidate HuR-Ago2 interactions.

A) Thirteen candidate sites were tested in T-REx-293 cells and NoDice 4-25 cells. The ratio of WT to miRNA seed mutant reporter activities indicates the regulatory effect of the mutation in different cell backgrounds. Blue asterisks indicate p-values < 0.05 in two-tailed paired t-test comparisons between WT construct and Mut construct luciferase activity in T-Rex-293 cells. Red asterisks indicate p-values < 0.05 in two-tailed Welch's t-test comparisons of WT/Mut ratios between T-REx-293 cells and NoDice 4-25 cells. B) Eleven of the miRNA-dependent repressive sites were tested in HuRKO 3-D8 cells to check HuR regulation of the miRNA-dependent repression. Green asterisks indicate p-values < 0.05 in two-tailed Welch's t-test comparisons of WT/Mut ratios between T-Rex-293 cells and HuRKO 3-D8 cells. Error bars indicate one standard deviation.

To further validate that the repressive activity that remains at these interactive sites in the absence of HuR is guided by specific miRNAs, we inhibited the most abundant specific targeting miRNA(s) by the respective antagomirs or LNAs in the HuR KO luciferase assays (Appendix D-Supplementary File 3). Inhibition of miR-25-3p caused a derepression of the BTG2 and CDK16 constructs, while combined inhibition of miR-19a/b-3p, miR-130b-3p, and the miR-17 family derepressed the MSMO1 construct, indicating the involvement of the miRNAs in the regulation (Figure 1.9). Importantly, derepression was not observed in the mutant constructs, demonstrating that the miRNAs functioned through the mutated targeting sites. In sum, the luciferase reporter experiments identified 3 candidate sites with altered activities in HuR KO cells, demonstrating that HuR interacts with miRNA machinery, either antagonistically or cooperatively, on some overlapping sites.

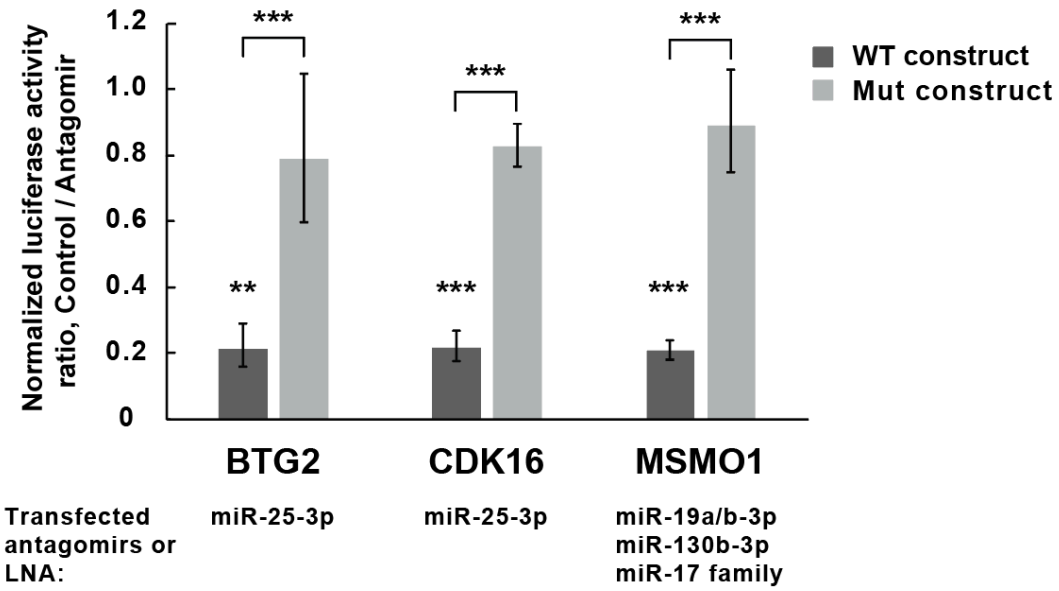

Figure 1.9. Specific miRNAs are responsible for repression at the identified sites of interaction.

Luciferase assays in the HuR KO 3-D8 cell line were performed with four replicates. Comparison of luciferase activity between the control and antagomir transfections was performed by two-tailed paired t-tests. Comparison of Control/Antagomir ratios between WT and mutant constructs was performed by two-tailed Welch's t-tests. Significance is indicated by asterisks: * $p<0.05$, ** $p<0.01$, *** $p<0.001$. Error bars indicate one standard deviation.

DISCUSSION

In the current study, we successfully applied a perturbation approach to identify global signatures of HuR-Ago2 interactions on mRNA 3′ UTRs through relative quantification of binding at individual sites. In addition to determining the site locations, measuring the CLIP signal of one RBP while manipulating the levels of the other allowed for the detection of HuR effects on Ago2 binding. Focusing on the RBP sites with the most

extreme changes for each 3′ UTR upon KD/KO of the other factor as the sites of interest for possible RBP interactions, we observed that Ago2 sites with maximal LFCs upon HuR KD can be antagonized by HuR presence on the same 3′ UTR (Figure 1.3D). HuR-miRNA antagonism has also been inferred from effects on mRNA differential expression upon HuR or miRNA KD (43,53). In agreement, our analyses further demonstrate that the interactive effects of HuR impinge directly on the binding of Ago2 to mRNAs. These global results are also in agreement with antagonistic regulation previously demonstrated on individual mRNAs (33,54-57). It should be noted that HuR has been shown to impact Ago2 activity even at distant binding sites, likely through an oligomerization property (34).

In addition to antagonistic interactions, measurement of Ago2 CLIP signal with and without HuR KD delineated a set of sites with minimal LFC (Figure 1.3C) that are enriched in cooperative interactions with HuR. Although individual examples of cooperation have been shown (58,59), such interactions have not been previously detected in transcriptome-wide studies. Here, the stratification of sites by their response to HuR KD permitted the global demonstration of this interaction mode. Furthermore, correlation analysis between maximal Ago2 and HuR LFCs on the same 3′ UTR detected a small but statistically significant effect, indicating that HuR-Ago2 interactions can be reciprocal at the level of binding. Altogether, our study globally demonstrated that RBP interactions can antagonistically and cooperatively affect the binding levels of their partners, providing a further perspective to understand their joint regulatory modes. It

should be noted that the identified interactions can occur due to direct Ago2-HuR contacts, or through intermediate adaptor proteins, which may impart additional regulation.

Although quantitative CLIP-seq comparison between conditions is able to detect significant global effects aggregated across all binding events, CLIP signal reproducibility among replicates at individual sites falls short of that seen in RNA-seq or small RNA-seq experiments (60). The reasons likely lie in the complex, multi-step procedure, the necessity to reverse-transcribe through crosslinked sites, and the indirect quantification by degenerate ligated barcode counts. Thus, statistical significance of differential binding is reached only for a handful of sites, precluding precise transcriptome-wide identification of all individual interactions. Further refinements or alternative cloning and quantification methods will be required to achieve this necessary goal. Despite the current deficiency in quantitative power, global analysis is a useful tool in detection of RBP overlap sites, coupled with downstream validation experiments, to uncover cases of co-regulation.

Examination of CLIP data demonstrated that approximately 10% of Ago2 sites and 18% of HuR sites overlap each other (Figure 1.5A). Importantly, the overlapping sites share strength characteristics and the expected sequence enrichment with solo sites, demonstrating their genuine nature. The extent and positional enrichment of the overlap indicates that Ago2 and HuR binding sites have evolved to frequently co-occur,

supporting the combinatorial model of mRNA regulation. These observations are in agreement with previous analyses of association for experimentally identified and bioinformatically predicted miRNA and RBP binding sites (36,39-42,61), as well as a broader picture where mRNAs contain "hotspot" binding sites for multiple RBPs, with undoubtedly complex and multivalent opportunities for control (37). Assessment of HuR's effect on Ago2 binding at overlapping sites by looking at changes in Ago2 occupancy upon HuR KD revealed a statistically weak trend toward cooperativity (Figure 1.6C). It should be noted that overlap in our analysis is defined to the extent of CLIP-seq peak resolution (34-44 nt, Figure 1.1C), and may not involve steric hindrance between the RBPs, allowing for cooperation at such sites. When examining HuR effects on Ago2 binding on the same 3′ UTR regardless of overlap, we observed both cooperative and antagonistic effects. Thus, there is a possibility that the effect from HuR sites on overlapping Ago2 binding are a mixture of both types of interactions that would be largely cancelled out in the above analysis. Additionally, HuR may exert functional effects on Ago2 regulation without displacing Ago2, but by attenuating its interactions with downstream adaptor proteins (TNRC6) and degradation machinery components (CCR4-NOT complex). Previous studies have shown that overlapping or adjacent HuR and miRNA sites have antagonistic effects on mRNA stability (36,43,53).

To complement the transcriptome-wide examination of overlapping sites, we individually characterized 13 high fidelity candidates in luciferase assays. For most of the sites (11/13), mutation of the predicted miRNA seed showed repression that was relieved in

Dicer-deficient cells, validating their miRNA dependence (Figure 1.8A). Thus, most of the overlapping candidates were confirmed to be genuine sites under Ago2 regulation, in agreement with the global analysis. Among these, the majority of the mutated sites de-repressed to a WT/mut ratio close to 1 (no site effect) in Dicer-null cells, indicating that miRNA activity is necessary for all of the regulation that occurs through the site itself. Interestingly, however, some sites (BTG2, CDK16, MSMO1, JOSD1) converted from repressive to activating in the absence of miRNAs, indicating that the mutated miRNA seed region overlaps a site necessary for the activity (potentially through direct binding) of an additional, protective factor. Therefore, direct steric competition with Ago proteins is expected at such sites. When tested in HuR KO cells, three of the 11 miRNA-regulated sites were shown to have an altered activity, indicating that HuR affects miRNA-mediated repression at those sites. For the BTG2 and CDK16 sites, HuR was antagonistic to Ago regulation (Figure 1.8B). The increased repression in HuR KO cells agrees with the activating function of BTG2 and CDK16 sites in Dicer-null cells, and suggests that HuR may be responsible for their stabilization in the absence of miRNAs as well. However, the binding site of MSMO1 exhibited a cooperativity between HuR and miRNAs. The specific mechanism of such interactive sites will require further study. Although stable, stoichiometric HuR-Ago2 association is not observed by co-IPs, co-regulation by RNA secondary structure rearrangement at specific sites, as observed for PUM-Ago interactions (35), is a potential mechanism for cooperation. Overall, the observation of positive and negative interactions at individual loci may explain the weak net HuR effects on Ago2 binding that were seen globally.

In summary, we present an integrated approach to identify HuR-Ago/miRNA interactions and validate candidate sites. Extrapolating the number of validated interactions to the total number of overlapping sites, we estimate that on the order of 100 HuR-Ago/miRNA interactions likely occur at overlapping sites throughout the transcriptome (assayed in a single cell line). In addition, long-range interactions, as well as those induced by stress or other cell transitions (33) and thus not detected in this study, increase the number of interactive cases further. In a global view, the involvement of other RBPs in pairwise and multivalent interactions with HuR and Ago/miRNA, as well as among themselves, predicts that the overall contribution of combinatorial regulation to mRNA control is very substantial. These and other approaches will be necessary to advance our understanding of the fascinating complexity of the post-transcriptional regulation network.

MATERIALS AND METHODS

Cell culture and knockdown experiments

T-REx-293 cells were obtained from Invitrogen, and 293T and NoDice (2-20) and NoDice (4-25) cells were a kind gift of B. Cullen. HuR knockout 3-D8 cells were previously described (51). Cells were grown in DMEM (Corning Cellgro) with 10 % Fetal Bovine Serum (HyClone) and 10 units/ml of Penicillin-Streptomycin (HyClone) in a humidified incubator at 37 °C with 5 % CO_2. For HuR knockdown, 5 replicates of T-REx-293 cells were separately transfected with two distinct siRNAs against HuR, or with

a GL3.1 siRNA control (Appendix E-Supplementary File 1a). *Trans*IT-TKO (Mirus) transfections with 100 nM siRNA were performed for the first 2 replicates, and calcium phosphate transfections with 25 nM siRNA were carried out for the later 3 replicates. For each replicate set, three successive transfections 2 days apart were performed to get sufficient knockdown of HuR. For each replicate/condition, three to six 15 cm plates of cells were collected for the CLIP procedure.

Ago2 and HuR HITS-CLIP

The Ago2 CLIP protocol was performed as previously described (44). HuR CLIP was carried out using the same protocol, excising the appropriate protein-RNA complex on the protein gel. Mouse anti-Ago2 (Santa Cruz, clone 4F9) and mouse anti-HuR (Santa Cruz, clone 3A2) antibodies were used for Ago2 CLIP and HuR CLIP, respectively. For HuR CLIP, three replicate sets of 293T cells (control), NoDice (2-20) and NoDice (4-25) cells were performed. Libraries were sequenced on an Illumina HiSeq2500 instrument with a multiplex of 6 libraries per lane.

Data analysis

CLIP library processing to generate binding peaks, annotations and associated readcounts was performed as before (44), except bowtie2 mapping was used instead of iterative bowtie. Further analysis was performed in R/Bioconductor (62,63). 3′ UTR peaks/sites were filtered for the presence of greater than a total of 15 readcounts across all replicates for Ago2 CLIP, and 9 readcounts for HuR CLIP, representing equivalent stringency for

the 15 and 9 CLIP samples, respectively. Peaks containing complements to nucleotides 3-7 of the knockdown siRNAs were eliminated to avoid off-targeting artefacts. Differential expression and the log2 fold changes (LFCs) for each CLIP site upon the respective perturbation (HuR knockdown or Dicer loss) were computed by DESeq2 (45). Ago2 site sequence motif enrichment was performed by DREME with a minimal 6-mer motif (64). mRNA abundance estimates for CLIP signal normalization in Figure 1.6A were obtained from the untreated RNAseq data in (44). For analysis of Ago2-HuR interactions on the same 3′ UTRs, the longest 3′ UTR isoform for each gene was considered. For each gene, the following values were computed: the number of Ago2 and HuR sites; the maximum, the minimum and the sum of LFCs among the Ago2 site signals on the 3′ UTR upon HuR knockdown; conversely, the max, min and sum of LFCs among HuR site signals in the NoDice/WT comparison. Pearson correlation values between maximal Ago2 and HuR site LFCs, as well as the sum of LFCs (for 3′ UTRs that contain both) were calculated. The correlation z-score was derived based on a background distribution of 1000 correlations where the Ago2 and HuR LFC values were independently permuted. For the cumulative distribution analysis of Ago2 site LFCs, the values were normalized to LFCs of mRNA abundance upon HuR knockdown reported in (43). Ago2 and HuR sites with at least 1 nt of overlap were considered overlapping. To calculate positional enrichment of CLIP sites relative to other features (CLIP sites, miRNA predicted sites, or HuR motifs), distances between the site and feature centers were calculated in a 1000 nt window around the site, and aggregated across all 3′ UTRs to generate the density profile (smoothed histogram) of distances. Background, random expectation distances were

computed 100 times by randomly shuffling CLIP site locations on the same UTR (preserving the number of sites per UTR), and the mean and standard deviation of their density profiles were calculated.

Reporter vector plasmid construction

We screened candidate Ago2-HuR overlapping sites for further experimental testing with the following selection criteria: (1) Ago2 site overlap with a HuR site from both our dataset and an independent HuR dataset generated with different crosslinking chemistry (PAR-CLIP) (65); (2) mRNA-normalized Ago2 CLIP signal strength among the top 20 sites (with the exception of WEE1, which is from the top 20 of unnormalized CLIP signal); (3) TargetScan (TargetScanHuman7 or TargetScan5.1) miRNA seed match predictions near the center of the site (with the exception of Myc, which does not have a TargetScan predicted miRNA seed match, but has a miRNA target site validated by a previous study (59)). Additionally, a MKNK2 site was filtered out due to the relatively low HuR site signal compared to surrounding HuR sites. This selection yields 13 overall candidates for testing, listed in Table 1.1.

Candidate Ago2 binding sites that overlap HuR, including 24-32 nt of flanking sequence (to avoid steric hindrance and to cover the full HuR peak sequences) were inserted as 4x concatamers into the luciferase reporter plasmid psiCHECK-2 (Promega), where the genomic coordinates of cloning monomers and HuR sites were shown in Supplementary File 1b and 1c (Appendix E), respectively. In addition to the WT reporters, to validate

miRNA activity, mutant constructs were created by disrupting Ago2 CLIP site miRNA seed matches corresponding to the most abundant miRNAs (Supplementary File 3), quantified by the miRmine database (66). miRNA seed sequences were shuffled by the Sequence Manipulation Suite (67). The WT and mutant monomer sequences are listed in Supplementary File 2 (Appendix C). Each monomer was constructed by overlapping PCR with 4 oligos (Appendix E-Supplementary File 1d), as shown in Supplementary Figure S1.2A (Appendix B), producing an amplicon with BsmBI sites near the ends that generate unique overhangs for subsequent Golden Gate cloning (GGC) to assemble the 4 monomers into the 3′ UTR of the Renilla luciferase gene in the psiCHECK-2 plasmid. The psiCHECK-2 plasmid was also correspondingly modified to contain two recipient BsmBI sites producing CACC and GTTT overhangs in its multiple cloning region for the Golden Gate reaction (Appendix E-Supplementary File 1d). The scheme for the GGC strategy is shown in Supplementary Figure S1.2B (Appendix B). The overhang sequences between plasmid and monomer, or between monomers are CACC, AACA, GGCT, TCAG, and GTTT, in 5′-3′ order. For the HuR target controls cfos and AU5, the monomer sequences were either PCR-amplified from oligos or directly synthesized and were inserted as 4x concatamers into the 3′ UTR of the luciferase gene in the pRL-TK plasmid by GGC (Appendix E-Supplementary File 1g and 1h). The vector plasmid pRL-TK was adapted to carry BsmBI sites and CACC and GTTT overhangs for GGC (Appendix E-Supplementary File 1f). The Golden Gate reaction conditions were adapted from (68) with 10-30 temperature cycles.

Plasmid transfection and luciferase assays

T-REx-293 cells were seeded in 96-well plates and transfected with 10 ng of reporter plasmid per well, with the exception of one replicate with 5ng of plasmid in both T-REx-293 and HuR KO cells. For the HuR target control, 10 ng of firefly luciferase plasmid pGL3 was transfected together with the reporter plasmid pRL-TK to normalize for transfection efficiency. Transfections were performed in three technical replicates, at approximately 70% confluency with the *Trans*IT-LT1 reagent (Mirus) following the manufacturer protocol. In antagomir experiments, calcium phosphate transfection was used to transfect 10 ng of reporter plasmid with 0.75 μM of individual antagomirs to cells at approximately 70% confluency in the 96-well plate. Anti-miR-19a, anti-miR-19b, anti-miR-130b, anti-miR-25 and the control antagomir were manufactured by Dharmacon. Anti-miR-17 family LNA and its control were obtained from Exiqon. WT and miRNA seed mutant reporters were transfected in parallel on the same plates. Cells were lysed after 24 hours with 20 μL of Passive Lysis Buffer (Promega). 5 μL of cell lysate were used for dual luciferase reporter measurements (Dual-Luciferase Reporter Assay System, Promega). Luciferase substrates were diluted 1:5 in use.

Luciferase assays data analysis

The Firefly luciferase on the same plasmid was used to normalize the reporter expression level. Technical replicates where signal was less than 5-fold of the background reading were filtered out. Four to 8 biological replicates were performed, and experiments with less than 50% coefficients of variability between the technical replicates were used for

further analysis, resulting in 3-5 replicates per each candidate reporter. Further, the WT luciferase activity was divided by mutant luciferase activity, and the ratio served as an indicator of the microRNA site regulatory activity under different cell conditions. Data in graphs are displayed in the original scale of measurement. However, averaging and statistical analysis of the WT/Mut ratios were performed after logarithmic transformation. To check whether sites are repressive in T-REx-293 cells, WT luciferase activity was compared with Mut luciferase activity by two-tailed paired t-test, which is mathematically equivalent to comparing WT/Mut ratios with 1 by two-tailed one-sample t-test. To check whether the repressive effects of the sites are miRNA-dependent, we compared the WT/Mut ratios in T-REx-293 and NoDice 4-25 cells by two-tailed Welch's t-test. Third, to check the HuR regulation of the miRNA-dependent repression of the site, we compared the WT/Mut ratios in T-REx-293 with HuRKO 3-D8 cells by two-tailed Welch's t-test. Significance was set at 0.05.

ACCESSION NUMBERS

CLIP-Seq datasets have been deposited in the NCBI GEO database under accession number GSE102321.

ACKNOWLEDGEMENT

The authors would like to thank the Raikhel lab for sharing reagents, Erin Sternburg for experimental assistance and all members of the Karginov lab for insightful discussions.

REFERENCES

1. Vogel, C. and Marcotte, E.M. (2012) Insights into the regulation of protein abundance from proteomic and transcriptomic analyses. *Nat Rev Genet*, **13**, 227-232.

2. McManus, J., Cheng, Z. and Vogel, C. (2015) Next-generation analysis of gene expression regulation--comparing the roles of synthesis and degradation. *Mol Biosyst*, **11**, 2680-2689.

3. Ghazalpour, A., Bennett, B., Petyuk, V.A., Orozco, L., Hagopian, R., Mungrue, I.N., Farber, C.R., Sinsheimer, J., Kang, H.M., Furlotte, N. *et al.* (2011) Comparative analysis of proteome and transcriptome variation in mouse. *PLoS Genet*, **7**, e1001393.

4. Battle, A., Khan, Z., Wang, S.H., Mitrano, A., Ford, M.J., Pritchard, J.K. and Gilad, Y. (2015) Genomic variation. Impact of regulatory variation from RNA to protein. *Science*, **347**, 664-667.

5. Schwanhausser, B., Busse, D., Li, N., Dittmar, G., Schuchhardt, J., Wolf, J., Chen, W. and Selbach, M. (2011) Global quantification of mammalian gene expression control. *Nature*, **473**, 337-342.

6. Li, J.J. and Biggin, M.D. (2015) Gene expression. Statistics requantitates the central dogma. *Science*, **347**, 1066-1067.

7. Kristensen, A.R., Gsponer, J. and Foster, L.J. (2013) Protein synthesis rate is the predominant regulator of protein expression during differentiation. *Mol Syst Biol*, **9**, 689.

8. Stadler, M. and Fire, A. (2013) Conserved translatome remodeling in nematode species executing a shared developmental transition. *PLoS Genet*, **9**, e1003739.

9. Aviner, R., Shenoy, A., Elroy-Stein, O. and Geiger, T. (2015) Uncovering Hidden Layers of Cell Cycle Regulation through Integrative Multi-omic Analysis. *PLoS Genet*, **11**, e1005554.

10. Robles, M.S., Cox, J. and Mann, M. (2014) In-vivo quantitative proteomics reveals a key contribution of post-transcriptional mechanisms to the circadian regulation of liver metabolism. *PLoS Genet*, **10**, e1004047.

11. Cheng, Z., Teo, G., Krueger, S., Rock, T.M., Koh, H.W., Choi, H. and Vogel, C. (2016) Differential dynamics of the mammalian mRNA and protein expression response to misfolding stress. *Mol Syst Biol*, **12**, 855.

12. Wu, L., Candille, S.I., Choi, Y., Xie, D., Jiang, L., Li-Pook-Than, J., Tang, H. and Snyder, M. (2013) Variation and genetic control of protein abundance in humans. *Nature*, **499**, 79-82.

13. Albert, F.W., Treusch, S., Shockley, A.H., Bloom, J.S. and Kruglyak, L. (2014) Genetics of single-cell protein abundance variation in large yeast populations. *Nature*, **506**, 494-497.

14. Khan, Z., Ford, M.J., Cusanovich, D.A., Mitrano, A., Pritchard, J.K. and Gilad, Y. (2013) Primate transcript and protein expression levels evolve under compensatory selection pressures. *Science*, **342**, 1100-1104.

15. Laurent, J.M., Vogel, C., Kwon, T., Craig, S.A., Boutz, D.R., Huse, H.K., Nozue, K., Walia, H., Whiteley, M., Ronald, P.C. *et al.* (2010) Protein abundances are more conserved than mRNA abundances across diverse taxa. *Proteomics*, **10**, 4209-4212.

16. Artieri, C.G. and Fraser, H.B. (2014) Evolution at two levels of gene expression in yeast. *Genome Res*, **24**, 411-421.

17. McManus, C.J., May, G.E., Spealman, P. and Shteyman, A. (2014) Ribosome profiling reveals post-transcriptional buffering of divergent gene expression in yeast. *Genome Res*, **24**, 422-430.

18. Wang, Z., Sun, X., Zhao, Y., Guo, X., Jiang, H., Li, H. and Gu, Z. (2015) Evolution of gene regulation during transcription and translation. *Genome Biol Evol*, **7**, 1155-1167.

19. Castello, A., Fischer, B., Hentze, M.W. and Preiss, T. (2013) RNA-binding proteins in Mendelian disease. *Trends Genet*, **29**, 318-327.

20. Berezikov, E. (2011) Evolution of microRNA diversity and regulation in animals. *Nat Rev Genet*, **12**, 846-860.

21. Bartel, D.P. (2009) MicroRNAs: target recognition and regulatory functions. *Cell*, **136**, 215-233.

22. Dueck, A., Ziegler, C., Eichner, A., Berezikov, E. and Meister, G. (2012) microRNAs associated with the different human Argonaute proteins. *Nucleic Acids Res*, **40**, 9850-9862.

23. Wang, D., Zhang, Z., O'Loughlin, E., Lee, T., Houel, S., O'Carroll, D., Tarakhovsky, A., Ahn, N.G. and Yi, R. (2012) Quantitative functions of Argonaute proteins in mammalian development. *Genes Dev*, **26**, 693-704.

24. Hafner, M., Landthaler, M., Burger, L., Khorshid, M., Hausser, J., Berninger, P., Rothballer, A., Ascano, M., Jr., Jungkamp, A.C., Munschauer, M. *et al.* (2010) Transcriptome-wide identification of RNA-binding protein and microRNA target sites by PAR-CLIP. *Cell*, **141**, 129-141.

25. Landthaler, M., Gaidatzis, D., Rothballer, A., Chen, P.Y., Soll, S.J., Dinic, L., Ojo, T., Hafner, M., Zavolan, M. and Tuschl, T. (2008) Molecular characterization of human Argonaute-containing ribonucleoprotein complexes and their bound target mRNAs. *RNA*, **14**, 2580-2596.

26. Simone, L.E. and Keene, J.D. (2013) Mechanisms coordinating ELAV/Hu mRNA regulons. *Curr Opin Genet Dev*, **23**, 35-43.

27. Srikantan, S., Tominaga, K. and Gorospe, M. (2012) Functional interplay between RNA-binding protein HuR and microRNAs. *Curr Protein Pept Sci*, **13**, 372-379.

28. Meisner, N.C. and Filipowicz, W. (2010) Properties of the regulatory RNA-binding protein HuR and its role in controlling miRNA repression. *Adv Exp Med Biol*, **700**, 106-123.

29. Reiter, F., Wienerroither, S. and Stark, A. (2017) Combinatorial function of transcription factors and cofactors. *Curr Opin Genet Dev*, **43**, 73-81.

30. Kishore, S., Luber, S. and Zavolan, M. (2010) Deciphering the role of RNA-binding proteins in the post-transcriptional control of gene expression. *Brief Funct Genomics*, **9**, 391-404.

31. Jiang, P. and Coller, H. (2012) Functional interactions between microRNAs and RNA binding proteins. *Microrna*, **1**, 70-79.

32. Iadevaia, V. and Gerber, A.P. (2015) Combinatorial Control of mRNA Fates by RNA-Binding Proteins and Non-Coding RNAs. *Biomolecules*, **5**, 2207-2222.

33. Bhattacharyya, S.N., Habermacher, R., Martine, U., Closs, E.I. and Filipowicz, W. (2006) Relief of microRNA-mediated translational repression in human cells subjected to stress. *Cell*, **125**, 1111-1124.

34. Kundu, P., Fabian, M.R., Sonenberg, N., Bhattacharyya, S.N. and Filipowicz, W. (2012) HuR protein attenuates miRNA-mediated repression by promoting miRISC dissociation from the target RNA. *Nucleic Acids Res*, **40**, 5088-5100.

35. Kedde, M., van Kouwenhove, M., Zwart, W., Oude Vrielink, J.A., Elkon, R. and Agami, R. (2010) A Pumilio-induced RNA structure switch in p27-3' UTR controls miR-221 and miR-222 accessibility. *Nat Cell Biol*, **12**, 1014-1020.

36. HafezQorani, S., Lafzi, A., de Bruin, R.G., van Zonneveld, A.J., van der Veer, E.P., Son, Y.A. and Kazan, H. (2016) Modeling the combined effect of RNA-binding proteins and microRNAs in post-transcriptional regulation. *Nucleic Acids Res*, **44**, e83.

37. Plass, M., Rasmussen, S.H. and Krogh, A. (2017) Highly accessible AU-rich regions in 3' untranslated regions are hotspots for binding of regulatory factors. *PLoS Comput Biol*, **13**, e1005460.

38. Sood, P., Krek, A., Zavolan, M., Macino, G. and Rajewsky, N. (2006) Cell-type-specific signatures of microRNAs on target mRNA expression. *Proc Natl Acad Sci U S A*, **103**, 2746-2751.

39. Jacobsen, A., Wen, J., Marks, D.S. and Krogh, A. (2010) Signatures of RNA binding proteins globally coupled to effective microRNA target sites. *Genome Res*, **20**, 1010-1019.

40. Galgano, A., Forrer, M., Jaskiewicz, L., Kanitz, A., Zavolan, M. and Gerber, A.P. (2008) Comparative analysis of mRNA targets for human PUF-family proteins suggests extensive interaction with the miRNA regulatory system. *PLoS One*, **3**, e3164.

41. Jiang, P., Singh, M. and Coller, H.A. (2013) Computational assessment of the cooperativity between RNA binding proteins and MicroRNAs in Transcript Decay. *PLoS Comput Biol*, **9**, e1003075.

42. Lebedeva, S., Jens, M., Theil, K., Schwanhausser, B., Selbach, M., Landthaler, M. and Rajewsky, N. (2011) Transcriptome-wide analysis of regulatory interactions of the RNA-binding protein HuR. *Mol Cell*, **43**, 340-352.

43. Mukherjee, N., Corcoran, D.L., Nusbaum, J.D., Reid, D.W., Georgiev, S., Hafner, M., Ascano, M., Jr., Tuschl, T., Ohler, U. and Keene, J.D. (2011) Integrative regulatory mapping indicates that the RNA-binding protein HuR couples pre-mRNA processing and mRNA stability. *Mol Cell*, **43**, 327-339.

44. Karginov, F.V. and Hannon, G.J. (2013) Remodeling of Ago2-mRNA interactions upon cellular stress reflects miRNA complementarity and correlates with altered translation rates. *Genes Dev*, **27**, 1624-1632.

45. Love, M.I., Huber, W. and Anders, S. (2014) Moderated estimation of fold change and dispersion for RNA-seq data with DESeq2. *Genome Biol*, **15**, 550.

46. Bogerd, H.P., Whisnant, A.W., Kennedy, E.M., Flores, O. and Cullen, B.R. (2014) Derivation and characterization of Dicer- and microRNA-deficient human cells. *RNA*, **20**, 923-937.

47. Ray, D., Kazan, H., Chan, E.T., Pena Castillo, L., Chaudhry, S., Talukder, S., Blencowe, B.J., Morris, Q. and Hughes, T.R. (2009) Rapid and systematic analysis of the RNA recognition specificities of RNA-binding proteins. *Nat Biotechnol*, **27**, 667-670.

48. Ray, D., Kazan, H., Cook, K.B., Weirauch, M.T., Najafabadi, H.S., Li, X., Gueroussov, S., Albu, M., Zheng, H., Yang, A. *et al.* (2013) A compendium of RNA-binding motifs for decoding gene regulation. *Nature*, **499**, 172-177.

49. Uren, P.J., Burns, S.C., Ruan, J., Singh, K.K., Smith, A.D. and Penalva, L.O. (2011) Genomic analyses of the RNA-binding protein Hu antigen R (HuR) identify a complex network of target genes and novel characteristics of its binding sites. *J Biol Chem*, **286**, 37063-37066.

50. Agarwal, V., Bell, G.W., Nam, J.W. and Bartel, D.P. (2015) Predicting effective microRNA target sites in mammalian mRNAs. *Elife*, **4**.

51. Estep, J.A., Sternburg, E.L., Sanchez, G.A. and Karginov, F.V. (2016) Immunoblot screening of CRISPR/Cas9-mediated gene knockouts without selection. *BMC Mol Biol*, **17**, 9.

52. Myer, V.E., Fan, X.C. and Steitz, J.A. (1997) Identification of HuR as a protein implicated in AUUUA-mediated mRNA decay. *EMBO J*, **16**, 2130-2139.

53. Lu, Y.C., Chang, S.H., Hafner, M., Li, X., Tuschl, T., Elemento, O. and Hla, T. (2014) ELAVL1 modulates transcriptome-wide miRNA binding in murine macrophages. *Cell Rep*, **9**, 2330-2343.

54. Zhuang, R., Rao, J.N., Zou, T., Liu, L., Xiao, L., Cao, S., Hansraj, N.Z., Gorospe, M. and Wang, J.Y. (2013) miR-195 competes with HuR to modulate stim1 mRNA stability and regulate cell migration. *Nucleic Acids Res*, **41**, 7905-7919.

55. Srikantan, S., Abdelmohsen, K., Lee, E.K., Tominaga, K., Subaran, S.S., Kuwano, Y., Kulshrestha, R., Panchakshari, R., Kim, H.H., Yang, X. *et al.* (2011) Translational control of TOP2A influences doxorubicin efficacy. *Mol Cell Biol*, **31**, 3790-3801.

56. Epis, M.R., Barker, A., Giles, K.M., Beveridge, D.J. and Leedman, P.J. (2011) The RNA-binding protein HuR opposes the repression of ERBB-2 gene expression by microRNA miR-331-3p in prostate cancer cells. *J Biol Chem*, **286**, 41442-41454.

57. Young, L.E., Moore, A.E., Sokol, L., Meisner-Kober, N. and Dixon, D.A. (2012) The mRNA stability factor HuR inhibits microRNA-16 targeting of COX-2. *Mol Cancer Res*, **10**, 167-180.

58. Glorian, V., Maillot, G., Poles, S., Iacovoni, J.S., Favre, G. and Vagner, S. (2011) HuR-dependent loading of miRNA RISC to the mRNA encoding the Ras-related small GTPase RhoB controls its translation during UV-induced apoptosis. *Cell Death Differ*, **18**, 1692-1701.

59. Kim, H.H., Kuwano, Y., Srikantan, S., Lee, E.K., Martindale, J.L. and Gorospe, M. (2009) HuR recruits let-7/RISC to repress c-Myc expression. *Genes Dev*, **23**, 1743-1748.

60. Ince-Dunn, G., Okano, H.J., Jensen, K.B., Park, W.Y., Zhong, R., Ule, J., Mele, A., Fak, J.J., Yang, C., Zhang, C. *et al.* (2012) Neuronal Elav-like (Hu) proteins regulate RNA splicing and abundance to control glutamate levels and neuronal excitability. *Neuron*, **75**, 1067-1080.

61. Mukherjee, N., Lager, P.J., Friedersdorf, M.B., Thompson, M.A. and Keene, J.D. (2009) Coordinated posttranscriptional mRNA population dynamics during T-cell activation. *Mol Syst Biol*, **5**, 288.

62. R Core Team. (2017). R Foundation for Statistical Computing, Vienna, Austria.

63. Huber, W., Carey, V.J., Gentleman, R., Anders, S., Carlson, M., Carvalho, B.S., Bravo, H.C., Davis, S., Gatto, L., Girke, T. *et al.* (2015) Orchestrating high-throughput genomic analysis with Bioconductor. *Nat Methods*, **12**, 115-121.

64. Bailey, T.L. (2011) DREME: motif discovery in transcription factor ChIP-seq data. *Bioinformatics*, **27**, 1653-1659.

65. Kishore, S., Jaskiewicz, L., Burger, L., Hausser, J., Khorshid, M. and Zavolan, M. (2011) A quantitative analysis of CLIP methods for identifying binding sites of RNA-binding proteins. *Nat Methods*, **8**, 559-564.

66. Panwar, B., Omenn, G.S. and Guan, Y. (2017) miRmine: a database of human miRNA expression profiles. *Bioinformatics*, **33**, 1554-1560.

67. Stothard, P. (2000) The sequence manipulation suite: JavaScript programs for analyzing and formatting protein and DNA sequences. *Biotechniques*, **28**, 1102, 1104.

68. Sanjana, N.E., Cong, L., Zhou, Y., Cunniff, M.M., Feng, G. and Zhang, F. (2012) A transcription activator-like effector toolbox for genome engineering. *Nat Protoc*, **7**, 171-192.

CHAPTER 2

Sequence Analysis of Minor Bands in HuR CLIP

ABSTRACT

High-throughput sequencing of RNA isolated by crosslinking immunoprecipitation (HITS-CLIP) allows for identification of RNA-binding protein binding sites across the transcriptome. In our HuR HITS-CLIP experiment, four bands appeared on the phosphorimage of the SDS-polyacrylamide gel. Among them, the band with the strongest signal (termed the major band) contained the target HuR-RNA complex and was used for analyzing HuR binding sequences in chapter 1. But the identities of the other three bands (termed minor bands) were unknown. Here, we determined the identities of minor bands through analyzing their contained RNA sequences. We found that the minor band libraries had different annotation breakdowns compared to major band libraries, and minor bands had more abundant miRNAs reads which are possibly derived from background binding. Moreover, no HuR motif was found in minor band libraries through de novo motif discovery, but this result could be explained by low sequencing depths of these libraries. Overall, our results imply that minor bands are not HuR bands; instead, they are largely attributable to background binding. Nevertheless, re-analysis of minor band libraries with higher sequencing depths is necessary to validate this preliminary conclusion.

INTRODUCTION

Identifying the binding targets of RNA-binding proteins (RBPs) is crucial for understanding the functions of RBPs. High-throughput sequencing of RNA isolated by crosslinking immunoprecipitation (HITS-CLIP) is a high-throughput RNA binding assay that identifies the RBP targets at the transcriptome-wide level (1). HITS-CLIP library construction starts with 254nm UV light treatment of cells that covalently crosslinks proteins and their proximal RNAs. Cells are then lysed, treated with RNases, and the protein of interest with attached RNAs (or together as the ribonucleoprotein (RNP) complex) are immunoprecipitated using a specific antibody to the RBP of interest. The 3' end of the RNA fragments within RNP complexes are radiolabeled by ligating with a RNA adapter while on bead. Then the RNP complexes are resolved on an SDS-polyacrylamide gel (SDS-PAGE), transferred to nitrocellulose membrane, and visualized by the radioactivity of RNA fragments in autoradiography. In theory, the size of the target RBP band on SDS-PAGE equals the addition of the size of the protein and the size of the bound RNA fragment. Accordingly, the band at the target RNP size is excised, from which RNAs are extracted, ligated with a 5' RNA adapter, followed by RNA sequencing. Among them, the band excision is a critical step for isolating the target RBP binding sequences.

In our HuR HITS-CLIP experiment, four bands appeared on the phosphorimage of SDS-PAGE (Figure 2.1). The band (termed the major band) with the strongest signal was at

around 43 kDa, which matched to the predicted size of the target HuR RNP complex, and therefore was used for analyzing HuR binding sequences in chapter 1. Additionally, motif analysis on the contained sequences showed the presence of putative HuR motifs, which further validated that they are true HuR bands. However, identities of the other three bands (termed minor bands) were unknown. Here, through comparing the annotation breakdowns of libraries, a clear difference was shown between minor bands and major bands, suggesting minor bands are unlikely to be HuR bands. Instead, they were suggested to have more background binding than major bands by the analysis of the involved miRNAs. Additionally, no HuR motifs were discovered in minor band libraries which could be either due to the lack of HuR binding sequences or their low sequencing depths. Correspondingly, re-analysis with consistently higher sequencing depths of minor band libraries is required for further validation of the current conclusion.

RESULTS

Minor and major bands in HuR CLIP

HITS-CLIP with a HuR antibody was performed in T-REx-293 and 293T cells. Due to the similarity of the cells, we considered them as biological replicates, with replicate 1 in T-REx-293 cells and replicates 2-4 in 293T cells. We named the four bands in each biological replicate as b1, b2, b3 and b4 in order of increasing band size. The major band, or b1, was the validated HuR band (Figure 2.1). The four replicates of b1, i.e. b1-rep1 through b1-rep4 were prepared into libraries as previously described (chapter 1). For

minor bands b2 to b4, we prepared only one library for each band. Specifically, the libraries of b3 and b4 were prepared from the first biological replicate and b2 was from the second biological replicate. To note, minor bands were deliberately sequenced at much lower sequencing depths compared to major bands, with an average sequencing coverage of 0.13 million reads versus 19 million reads (Table 2.1). In our library preparation, barcode sequences were introduced during adapter ligation to remove PCR duplicates, and therefore the barcode counts of reads were used to analyze the amount of sequences at identical locations.

We first asked whether the minor bands and major bands have cross-contamination which could be possibly introduced during gel purification steps. To address this, we examined the correlation of the levels of identical reads from CLIP libraries, where a high correlation is expected for cross-contamination. CLIP libraries prepared from the same SDS-PAGEs were examined in this analysis, including replicate 1 samples b1-rep1, b3 and b4, and replicate 2 samples b1-rep2 and b2. Comparisons between libraries from different biological replicates, i.e. b1-rep1 and b1-rep2/b2, were negative controls for cross-contamination. The correlations for libraries from the same biological replicates (R^2 = 0.51-0.62, Figure 2.2A and B) were numerically close to that for controls (R^2 = 0.47 and 0.55), indicating that the minor bands are unlikely to be cross-contaminated with the major bands on the same gels.

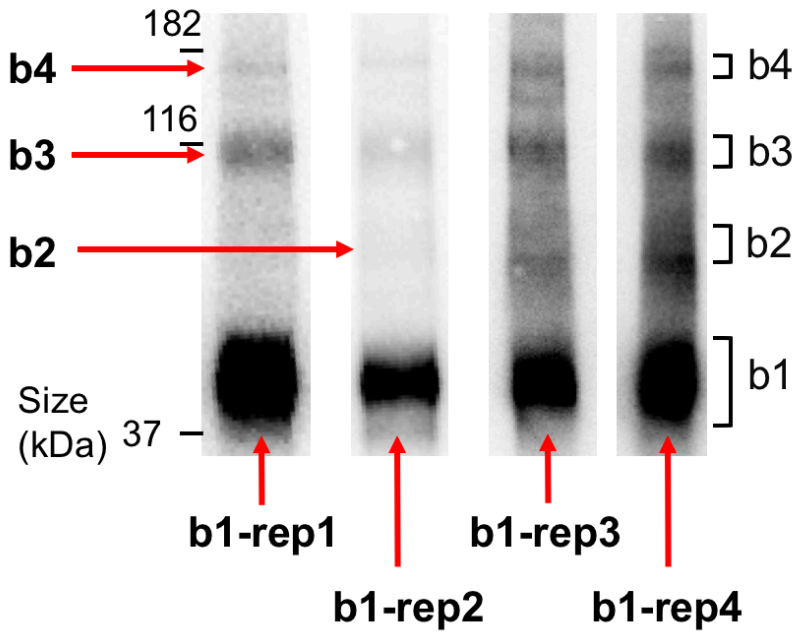

Figure 2.1. Phosphorimages of SDS-polyacrylamide gels show four radiolabeled ribonucleoprotein (RNP) bands in HuR CLIP.

Phosphorimages of four HuR CLIP biological replicates are shown and the excised regions are indicated by brackets. Samples for this analysis are indicated by red arrows.

Table 2.1. Read counts and barcode counts of HuR CLIP libraries.

Bands	Major				Minor		
	b1-rep1	b1-rep2	b1-rep3	b1-rep4	b2	b3	b4
Read counts	2,764,221	2,010,924	34,657,578	36,912,244	137,461	57,728	187,530
Barcode counts	28,070	41,083	473,331	341,030	2,339	3,699	1,615

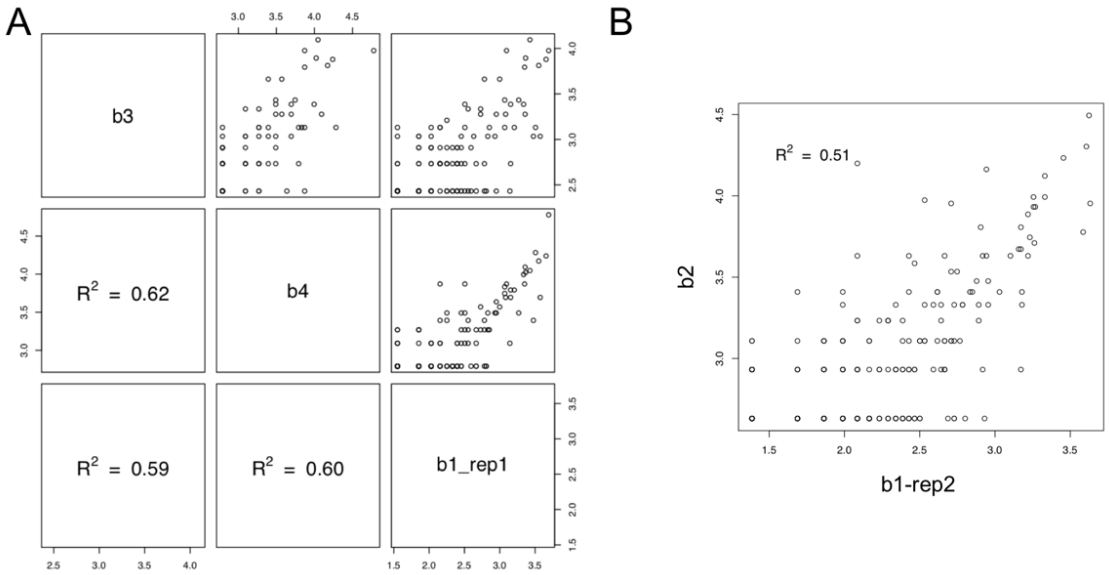

Figure 2.2. Correlations of the barcode counts of identical reads between libraries prepared from same SDS-PAGE gels.

A). Correlations for samples from replicate 1 including b1-rep1, b3 and b4. Scatterplot matrices of the log RPM (read per million) of identical reads from each data set are shown in upper panels with coefficient of determination values (R^2) displayed in lower panels. B). Correlations for samples from replicate 2 including b1-rep2 and b2. The log RPM of identical reads from the samples are plotted.

Annotation breakdown of the reads in CLIP libraries

We then compared the annotation breakdowns of the reads between major and minor band libraries (Figure 2.3). The annotation breakdowns were similar across the major bands, while the minor bands showed different patterns compared to the major bands. The difference of annotation breakdown was largely attributed to the top most abundant annotation classes. The top enriched classes in minor bands were intron, miRNA and 3'UTR. The high-abundance intron and 3'UTR reads also exist in the major bands as well as the previous HuR PAR-CLIP and iCLIP results (2-4). However, the large portion of miRNA reads was only observed in the three minor band libraries but not major bands,

though the difference between the two groups was only marginally significant due to high variance in the data (p-value=0.082, Welch's t-test). Additionally, the minor band libraries contained less introns (p-value=0.048, Welch's t-test) and less transposons (p-value=0.0032, Welch's t-test). The different annotation breakdowns of minor and major bands suggest that they are not from the same source, and thus, the minor bands are less likely to HuR bands. Furthermore, the annotation breakdowns of the three minor bands are different from each other, indicating that these minor bands could have different identities.

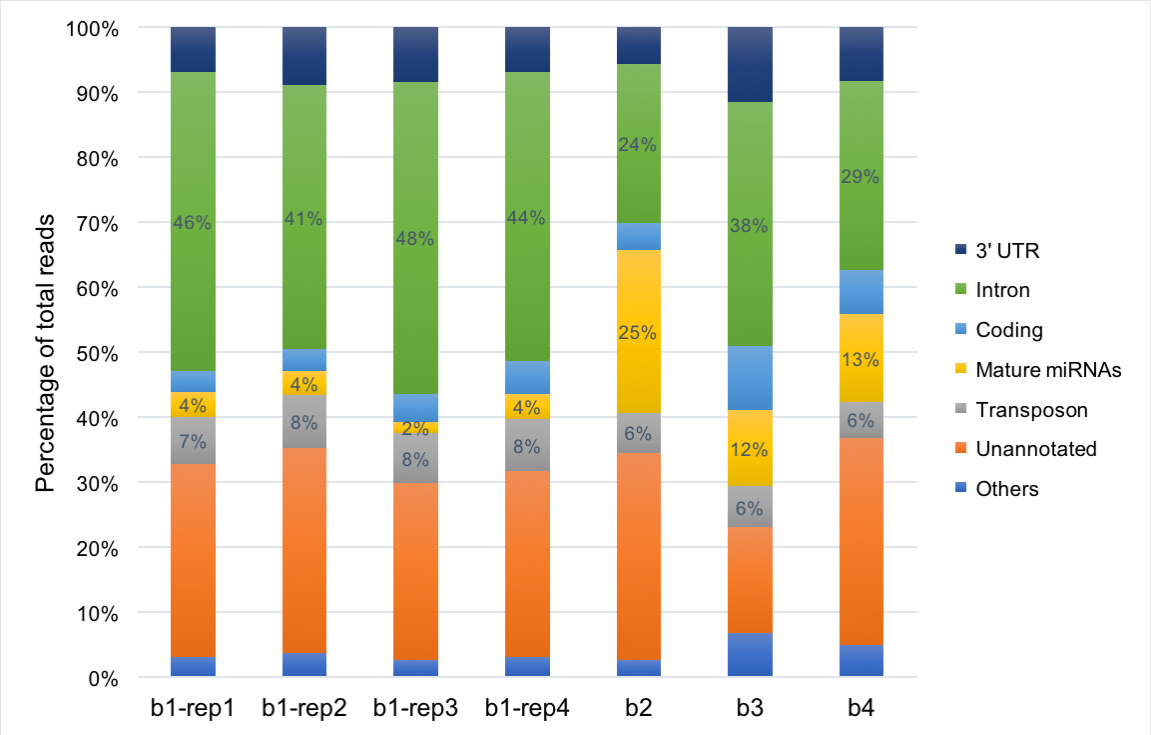

Figure 2.3. Annotation breakdown of unique locations from HuR CLIP libraries.

We combined the annotation class 'non-coding RNAs', '5'UTR', 'pre-miRNA', 'Simple RNA' and 'structural RNAs' into "Others" category because each of them occupied less than 4% of the barcode counts in libraries.

miRNA species in HuR CLIP libraries

In the annotation breakdown analysis, 2-4% of miRNA reads were in major bands, whereas this percentage was as high as 12-25% in minor bands. To find out the potential reason for the abundance of miRNAs in minor bands, we examined the involved miRNA species. The number of miRNAs in the seven CLIP libraries ranges from 31 to 232, which is positively correlated with the sizes of the libraries. Twenty-five miRNAs were overlapping among the seven CLIP libraries. This group of miRNAs altogether occupied 79-94% of the barcode counts of the miRNA category in all libraries, indicating that they can largely represent the miRNA population in those libraries. Consistently, those miRNAs were abundant miRNAs of all libraries, of which the abundance ranks were high in each library (Table 2.2). Additionally, the top 10 most abundant miRNAs of each library were largely overlapping across libraries (Table 2.2), further supporting the similarity of miRNA population in those libraries. We also found that those overlapping miRNAs were enriched with the most abundant cellular miRNAs, out of which nineteen were the top 100 most abundant miRNAs in 293T cells collected from the miRmine database (5). These results suggest that the miRNA content is largely similar among the libraries, and therefore they could be derived from the same source: very likely, the non-specific background binding. Taken together, despite the difference in percentage, the major band and minor bands have very similar collections of miRNA species, which were possibly derived from background binding. In turn, minor bands are likely to have more background binding than major bands.

Table 2.2. Twenty-five overlapping miRNAs were enriched in all CLIP libraries.

For each overlapping miRNA, its enrichment ranks for different data sets are shown and the top 10 ranks are highlighted in bold red.

No.	miRNAs	b1-rep1	b1-rep2	b1-rep3	b1-rep4	b2	b3	b4
1	miR-196b-5p	**2**	**2**	**2**	**2**	**3**	**1**	**1**
2	miR-30e-5p	**1**	**1**	**4**	**4**	**4**	**2**	**2**
3	miR-374a-5p	**7**	**5**	**1**	**1**	**1**	**4**	**7**
4	miR-30a-5p	**3**	**3**	**7**	**7**	**10**	**6**	**3**
5	miR-31-5p	**4**	**4**	**10**	**8**	**5**	**8**	**4**
6	miR-19a-3p	**5**	**6**	**9**	11	11	**3**	**5**
7	miR-20a-5p	**9**	**7**	**5**	**5**	**6**	**7**	11
8	miR-30d-5p	**6**	**8**	12	**10**	12	**5**	**6**
9	miR-21-5p	**10**	**9**	**6**	**6**	**8**	13	12
10	miR-142-3p	11	15	**3**	**3**	**2**	23	13
11	miR-34a-5p	12	**10**	14	14	13	**9**	**10**
12	miR-708-5p	**8**	12	16	15	15	11	**8**
13	miR-17-5p	16	13	13	13	14	**10**	**9**
14	miR-374b-5p	13	11	15	16	16	14	31
15	miR-93-5p	20	16	18	17	24	15	19
16	miR-186-5p	17	19	17	18	31	12	17
17	miR-221-3p	15	20	21	22	22	19	18
18	miR-188-5p	18	17	22	21	18	26	24
19	miR-18a-5p	44	22	29	32	21	18	14
20	miR-25-3p	31	27	28	28	36	20	26
21	miR-27b-3p	26	26	27	23	49	21	27
22	miR-324-3p	32	24	25	25	20	46	29
23	miR-222-3p	19	23	33	30	35	42	25
24	miR-15a-5p	42	41	31	31	26	25	16
25	miR-185-5p	43	36	36	46	46	22	23

Motif analysis on minor and major band data sets

Motif discovery and HuR motif searching

To further characterize the RNA sequences contained in the bands, we carried out motif analysis on the data. First we called peaks from the reads in CLIP libraries and performed de novo motif discovery using DREME (6). Major band libraries had more peaks and motifs compared to minor band libraries which were correlated to the higher sequencing depths of the libraries (Table 2.1, 2.3). The most enriched motifs of each library are displayed in Figure 2.4A.

To ask whether a band is a HuR band, we search for HuR motifs from the discovered motifs in each data set. HuR motifs are generally a poly U stretch or two poly U stretches inserted with a single guanosine or another nucleotide in the middle which were defined in current large-scale HuR binding sites studies (2-4,7-9). HuR motifs from RNAcompete were used as references (9), and motifs that assemble those motifs were counted as HuR motifs in this work. Motif comparison analysis was performed by TOMTOM using default settings (10). As expected, all major band libraries had HuR motifs, with counts ranging from 2-16. Whereas, notably, minor band libraries had no HuR motifs (Table 2.3). This difference in HuR motifs was also reflected in the most enriched motifs of all data sets. Motif T, as a HuR motif, was one of the most enriched motifs of major band data sets while it did not appear in minor band data sets (Figure 2.4A, Table 2.4). The absence of HuR motifs in minor band data sets could be caused by either the lack of HuR

binding sequences, or simply insufficient sequences due to lower sequencing depth of the minor band libraries.

To check the second possibility, we normalized the sequencing depth for all CLIP libraries to re-detect the enriched motifs. The CLIP libraries were subsampled to the lowest sequencing depth among them, which was 57,728 reads from the b3 library. Three sets of subsamples were analyzed, and the average number of peaks, motifs and HuR motifs were compared (Table 2.3). As expected, no HuR motifs were found in the subsampled minor band libraries. However, two of the subsampled b1 libraries did not have any HuR motifs, and the other two only had one HuR motif, indicating that the number of HuR motifs in the known HuR bands were at the detectable boundary with the low sequencing depth. Thus, we cannot rule out the possibility that the low sequencing depth led to the lack of HuR motifs in minor band libraries. Taken together, although minor band libraries did not have HuR motifs while the major bands did, we cannot firmly conclude that minor bands were not HuR bands in this analysis because the difference in HuR motifs could be due to the inconsistency in sequencing depths of the libraries. Correspondingly, a consistently higher sequencing depth on those libraries is required to determine the identity of minor bands.

Table 2.3. Comparison of motifs from major and minor band libraries and their subsampled libraries.

The motif counts in subsampled libraries were the average numbers of motifs from three subsamples.

Bands		b1-rep1	b1-rep2	b1-rep3	b1-rep4	b2	b3	b4
Original libraries	Peak counts	23,213	29,334	332,821	218,202	1,281	3,009	1,067
	Motif counts	20	27	79	73	2	4	1
	HuR motif counts	4	2	16	10	0	0	0
Subsampled libraries	Peak counts	605	1487	2,529	2,899	591	3,009	356
	Motif counts	1	3.3	4.7	5	1.3	4	1.3
	HuR motif counts	0	0	1	1	0	0	0

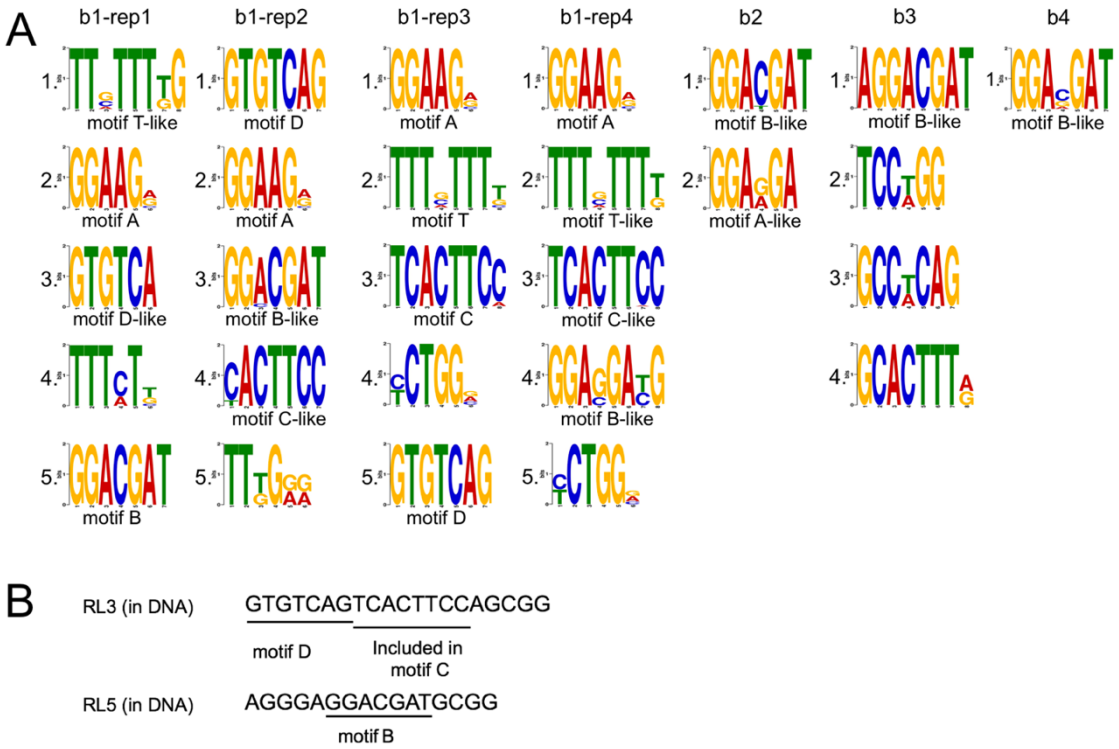

Figure 2.4. Top enriched motifs from HuR CLIP data sets and some of them matched with adapter sequences.

A). The top 5 most enriched motifs for major band data sets and all motifs for minor band data sets. B). Some of the most enriched motifs matched with RNA adapter sequences. The motif variations were indicated with the suffix "-like" and were counted as the original motifs. The ranks were based on the p-values for enrichment.

Other highly enriched motifs in HuR CLIP data sets

In addition to motif T, motif A-D were discovered as highly statistically enriched motifs in CLIP data sets (Figure 2.4A). GGAAGV, or motif A, presented in all four major band data sets and the b2 data set, occupied 12-13% of peak sequences on average, which was even higher than motif T (Table 2.4). It was the top enriched motif in filtered data sets where only peaks with more than 5 reads were kept (data not shown), suggesting that it

may be not simply due to random noise. Interestingly, a few similar motifs were discovered in Ago2, Pum1 and Pum2 CLIP data sets from our lab (8,11), including ARGGAR from Ago2 CLIP, DGGAAD, GGAGGYGG from Pum1 CLIP, and GGAAGR from Pum2 CLIP, indicating the prevalence of G-rich motifs across different RBP CLIPs.

The other top enriched motifs, motif B, C and D, have very definite sequences and match with parts of RNA adapter sequences used in the ligation reactions (Figure 2.4A, B, Table 2.4). Motifs B and C match with the middle part of the 5' adapter and 3' adapter, respectively, and motif D matches with the first 6 bases of 3' adapter. In addition to motif B-D, a few other discovered motifs also match with adapter sequences (data not shown). Motif B appeared in all HuR CLIP data sets, whereas motifs C and D appeared only in major band data sets (Table 2.4). Similarly, the absence of these motifs in minor band data sets could be due to the limited size of the data sets. Motif B, C, D were present at low frequency (less than 3%) in CLIP data sets (Table 2.4), and the high statistical enrichment could be due to the specificity of their sequences.

In sum, motifs A to D appeared in both major and minor band data sets, indicating the universality of their presence in our HuR CLIP data sets.

Table 2.4. Top enriched motifs and their occurrences in major and minor band data sets.

Motifs	Sequence logos	Sequences	Match	Occurrence of the motifs/variants in		Frequency (Average ± SEM)
				major bands	minor bands	
Motif T		TTTVTTTB	HuR motif	3	0	6.39 ± 0.60%
Motif A		GGAAGV	unknown	4	1	12.45 ± 1.27%
Motif B		GGACGAT	RL5 (adapter)	4	3	2.72 ± 1.30%
Motif C		TCACTTCM	RL3 (adapter)	4	0	0.65 ± 0.12%
Motif D		GTGTCAG	RL3 (adapter)	4	0	1.23 ± 0.37%

DISCUSSION

To distinguish the target RBP band from non-specific bands, a common practice is to set controls in parallel, e.g. an IgG antibody control and a HuR KO cell control, where the band not showing in control but present in the experimental sample is the target band. When the control is not available, or multiple bands are exclusively in the experimental sample, analyzing the sequences within the unknown bands is an alternate method to determine their identities. In the study first introducing Ago2 HITS-CLIP (12), two

discrete bands at 110 and 130 kDa appeared on the phosphorimage of the Ago2 IP sample while not observed in IgG control. Both bands could be the Ago2-mRNA complex since the sizes of the bands were higher than the size of individual Ago2 protein at 97 kDa. Through sequencing analysis, the majority (~80%) of the RNAs from 130 kDa band were aligned to genomic sequences while 110kDa band were to miRNAs, indicating that the 130 kDa is the target band for Ago2-mRNA complex while the 110 kDa band is mainly composed of Ago-miRNA complex. In our study, since we did not set the controls in the first place, we took advantage of the available minor band libraries, and determined the identities of minor bands using sequencing analysis.

We found that minor band and major band libraries had different annotation breakdowns. Notably, minor bands had more miRNAs than major bands, despite that their enriched miRNA species were highly similar. Their shared miRNAs were largely overlapping with most abundant cellular miRNAs, supporting the idea that the miRNAs come from non-specific binding in CLIP procedure. How come miRNAs are more abundant in minor bands? One hypothesis is that the minor bands have few RNAs and therefore the non-specific binding could be more predominant, and particularly, among all the non-specific binding sequences miRNAs have higher cloning efficiency in the CLIP procedure due to the following two properties, i.e., first, miRNAs are short RNAs with simple structure so may be cloned more efficiently; and second, miRNAs have a 3' hydroxyl group which possibly facilitates the 3' adapter ligation.

In addition to HuR motifs, we found a G-rich motif highly enriched across HuR CLIP data sets. Yet, G-rich motifs also appeared in other studies with controversial implications of functionality. Leung et al. showed that Ago2 HITS-CLIP in mouse embryonic cells yielded a consensus G-rich motif that modulated miRNA-mediated repression (13). The function of the G-rich motif suggests that it may not be a CLIP artifact but rather a de novo RBP motif. Additionally, Taliaferro et al. reported that in the Ago2 iCLIP of drosophila S2 cell nuclear extract, a G-rich stretch GGCGG, as the most enriched 5mer, was close to the mutation site/crosslinking site (14), suggesting its potential functionality. In contrast, a G-rich motif from HuR PAR-CLIP was implicated to be functionally irrelevant (15). This G-rich motif was the most enriched motif in background bands, suggesting that it is perhaps derived from background binding sequences.

Interestingly, several top enriched motifs match with either 5' or 3' RNA adapter sequence. Motif D was interpreted as a mispriming product of CLIP in (16). Specifically, random genome sequences with sequences match to the 5'end of 3' RNA adapter could be anchored by reverse transcription primer and then introduced into the final reads. Indeed, mispriming may occur, however, the bioinformatic 3' adapter clipping process removes the adapter sequences so the mispriming products will not be kept in the final product (see methods). Therefore, mispriming cannot account for the sources of the motif in our data sets. Instead, mistakes in cloning reactions could bring in those sequences into

the final reads, such as the partial duplication in PCR. Further investigations are required to validate this possibility.

Motifs analysis is a straightforward way to detect enriched sequences and is therefore powerful for examining the band identity. We show that the minor bands lack HuR motifs but this result can be explained by the insufficient sequencing depth of minor band libraries. To validate the current results, equal and sufficient sequencing depths for all the studied bands are required for motif analysis. In addition, with the same sequence depth, we could apply other comparative methods such as analyzing overlapping sites to examine the similarity of the libraries.

In summary, we determined the identities of minor bands in HuR HITS-CLIP by sequence analysis. The annotation breakdowns of minor and major bands are statistically different, suggesting that they are not from the same source. Analysis of miRNAs within these bands indicated that minor bands are largely attributable to background binding. Motif analysis in the minor band libraries is suggestive of their sources, but solid interpretations were hampered by low sequencing depth. Instead, high sequencing depth of minor band libraries will be useful in validating the minor band identities.

MATERIALS AND METHODS

HuR HITS-CLIP data analysis

Four HuR HITS-CLIP experiments were performed. Data analysis is the same as in chapter 1, except that peaks were called individually for each of the libraries. In brief, 3' adapter sequences in the raw reads were removed by fastx_clipper. Reads with identical sequences were collapsed and their barcodes were counted as the barcode count. Reads that are equal to or longer than 15nt were kept. Reads were annotated by bowtie2 and tophat. Peaks were called by FindPeaks.

Motif discovery and motif comparisons

Motifs were discovered by DREME (6) with default settings, except that the minimum width of motif was set at 6nt. The example code is:

dreme -oc sample.dreme -p sample.fasta -norc -mink 6

Represented motifs and their variations were counted together for each of the data sets as shown in Table 2.3. The variations of motifs were one base offset or (and) up-to-two bases mismatches, where the mismatched symbols were required to share at least one nucleotide.

Motifs were compared to motifs from the motif database "2013RNAcompete homo sapiens (DNA encoded RNA)" in TOMTOM with default settings (9,10). Reverse

complement matches were removed. HuR motifs were manually selected from the output. The example code is:

tomtom -no-ssc -oc . -verbosity 1 -min-overlap 5 -dist pearson -evalue -thresh 10.0 dremeoutput.txt Ray2013_rbp_Homo_sapiens.dna_encoded.meme

Correlation analysis in cross-contamination checks

Identical reads were selected through bedtools and manual filtering in Excel. First, bedtools were used to select reads from the first data set that are included in the reads from the second data set. Filter function in Excel was used to screen the identical reads. The example code used in bedtools is:

bedtools intersect -s -f 1 -r -a sample1.bed -b sample2bed -wa -wb > sample1_sample2.bed

The RPM of identical reads of two data sets were plotted in scatterplot and the corresponding correlations were calculated.

Ago2, Pum1 and 2 CLIP data sets

The Ago2, Pum1 and 2 CLIP data sets used in motif analysis were from CLIP experiments performed in our lab and the data were used in (11). Peaks were called from the pooled data of each CLIP.

REFERENCES

1. Licatalosi, D.D., Mele, A., Fak, J.J., Ule, J., Kayikci, M., Chi, S.W., Clark, T.A., Schweitzer, A.C., Blume, J.E., Wang, X. *et al.* (2008) HITS-CLIP yields genome-wide insights into brain alternative RNA processing. *Nature*, **456**, 464-469.

2. Mukherjee, N., Corcoran, D.L., Nusbaum, J.D., Reid, D.W., Georgiev, S., Hafner, M., Ascano, M., Jr., Tuschl, T., Ohler, U. and Keene, J.D. (2011) Integrative regulatory mapping indicates that the RNA-binding protein HuR couples pre-mRNA processing and mRNA stability. *Mol Cell*, **43**, 327-339.

3. Lebedeva, S., Jens, M., Theil, K., Schwanhausser, B., Selbach, M., Landthaler, M. and Rajewsky, N. (2011) Transcriptome-wide analysis of regulatory interactions of the RNA-binding protein HuR. *Mol Cell*, **43**, 340-352.

4. Uren, P.J., Burns, S.C., Ruan, J., Singh, K.K., Smith, A.D. and Penalva, L.O. (2011) Genomic analyses of the RNA-binding protein Hu antigen R (HuR) identify a complex network of target genes and novel characteristics of its binding sites. *J Biol Chem*, **286**, 37063-37066.

5. Panwar, B., Omenn, G.S. and Guan, Y. (2017) miRmine: a database of human miRNA expression profiles. *Bioinformatics*, **33**, 1554-1560.

6. Bailey, T.L. (2011) DREME: motif discovery in transcription factor ChIP-seq data. *Bioinformatics*, **27**, 1653-1659.

7. Nicholson, C.O., Friedersdorf, M. and Keene, J.D. (2017) Quantifying RNA binding sites transcriptome-wide using DO-RIP-seq. *RNA*, **23**, 32-46.

8. Li, Y., Estep, J.A. and Karginov, F.V. (2018) Transcriptome-wide Identification and Validation of Interactions between the miRNA Machinery and HuR on mRNA Targets. *J Mol Biol*, **430**, 285-296.

9. Ray, D., Kazan, H., Cook, K.B., Weirauch, M.T., Najafabadi, H.S., Li, X., Gueroussov, S., Albu, M., Zheng, H., Yang, A. *et al.* (2013) A compendium of RNA-binding motifs for decoding gene regulation. *Nature*, **499**, 172-177.

10. Gupta, S., Stamatoyannopoulos, J.A., Bailey, T.L. and Noble, W.S. (2007) Quantifying similarity between motifs. *Genome Biol*, **8**, R24.

11. Sternburg, E.L., Estep, J.A., Nguyen, D.K., Li, Y. and Karginov, F.V. (2018) Antagonistic and cooperative AGO2-PUM interactions in regulating mRNAs. *Scientific Reports*, **8**.

12. Chi, S.W., Zang, J.B., Mele, A. and Darnell, R.B. (2009) Argonaute HITS-CLIP decodes microRNA-mRNA interaction maps. *Nature*, **460**, 479-486.

13. Leung, A.K., Young, A.G., Bhutkar, A., Zheng, G.X., Bosson, A.D., Nielsen, C.B. and Sharp, P.A. (2011) Genome-wide identification of Ago2 binding sites from mouse embryonic stem cells with and without mature microRNAs. *Nat Struct Mol Biol*, **18**, 237-244.

14. Taliaferro, J.M., Aspden, J.L., Bradley, T., Marwha, D., Blanchette, M. and Rio, D.C. (2013) Two new and distinct roles for Drosophila Argonaute-2 in the nucleus: alternative pre-mRNA splicing and transcriptional repression. *Genes Dev*, **27**, 378-389.

15. Friedersdorf, M.B. and Keene, J.D. (2014) Advancing the functional utility of PAR-CLIP by quantifying background binding to mRNAs and lncRNAs. *Genome Biol*, **15**, R2.

16. Gillen, A.E., Yamamoto, T.M., Kline, E., Hesselberth, J.R. and Kabos, P. (2016) Improvements to the HITS-CLIP protocol eliminate widespread mispriming artifacts. *BMC Genomics*, **17**, 338.

APPENDICES

Appendix A

Identifying the HuR Regulatory Sites for HuR-miRNA Interactions

Previous studies have shown that the on the three HuR-miRNA overlapping sites, miRNA repression on the sites were affected by HuR presence, where antagonistic with HuR on BTG2 and CDK16 sites and cooperative with HuR on MSMO1. Here, we want to further investigate the interactions by identifying the HuR binding sites that are involved in interacting with miRNA regulation.

To select candidate HuR binding sites to test, top 10 6mers from HuR CLIP data sets and any AU stretch that are longer than 4nt within the study sequences were considered. Overall, one site from BTG2 and CDK16 and three sites from MSMO1 were selected. Two or three nucleotides within the sites were mutated to abolish potential HuR effect. We expected to see that in WT cell conditions the miRNA site activity altered in constructs with mHuR sites, compared to constructs with WT HuR sites (wHuR). Among the five sites, the mHuR site on BTG2 and the second mHuR sites on MSMO1 were shown to affect the miRNA site activities. In BTG2, the mHuR site context leads to a decreased activity from miRNA sites compared to that with wHuR site (Figure AA1), suggesting that the candidate HuR site antagonizes with miRNA's repression. This result is in line with the previous identified HuR-miRNA antagonism on the site (Chapter 1).

Interestingly, there is a further decrease in site activity when the mHuR constructs were tested in HuR KO cells (Figure AA1), which indicates that the mutated HuR site may not be the only site that HuR binds to and antagonizes with miRNAs on the BTG2 site.

In contrast, the mH2 site of MSMO1 increased site activity (Figure AA1), suggesting that the tested HuR site cooperates with miRNA's regulation, which agrees with previous HuR-miRNA cooperation model. However, in HuR KO cells, miRNA site activity with mHuR site is higher compared to that with wHuR site (Figure AA1), suggesting that the site has a repressive function independent from HuR protein. Therefore, it is possible that the candidate HuR site is regulated by not only HuR protein but also some other AU-rich binding proteins and the overall effect of the site is cooperation with miRNA's regulation.

Taken together, we validate a potential HuR binding site that HuR antagonizes with miRNA activity on BTG sites, though this site may not be the only HuR site that is responsible for the HuR-miRNA antagonism. we also find a site that cooperatively affects miRNA repression on MSMO1 site, which is likely bound by HuR and some other cooperative factors.

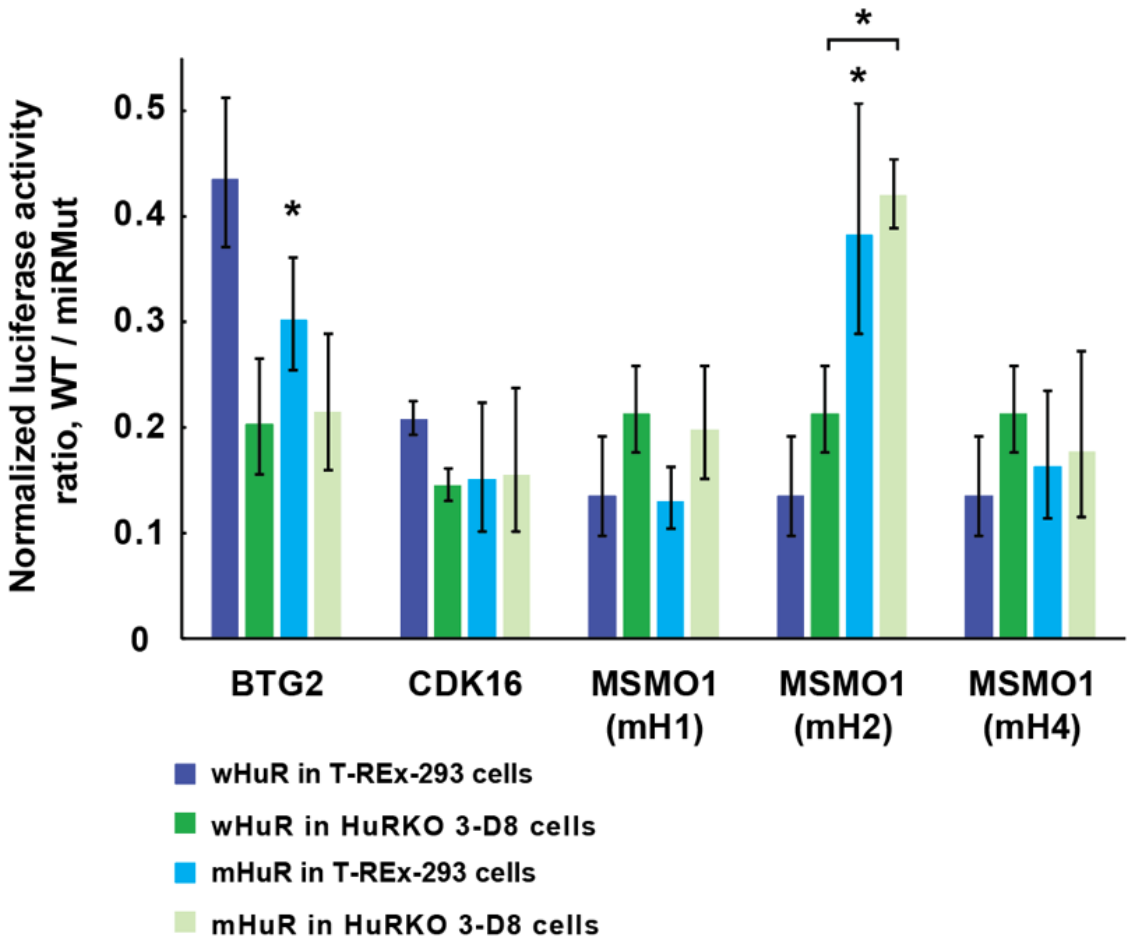

Figure AA1. Luciferase assay testing of candidate HuR binding sites.

wHuR construct testing in T-REx-293 and HuRKO 3-D8 cells were taken from a previous figure and added for comparison without significance asterisks. Comparison of WT/miRMut ratios between two groups was performed by two-tailed Welch's t-tests. Significance is indicated by asterisks: * $p<0.05$. Asterisk on top of bar indicates the group was compared to wHuR in T-REx-293 cells, other comparisons were indicated by a bracket. Error bars indicate one standard deviation.

Appendix B

Supplementary Figure S1.1-1.3

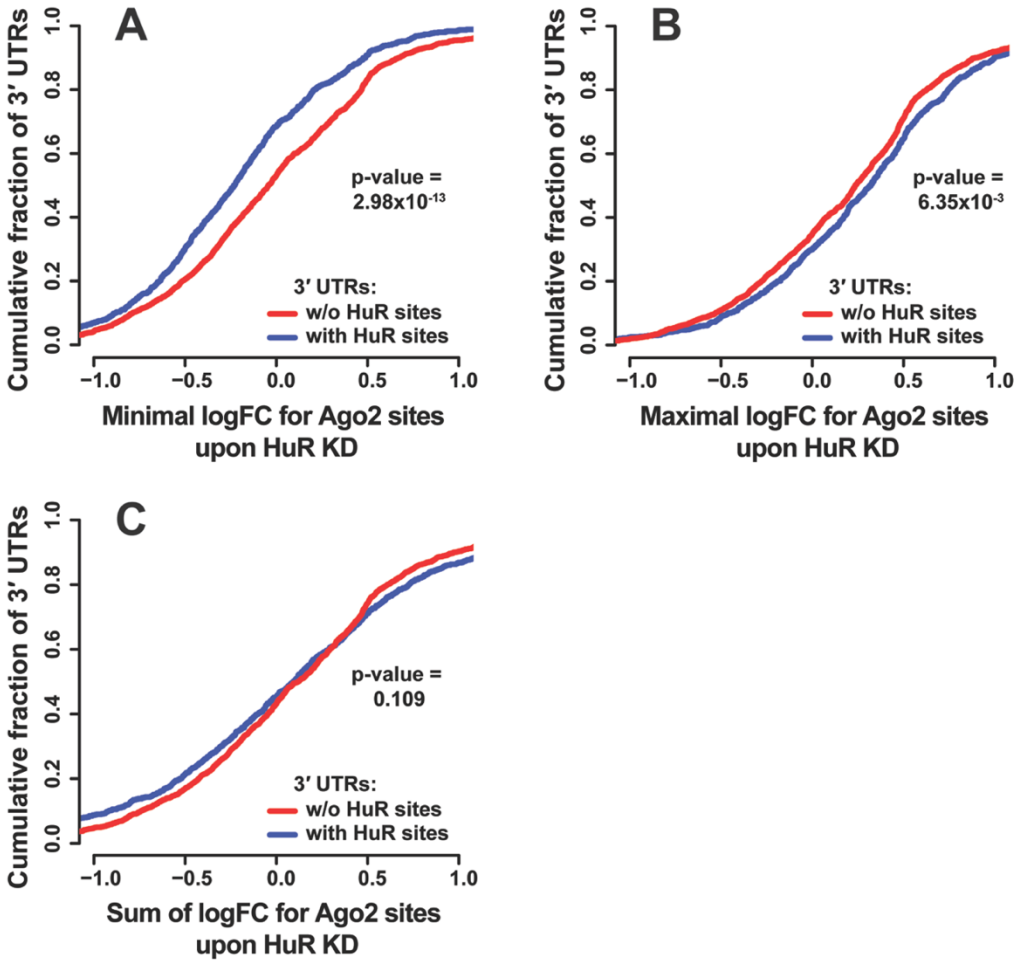

Figure S1.1. CLIP-Seq analysis of HuR-Ago2 interactions on the same 3′ UTR without mRNA level normalization.

Cumulative fraction plots of minimal (A), maximal (B), and sum (C) of the log fold change (logFC) of Ago2 sites upon HuR KD on 3′ UTRs with and without HuR.

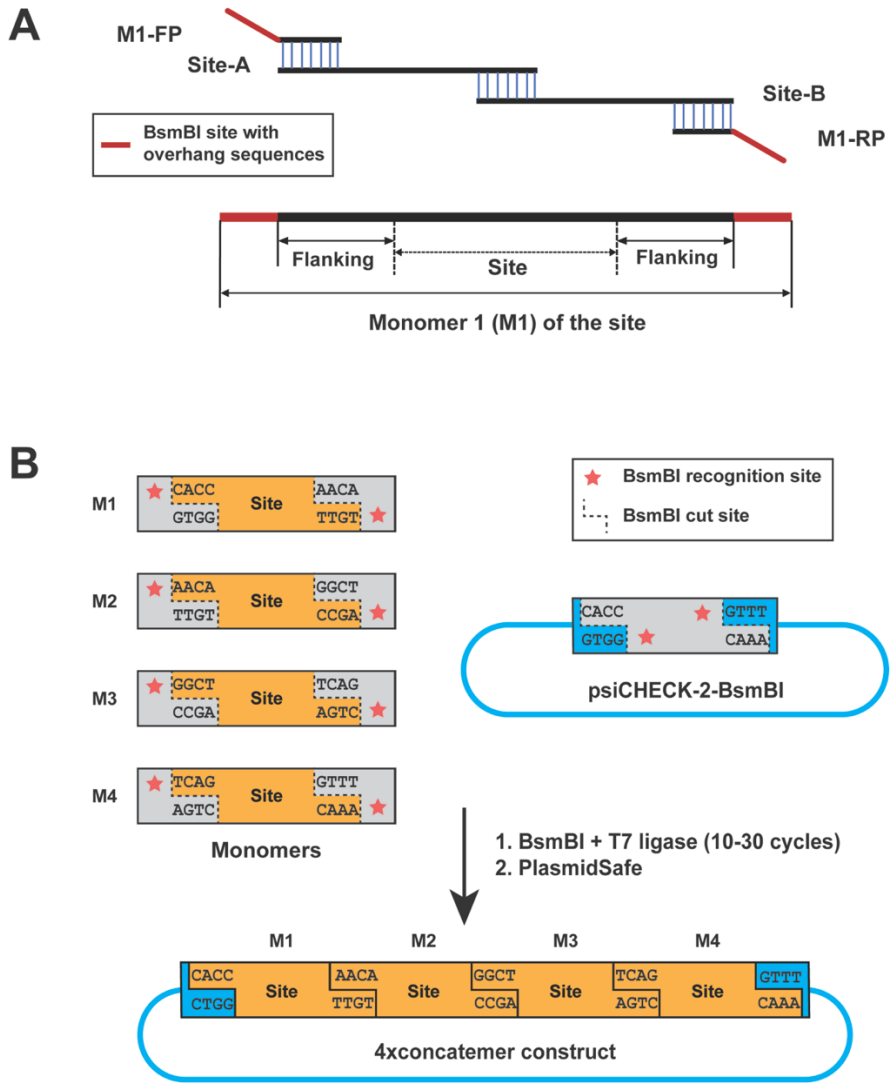

Figure S1.2. PCR design for monomer cloning and Golden Gate cloning design for luciferase reporter plasmid construction.

A) PCR design to clone monomers. Due to oligo length limits, the monomer was synthesized in two parts, A and B, with approximately 25 nts of overlap. Two outside primers were used to introduce GGC enzyme sites and unique overhangs by PCR. B) Golden Gate cloning design for luciferase reporter plasmid construction. The four monomers were assembled in the desired order guided by unique overhang sequences attached to each monomer.

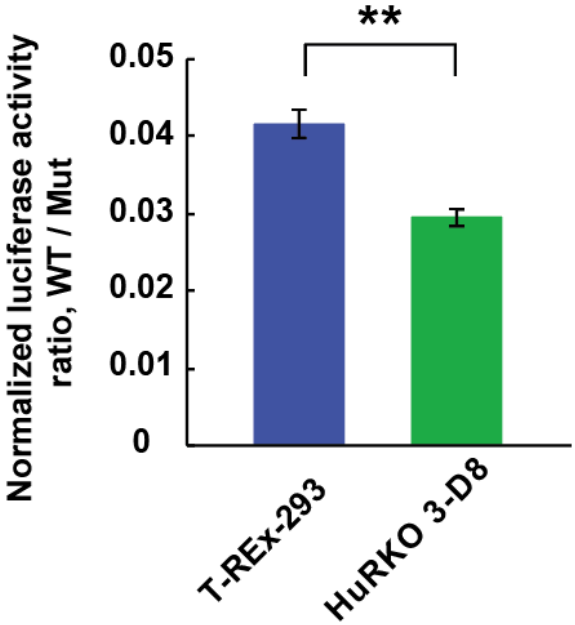

Figure S1.3. Luciferase assays of HuR-responsive positive control AU5.

Effects of the known HuR motif (a synthetic repetitive AUUUA-containing sequence) was tested by comparing luciferase activities of WT and mutant site constructs, i.e. WT/Mut ratio. HuR regulation of the site was assayed by comparing the WT/Mut ratio in T-REx-293 cells and HuRKO 3-D8 cells and statistically tested by two-tailed Welch's t-tests. Significance is indicated by asterisks: ** $p<0.01$. Error bars indicate one standard deviation.

Appendix C

Supplementary File 2

Monomer sequences of 4x concatenated candidate sites. The Ago2 CLIP and HuR CLIP sequences are indicated. The predicted miRNA seed and mutated nucleotides in mutant constructs are shown.

Legend:

Black/Default: Overlapping Ago2 site sequences.

Underline: Overlapping HuR site sequences.

Blue: (24-32nt) flanking sequences of Ago2 sites on each side.

Box: Predicted microRNA seed by TS7 or TS5.1.

Red: The mutated nucleotides.

>Myc_WT
CTTGTTTCAAATGCATGATCAAATGCAACCTCACAACCTTGGCTGAGTCT
TGAGACTGAAAGATTTAGCCATAATGTAAACTGCCTCAAATTGGACTTTG
GGCATAAAAGAACTTTTTTA

Mutate let-7 seed:
TGCCTCA → GGCAGGA

>BTG2_WT
CCGTATTTTCTAGGACAAGAGTTCTCAGTCACTGTGCAATATGCCCCCTG
GGTCCCAGGAGGGTCTGGAGGAAAACTGGCTATCAGAACCTCCTGATGCC
CTGG

Mutate miR-25-3p seed (also part of miR-128-3p seed):
GTGCAATA → ATACGTGA

>SNX17_WT
GAGCTGGCCCTCGATGCCAAATTAGCATTTAGTATTTTGCACAAAGTCTA
AGGGACCATGGCTGCCTGCCTTGGGGAGGAACCATATCTCCCTCT

Mutate part of the miR-19-3p seed:
TTTGCAC → ATTCGCT

>NEFL_WT
TCCTTTGAACCTTCGGTGGTTAGCAATTAAAGACCCTGAGTTATGTGCAATAAATAGTAAATAA
AGTTATACCGAATGATGTAT

Mutate part of miR-25 and 137 seed:
GCAATA → ACTGAA

>TIMM17B_WT
ACTGCCACCATGGGAGCTACTTCTCGGTTCCCTCCCCGATGGTCTACCTC
GAAGGGAGGGCTGGCTCCCAGTTAGCCCTGGGACCCTCCAGAGAGG

Mutate let-7-5p seed:
CTACCTC → CTCCTCA

>MSMO1_WT
TTAAAAACTGTATCTTGAAACTTTGTGAACTGACTTGCTGTATTTGCACT
TTGAGCTCTTGAAATAAATGTGATTTTTGTGTGATTATCTGGT

Mutate miR-130-3p seed (also covers part of the miR-19-3p and 17-5p seed):
TTGCACT → CATGTTC

>FAM98A_WT
TGGAAGAAATGCACTACAAAGTTAAGACAGATTTTTGCTAAGTGCAGGAG
GCCCTTTATTATTGCTGCAGAAAACAAAAGCCTGGCTGAGTTGATGTTTT
ACATTCTCCCTTA

Mutate miR-103-3p seed (also covers part of the miR-544 seed):
TGCTGCA → AGCTTCG

>JOSD1_WT
GCTTTTTGTTTTTCTTGCTTTTATTCCTTTTTGTTGTTGGCCTTGTGCTG
CGTTTGTTTACAAAAGATGTATTTTGTTTAACCAAATATTAAAA

Mutate part of the miR-30-5p seed (also covers part of the miR-495-3p seed):
TGTTTAC → TTTATGC

>PNRC1_WT
AATTTTAAGTGTGTGCTAAGGCACATGGAAGACCGATTTTATTTGCACAA
GGTACTGAGATTTTTTTCAAGAAACAGCTGT

Mutate part of the miR-19-3p seed:
TTTGCAC → CTATCTG

>HOXA10_WT
TACTTCTAATCTTAAATCAGAATAAATTAATATTGTATTGCTGCTGTGCG
TGGAAAAAGACGATGTTTATGTTCTTATAGAATAAAAGCT

Mutate miR-15-5p seed:
TGCTGCT → CTGTCGT

>RNF167_WT
TCCTGGTCTAATAACCCCCCACACATACACCTCTGGTGACCTATTTGCAC
AGACCGTCGTCTTCCCTCCAGTCTTCTGAGGG

Mutate part of the miR-19-3p seed and part of the miR-370-5p seed:
GACCTATTTGC → TTCTACGCAGT

>CDK16_WT
CCACCCCCTGCGTGTGGCCCTCCCACAGTATTTTGTGCAATGAAGCCCTG
CTCCCAGCCTTTCAGAGACAGGGACACAGCCCC

Mutate miR-25-3p seed:
GTGCAAT → TTACGGA

>WEE1_WT
ATCTTATATTTCTTTTTTTTTTAATTGTGAATTAGACTTGTATATCCCAC
TGGGAGCACTTTGTAGGCATTGCATGAACCATGGGATGATGATTCTGT

Mutate part of the miR-300 seed, and miR-17-5p seed (also covers part of the miR-302-3p seed):
CTTGTAT → TTACTTG
GCACTTT → ACGTCTT

Appendix D

Supplementary File 3

Supplementary File 3. Expression levels of candidate miRNAs.

Selecting candidate miRNAs combining information from the predicted miRNA target sites on overlapping sites and miRNA expression levels in the cells.

No.	Gene	miRNAs predicted to target the candidate sites by TargetScanHuman 7 or TargetScan 5.1 *	miRNA family members with high expression values **	Expression values (RPM) in HEK-293 cells ***
1	Myc	let-7b/c-5p	let-7b-5p	below 100
			let-7c-5p	438.7
2	BTG2	miR-25-3p/32-5p/92-3p/363-3p/367-3p	miR-25-3p	35906.7
			miR-92a-3p	29265.8, 27665.4
			miR-92b-3p	4176.4
			miR-363-3p	229.6
		miR-128-3p/216-3p/3681-3p	miR-128-3p	1905.9, 1757.2
		miR-146-5p/7153-5p	miR-146b-5p	192.3
3	SNX17	miR-19-3p	miR-19a-3p	427.6
			miR-19b-3p	461.2, 465
		miR-133-3p.1		below 100
		miR-182-5p		15354.7
		miR-96-5p/1271-5p		below 100
4	NEFL	miR-25-3p/32-5p/92-3p/363-3p/367-3p	see BTG2 for miR-25 family	
		miR-137		below 100
5	TIMM17B	let-7-5p/98-5p/4458/4500	let-7f-5p	5500, 5674.5
			let-7e-5p	1737.4
			let-7a-5p	1442.9, 1447.7, 1476.1
			let-7c-5p	438.7
			let-7i-5p	397.2
			let-7g-5p	357.1
6	MSMO1	miR-130-3p/301-3p/3666/4295/454-3p	miR-130a-3p	596.2
			miR-130b-3p	2127.2
			miR-301a-3p	3012.2
			miR-301b-3p	793.4
			miR-454-3p	132.4

		miR-19-3p	see SNX17 for miR-19-3p	
		miR-17-5p/20-5p/93-5p/106-5p/519-3p/526-3p	miR-17-5p	822.4
			miR-20a-5p	308.9
			miR-93-5p	7197.1
			miR-106b-5p	1360.2
		miR-223-3p		below 100
		miR-23-3p/103a-5p	miR-23b-3p	123.9
7	FAM98A	miR-103-3p/107	miR-103a-3p	5628.9, 5634.5
			miR-107	2204
		miR-544		below 100
8	JOSD1	miR-30-5p	miR-30a-5p	25806.2
			miR-30e-5p	7866.5
			miR-30d-5p	6123.6
			miR-30c-5p	1503.7, 1504.1
			miR-30b-5p	949
		miR-495-3p/5688		below 100
9	PNRC1	miR-19-3p	see SNX17 for miR-19-3p	
		miR-455-5p		131.6
		miR-216a-5p		below 100
10	HOXA10	miR-15-5p/16-5p/195-5p/424-5p/497-5p/6838-5p	miR-15b-5p	391.2
			miR-16-5p	9824.3, 9824.7
			miR-424-5p	149
11	RNF167	miR-370-5p		below 100
		miR-19-3p	see SNX17 for miR-19-3p	
12	CDK16	miR-25-3p/32-5p/92-3p/363-3p/367-3p	see BTG2 for miR-25 family	
		miR-200bc-3p/429		below 100
13	WEE1	miR-300/381-3p		below 100
		miR-302-3p/372-3p/373-3p/520-3p		below 100
		miR-17-5p/20-5p/93-5p/106-5p/519-3p/526-3p	see MSMO1 for miR-17 family	

* 1. miRNA sites disrupted in the mutant constructs are indicated in red. miRNA sites contained in the constructs' flanking regions outside of the Ago2 CLIP sites are indicated by the underline and were not mutated. 2. Myc is an exception, which was experimentally demonstrated by Kim, Kuwano *et al*, Genes & Dev. 2009
** High expression was defined as RPM >=100 from miRmine database: Panwar *et al*, Bioinformatics 2017
*** The multiple values were the expressions of miRNAs derived from multiple precursor miRNAs.

Appendix E

Supplementary File 1

Oligos information and site coordinates information.

Supplementary File 1a. siHuR sequences.

Name	Sequence
dsiHuR_2_guide	UUGAUCACCUCUGAGCUCGGG
dsiHuR_2_pass	CGAGCUCAGAGGUGAUCAAUU
dsiHuR_5_guide	UUGGCUGCAAACUUCACUGUG
dsiHuR_5_pass	CAGUGAAGUUUGCAGCCAAUU
gl3.1 sense	CUUACGCUGAGUACUUCGAUU
gl3.1 antisense	UCGAAGUACUCAGCGUAAGUU

Supplementary File 1b. Monomers coordinates.

Extended candidate Ago2 sites with flanking sequences (monomers)							
NO.	Gene	Strand	Ago2 site coordinates (BED format)			Length/nt	Flanking sequence length/nt
			Chr.	Start	End		
1	MYC	+	chr8	128753262	128753382	120	52
2	BTG2	+	chr1	203277591	203277695	104	52
3	SNX17	+	chr2	27599788	27599883	95	52
4	NEFL	-	chr8	24809886	24809970	84	52
5	TIMM17B	-	chrX	48750908	48751004	96	48
6	MSMO1	+	chr4	166264138	166264231	93	56
7	FAM98A	-	chr2	33808855	33808968	113	58
8	JOSD1	-	chr22	39081638	39081732	94	56
9	PNRC1	+	chr6	89794204	89794285	81	50
10	HOXA10	-	chr7	27210233	27210323	90	52
11	RNF167	+	chr17	4848300	4848382	82	52
12	CDK16	+	chrX	47088741	47088824	83	54
13	WEE1	+	chr11	9610573	9610671	98	52

Supplementary File 1c. HuR sites coordinates.

HuR sites that overlap with candidate Ago2 sites						
NO.	Gene	Strand	HuR site coordinates (BED format)			Length/nt
			Chr.	Start	End	
1	MYC	+	chr8	128753299	128753360	61
2	BTG2	+	chr1	203277617	203277644	27
3	SNX17	+	chr2	27599814	27599835	21
4	NEFL	-	chr8	24809912	24809937	25
5	TIMM17B	-	chrX	48750943	48750967	24
6	MSMO1	+	chr4	166264154	166264196	42
7	FAM98A	-	chr2	33808882	33808931	49
8	JOSD1	-	chr22	39081681	39081708	27
9	PNRC1	+	chr6	89794230	89794259	29
10	HOXA10	-	chr7	27210248	27210293	45
11	RNF167	+	chr17	4848334	4848355	21
12	CDK16	+	chrX	47088770	47088816	46
13	WEE1	+	chr11	9610580	9610639	59

Supplementary File 1d. Sequences for introducing BsmBI sites into psiCHECK-2.

The cutting sites were XhoI and NotI in multiple cloning sites region.

Sequences that introduce the BsmBI sites.

Forward strand 5'-3'	TCGACACCAGAGACGGACGTCTCTGTTT
reverse strand 5'-3'	GGCCAAACAGAGACGTCCGTCTCTGGTG

Sequencing primers

sequencing primer P1, 5'-3'	CGAGTTCGTGAAGGTGAAG
sequencing primer P2, 5'-3'	GTCAGACAAACCCTAACCAC

Supplementary File 1e. Oligos for monomer cloning.

A. Oligos for cloning templates

Name	Sequence
Myc-A	CTTGTTTCAAATGCATGATCAAATGCAACCTCACAACCTTGGCTGAGTCTTGAGACTGAAAGATTTAGCCATA
BTG2-WT-A	CCGTATTTTCTAGGACAAGAGTTCTCAGTCACTGTGCAATATGCCCCCTGGGTCCCAGGAGGGT
BTG2-mut-A	CCGTATTTTCTAGGACAAGAGTTCTCAGTCACTATACGTGATGCCCCCTGGGTCCCAGGAGGGT
SNX17-WT-A	GAGCTGGCCCTCGATGCCAAATTAGCATTTAGTATTTTGCACAAAGTCTAAGGGACCATGGC
SNX17-mut-A	GAGCTGGCCCTCGATGCCAAATTAGCATTTAGTATATTCGCTAAAGTCTAAGGGACCATGGC
NEFL-A	TCCTTTGAACCTTCGGTGGTTAGCAATTAAAGACCCTGAGTTATGT
TIMM17B-A	ACTGCCACCATGGGAGCTACTTCTCGGTTCCCTCCCCGATGGT
MSMO1-A	TTAAAAACTGTATCTTGAAACTTTGTGAACTGACTTGCTGTAT
FAM98A-A	TGGAAGAAATGCACTACAAAGTTAAGACAGATTTTTGCTAAGTGCAGGAGGCCCTTTATTAT
JOSD1-A	GCTTTTTGTTTTTCTTGCTTTTATTCCTTTTTGTTGTTGGCCTTGTGCTGCGTT
Myc-WT-B	TAAAAAAGTTCTTTTATGCCCAAAGTCCAATTTGAGGCAGTTTACATTATGGCTAAATCTTTCAGTCTCAAG
Myc-mut-B	TAAAAAAGTTCTTTTATGCCCAAAGTCCAATTTCCTGCCGTTTACATTATGGCTAAATCTTTCAGTCTCAAG
BTG2-B	CCAGGGCATCAGGAGGTTCTGATAGCCAGTTTTCCTCCAGACCCTCCTGGGACCCAGGGGGCA
SNX17-B	AGAGGGAGATATGGTTCCTCCCCAAGGCAGGCAGCCATGGTCCCTTAGACTTT
NEFL-WT-B	ATACATCATTCGGTATAACTTTATTTACTATTTATTGCACATAACTCAGGGTCTTTAA
NEFL-mut-B	ATACATCATTCGGTATAACTTTATTTACTATTTTCAGTACATAACTCAGGGTCTTTAA
TIMM17B-WT-B	CCTCTCTGGAGGGTCCCAGGGCTAACTGGGAGCCAGCCCTCCCTTCGAGGTAGACCATCGGGGAGGGAACCGA

TIMM17B-mut-B	CCTCTCTGGAGGGTCCCAGGGCTAACTGGGAGCCAGCCCTCCCTTCTGAGGAGACCATCGGGGAGGGAACCGA
MSMO1-WT-B	ACCAGATAATCACACAAAAATCACATTTATTTCAAGAGCTCAAAGTGCAAATACAGCAAGTCAGTTCACA
MSMO1-mut-B	ACCAGATAATCACACAAAAATCACATTTATTTCAAGAGCTCAAGAACATGATACAGCAAGTCAGTTCACA
FAM98A-WT-B	TAAGGGAGAATGTAAAACATCAACTCAGCCAGGCTTTTGTTTTCTGCAGCAATAATAAAGGGCCTCCTGCA
FAM98A-mut-B	TAAGGGAGAATGTAAAACATCAACTCAGCCAGGCTTTTGTTTTCCGAAGCTATAATAAAGGGCCTCCTGCA
JOSD1-WT-B	TTTTAATATTTGGTTAAACAAAATACATCTTTTGTAAACAAACGCAGCACAAGGCCAACA
JOSD1-mut-B	TTTTAATATTTGGTTAAACAAAATACATCTTTTGCATAAAAACGCAGCACAAGGCCAACA
PNRC1-WT-A	AATTTTAAGTGTGTGCTAAGGCACATGGAAGACCGATTTTATTTGCACAAGGT
PNRC1-WT-B	ACAGCTGTTTCTTGAAAAAAATCTCAGTACCTTGTGCAAATAAAATCGGTCTT
PNRC1-mut-A	AATTTTAAGTGTGTGCTAAGGCACATGGAAGACCGATTTTACTATCTGAAGGT
PNRC1-mut-B	ACAGCTGTTTCTTGAAAAAAATCTCAGTACCTTCAGATAGTAAAATCGGTCTT
HOXA10-WT-A	TACTTCTAATCTTAAATCAGAATAAATTAATATTGTATTGCTGCTGTGCGTGGAAAA
HOXA10-WT-B	AGCTTTTATTCTATAAGAACATAAACATCGTCTTTTTCCACGCACAGCAGCAATACA
HOXA10-mut-A	TACTTCTAATCTTAAATCAGAATAAATTAATATTGTATCTGTCGTGTGCGTGGAAAA
HOXA10-mut-B	AGCTTTTATTCTATAAGAACATAAACATCGTCTTTTTCCACGCACACGACAGATACA
RNF167-WT-A	TCCTGGTCTAATAACCCCCCACACATACACCTCTGGTGACCTATTTGCACAGA
RNF167-WT-B	CCCTCAGAAGACTGGAGGGAAGACGACGGTCTGTGCAAATAGGTCACCAGAGG
RNF167-mut-A	TCCTGGTCTAATAACCCCCCACACATACACCTCTGGTTTCTACGCAGTACAGA
RNF167-mut-B	CCCTCAGAAGACTGGAGGGAAGACGACGGTCTGTACTGCGTAGAAACCAGAGG
CDK16-WT-A	CCACCCCCTGCGTGTGGCCCTCCCACAGTATTTTGTGCAATGAAGCCCTGCTCC

CDK16-WT-B	GGGGCTGTGTCCCTGTCTCTGAAAGGCTGGGAGCAGGGCTTCATTGCACAAAAT
CDK16-mut-A	CCACCCCCTGCGTGTGGCCCTCCCACAGTATTTTTTACGGAGAAGCCCTGCTCC
CDK16-mut-B	GGGGCTGTGTCCCTGTCTCTGAAAGGCTGGGAGCAGGGCTTCTCCGTAAAAAAT
WEE1-WT-A	ATCTTATATTTCTTTTTTTTTTAATTGTGAATTAGACTTGTATATCCCACTGGGAGCACTTT
WEE1-WT-B	ACAGAATCATCATCCCATGGTTCATGCAATGCCTACAAAGTGCTCCCAGTGGGATATACAAG
WEE1-mut-A	ATCTTATATTTCTTTTTTTTTTAATTGTGAATTAGATTACTTGATCCCACTGGGAACGTCTT
WEE1-mut-B	ACAGAATCATCATCCCATGGTTCATGCAATGCCTACAAGACGTTCCCAGTGGGATCAAGTAA

B. Oligos for primers

Name	Sequence
Myc_M1_FP	GCGTCTCTCACCCTT GTT TCA AAT GCA TGA TCA AAT
Myc_M1_RP	GCGTCTCTTGTTTAA AAA AGT TCT TTT ATG CCC AAA G
Myc_M2_FP	GCGTCTCTAACACTT GTT TCA AAT GCA TGA TCA AAT
Myc_M2_RP	GCGTCTCTAGCCTAA AAA AGT TCT TTT ATG CCC AAA G
Myc_M3_FP	GCGTCTCTGGCTCTT GTT TCA AAT GCA TGA TCA AAT
Myc_M3_RP	GCGTCTCTCTGATAA AAA AGT TCT TTT ATG CCC AAA G
Myc_M4_FP	GCGTCTCTTCAGCTT GTT TCA AAT GCA TGA TCA AAT
Myc_M4_RP	GCGTCTCTAAACTAA AAA AGT TCT TTT ATG CCC AAA G
BTG2_M1_FP	GCGTCTCTCACCCCG TAT TTT CTA GGA CAA GAG TTC TC
BTG2_M1_RP	GCGTCTCTTGTTCCA GGG CAT CAG GAG GT
BTG2_M2_FP	GCGTCTCTAACACCG TAT TTT CTA GGA CAA GAG TTC TC
BTG2_M2_RP	GCGTCTCTAGCCCCA GGG CAT CAG GAG GT
BTG2_M3_FP	GCGTCTCTGGCTCCG TAT TTT CTA GGA CAA GAG TTC TC
BTG2_M3_RP	GCGTCTCTCTGACCA GGG CAT CAG GAG GT
BTG2_M4_FP	GCGTCTCTTCAGCCG TAT TTT CTA GGA CAA GAG TTC TC
BTG2_M4_RP	GCGTCTCTAAACCCA GGG CAT CAG GAG GT
SNX17_M1_FP	GCGTCTCTCACCGAG CTG GCC CTC GAT GC
SNX17_M1_RP	GCGTCTCTTGTTAGA GGG AGA TAT GGT TCC TCC C
SNX17_M2_FP	GCGTCTCTAACAGAG CTG GCC CTC GAT GC
SNX17_M2_RP	GCGTCTCTAGCCAGA GGG AGA TAT GGT TCC TCC C

SNX17_M3_FP	GCGTCTCTGGCTGAG CTG GCC CTC GAT GC
SNX17_M3_RP	GCGTCTCTCTGAAGA GGG AGA TAT GGT TCC TCC C
SNX17_M4_FP	GCGTCTCTTCAGGAG CTG GCC CTC GAT GC
SNX17_M4_RP	GCGTCTCTAAACAGA GGG AGA TAT GGT TCC TCC C
NEFL_M1_FP	GCGTCTCTCACCTCC TTT GAA CCT TCG GTG
NEFL_M1_RP	GCGTCTCTTGTTATA CAT CATTCG GTA TAA CTT TAT TT
NEFL_M2_FP	GCGTCTCTAACATCC TTT GAA CCT TCG GTG
NEFL_M2_RP	GCGTCTCTAGCCATA CAT CATTCG GTA TAA CTT TAT TT
NEFL_M3_FP	GCGTCTCTGGCTTCC TTT GAA CCT TCG GTG
NEFL_M3_RP	GCGTCTCTCTGAATA CAT CATTCG GTA TAA CTT TAT TT
NEFL_M4_FP	GCGTCTCTTCAGTCC TTT GAA CCT TCG GTG
NEFL_M4_RP	GCGTCTCTAAACATA CAT CATTCG GTA TAA CTT TAT TT
TIMM17B_M1_FP	GCGTCTCTCACCACT GCC ACC ATG GGA GCT
TIMM17B_M1_RP	GCGTCTCTTGTTCCT CTC TGG AGG GTC CCA G
TIMM17B_M2_FP	GCGTCTCTAACAACT GCC ACC ATG GGA GCT
TIMM17B_M2_RP	GCGTCTCTAGCCCCT CTC TGG AGG GTC CCA G
TIMM17B_M3_FP	GCGTCTCTGGCTACT GCC ACC ATG GGA GCT
TIMM17B_M3_RP	GCGTCTCTCTGACCT CTC TGG AGG GTC CCA G
TIMM17B_M4_FP	GCGTCTCTTCAGACT GCC ACC ATG GGA GCT
TIMM17B_M4_RP	GCGTCTCTAAACCCT CTC TGG AGG GTC CCA G
MSMO1_M1_FP	GCGTCTCTCACCTTA AAA ACT GTA TCT TGA AAC TTT G
MSMO1_M1_RP	GCGTCTCTTGTTACC AGA TAA TCA CAC AAA AAT C
MSMO1_M2_FP	GCGTCTCTAACATTA AAA ACT GTA TCT TGA AAC TTT G
MSMO1_M2_RP	GCGTCTCTAGCCACC AGA TAA TCA CAC AAA AAT C
MSMO1_M3_FP	GCGTCTCTGGCTTTA AAA ACT GTA TCT TGA AAC TTT G
MSMO1_M3_RP	GCGTCTCTCTGAACC AGA TAA TCA CAC AAA AAT C
MSMO1_M4_FP	GCGTCTCTTCAGTTA AAA ACT GTA TCT TGA AAC TTT G
MSMO1_M4_RP	GCGTCTCTAAACACC AGA TAA TCA CAC AAA AAT C
FAM98A_M1_FP	GCGTCTCTCACCTGG AAG AAA TGC ACT ACA AAG
FAM98A_M1_RP	GCGTCTCTTGTTTAA GGG AGA ATG TAA AAC ATC AA
FAM98A_M2_FP	GCGTCTCTAACATGG AAG AAA TGC ACT ACA AAG
FAM98A_M2_RP	GCGTCTCTAGCCTAA GGG AGA ATG TAA AAC ATC AA
FAM98A_M3_FP	GCGTCTCTGGCTTGG AAG AAA TGC ACT ACA AAG
FAM98A_M3_RP	GCGTCTCTCTGATAA GGG AGA ATG TAA AAC ATC AA
FAM98A_M4_FP	GCGTCTCTTCAGTGG AAG AAA TGC ACT ACA AAG
FAM98A_M4_RP	GCGTCTCTAAACTAA GGG AGA ATG TAA AAC ATC AA
JOSD1_M1_FP	GCGTCTCTCACCGCT TTT TGT TTT TCT TGC TT

JOSD1_M1_RP	GCGTCTCTTGTTTTT TAA TAT TTG GTT AAA CAA AAT AC
JOSD1_M2_FP	GCGTCTCTAACAGCT TTT TGT TTT TCT TGC TT
JOSD1_M2_RP	GCGTCTCTAGCCTTT TAA TAT TTG GTT AAA CAA AAT AC
JOSD1_M3_FP	GCGTCTCTGGCTGCT TTT TGT TTT TCT TGC TT
JOSD1_M3_RP	GCGTCTCTCTGATTT TAA TAT TTG GTT AAA CAA AAT AC
JOSD1_M4_FP	GCGTCTCTTCAGGCT TTT TGT TTT TCT TGC TT
JOSD1_M4_RP	GCGTCTCTAAACTTT TAA TAT TTG GTT AAA CAA AAT AC
PNRC1_M1_FP	GCGTCTCTCACCAAT TTT AAG TGT GTG CTA AGG C
PNRC1_M1_RP	GCGTCTCTTGTTACA GCT GTT TCT TGA AAA AAA TCT
PNRC1_M2_FP	GCGTCTCTAACAAAT TTT AAG TGT GTG CTA AGG C
PNRC1_M2_RP	GCGTCTCTAGCCACA GCT GTT TCT TGA AAA AAA TCT
PNRC1_M3_FP	GCGTCTCTGGCTAAT TTT AAG TGT GTG CTA AGG C
PNRC1_M3_RP	GCGTCTCTCTGAACA GCT GTT TCT TGA AAA AAA TCT
PNRC1_M4_FP	GCGTCTCTTCAGAAT TTT AAG TGT GTG CTA AGG C
PNRC1_M4_RP	GCGTCTCTAAACACA GCT GTT TCT TGA AAA AAA TCT
HOXA10_M1_FP	GCGTCTCTCACCTAC TTC TAA TCT TAA ATC AGA ATA AA
HOXA10_M1_RP	GCGTCTCTTGTTAGC TTT TAT TCT ATA AGA ACA TAA AC
HOXA10_M2_FP	GCGTCTCTAACATAC TTC TAA TCT TAA ATC AGA ATA AA
HOXA10_M2_RP	GCGTCTCTAGCCAGC TTT TAT TCT ATA AGA ACA TAA AC
HOXA10_M3_FP	GCGTCTCTGGCTTAC TTC TAA TCT TAA ATC AGA ATA AA
HOXA10_M3_RP	GCGTCTCTCTGAAGC TTT TAT TCT ATA AGA ACA TAA AC
HOXA10_M4_FP	GCGTCTCTTCAGTAC TTC TAA TCT TAA ATC AGA ATA AA
HOXA10_M4_RP	GCGTCTCTAAACAGC TTT TAT TCT ATA AGA ACA TAA AC
RNF167_M1_FP	GCGTCTCTCACCTCC TGG TCT AAT AAC CCC C
RNF167_M1_RP	GCGTCTCTTGTTCCC TCA GAA GAC TGG AGG
RNF167_M2_FP	GCGTCTCTAACATCC TGG TCT AAT AAC CCC C
RNF167_M2_RP	GCGTCTCTAGCCCCC TCA GAA GAC TGG AGG
RNF167_M3_FP	GCGTCTCTGGCTTCC TGG TCT AAT AAC CCC C
RNF167_M3_RP	GCGTCTCTCTGACCC TCA GAA GAC TGG AGG
RNF167_M4_FP	GCGTCTCTTCAGTCC TGG TCT AAT AAC CCC C
RNF167_M4_RP	GCGTCTCTAAACCCC TCA GAA GAC TGG AGG
CDK16_M1_FP	GCGTCTCTCACCCCA CCC CCT GCG TGT GGC
CDK16_M1_RP	GCGTCTCTTGTTGGG GCT GTG TCC CTG TCT CTG AAA G
CDK16_M2_FP	GCGTCTCTAACACCA CCC CCT GCG TGT GGC
CDK16_M2_RP	GCGTCTCTAGCCGGG GCT GTG TCC CTG TCT CTG AAA G
CDK16_M3_FP	GCGTCTCTGGCTCCA CCC CCT GCG TGT GGC
CDK16_M3_RP	GCGTCTCTCTGAGGG GCT GTG TCC CTG TCT CTG AAA G

CDK16_M4_FP	GCGTCTCTTCAGCCA CCC CCT GCG TGT GGC
CDK16_M4_RP	GCGTCTCTAAACGGG GCT GTG TCC CTG TCT CTG AAA G
WEE1_M1_FP	GCGTCTCTCACCATC TTA TAT TTC TTT TTT TTT TAA TT
WEE1_M1_RP	GCGTCTCTTGTTACA GAA TCA TCA TCC CAT
WEE1_M2_FP	GCGTCTCTAACAATC TTA TAT TTC TTT TTT TTT TAA TT
WEE1_M2_RP	GCGTCTCTAGCCACA GAA TCA TCA TCC CAT
WEE1_M3_FP	GCGTCTCTGGCTATC TTA TAT TTC TTT TTT TTT TAA TT
WEE1_M3_RP	GCGTCTCTCTGAACA GAA TCA TCA TCC CAT
WEE1_M4_FP	GCGTCTCTTCAGATC TTA TAT TTC TTT TTT TTT TAA TT
WEE1_M4_RP	GCGTCTCTAAACACA GAA TCA TCA TCC CAT

Supplementary File 1f. Sequences for introducing BsmBI sites into pRL-TK.

The cutting sites were XbaI and NotI in multiple cloning sites region.

Sequences that introduce the BsmBI sites.

Forward strand 5'-3'	CTAGCACCAGAGACGGACGTCTCTGTTT
reverse strand 5'-3'	GGCCAAACAGAGACGTCCGTCTCTGGTG

Sequencing primers

sequencing primer P1, 5'-3'	GTCTTCATTTTTCGCAAGAA
sequencing primer P2, 5'-3'	ATTCTAGTTGTGGTTTGTCC

Supplementary File 1g. Monomer sequences of known HuR target AU5.

Monomer	Sequence
AU5 WT	ATTTATTTATTTATTTATTTA
AU5 Mut	AGGTAGGTAGGTAGGTAGGTA

Red indicates the nucleotides being mutated.

Supplementary File 1h. Oligos for HuR target cloning.

Name	Sequence
4X AU5_WT_M1_FP	GCGTCTCTCACCATTTATTTATTTATTTATTTAAAC AAG AGA CGC
4X AU5_WT_M2_FP	GCGTCTCTAACAATTTATTTATTTATTTATTTAGGC TAG AGA CGC
4X AU5_WT_M3_FP	GCGTCTCTGGCTATTTATTTATTTATTTATTTATCA GAG AGA CGC
4X AU5_WT_M4_FP	GCGTCTCTTCAGATTTATTTATTTATTTATTTAGTT TAG AGA CGC
4X AU5_WT_M1_RP	GCGTCTCTTGTTTAAATAAATAAATAAATAAATGGTGAGAGACGC
4X AU5_WT_M2_RP	GCGTCTCTAGCCTAAATAAATAAATAAATAAATTGTTAGAGACGC
4X AU5_WT_M3_RP	GCGTCTCTCTGATAAATAAATAAATAAATAAATAGCCAGAGACGC
4X AU5_WT_M4_RP	GCGTCTCTAAACTAAATAAATAAATAAATAAATCTGAAGAGACGC
4X AU5_mut_M1_FP	GCGTCTCTCACCAGGTAGGTAGGTAGGTAGGTAAAC AAG AGA CGC
4X AU5_mut_M2_FP	GCGTCTCTAACAAGGTAGGTAGGTAGGTAGGTAGGC TAG AGA CGC
4X AU5_mut_M3_FP	GCGTCTCTGGCTAGGTAGGTAGGTAGGTAGGTATCA GAG AGA CGC
4X AU5_mut_M4_FP	GCGTCTCTTCAGAGGTAGGTAGGTAGGTAGGTAGTT TAG AGA CGC
4X AU5_mut_M1_RP	GCGTCTCTTGTTTACCTACCTACCTACCTACCTGGTGAGAGACGC
4X AU5_mut_M2_RP	GCGTCTCTAGCCTACCTACCTACCTACCTACCTTGTTAGAGACGC
4X AU5_mut_M3_RP	GCGTCTCTCTGATACCTACCTACCTACCTACCTAGCCAGAGACGC
4X AU5_mut_M4_RP	GCGTCTCTAAACTACCTACCTACCTACCTACCTCTGAAGAGACGC